Purinergic Regulation of transepithelial ion transport in Cultured Equine Sweat Gland Epithelia

A thesis submitted for the degree of
Master of Philosophy
in Basic Medical Sciences

By

Vincent, Wai-ip Law

Department of Physiology
Division of Basic Medical Sciences
Faculty of Medicine
The Chinese University of Hong Kong

June, 1998

UL


香港大學
中文大學
圖書館系統
15 JUL 1999
UNIVERSITY
LIBRARY SYSTEM
THE UNIVERSITY OF HONG KONG

Declaration

This is to declare that the work presented in this thesis is my own and has not been submitted to this or any other institution for any degree, diploma or other qualification.

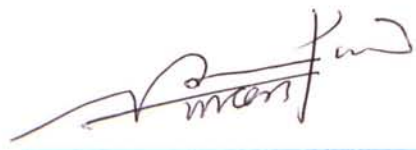

Vincent, Wai-ip Law

Candidate for M.Phil. Degree
Department of Physiology
Faculty of Medicine
The Chinese University of Hong Kong

Acknowledgment

First of all, I would like to express my sincere gratitude to my supervisor Prof. W. H. Ko for his patient guidance, helpful advice and constructive criticism throughout the past two years. Without his supervision and inspiration, all the work would not have been possible.

I would also like to thank Dr. S. M. Wilson, Prof. H.C. Chan, Prof. Y. Huang and Prof. P.Y.D. Wong for their helpful comments and suggestions.

I am also grateful to Mr. C.Y. Yip for his skilled technical assistance and preparation throughout the experiment. Thanks are also extended to Miss Karen Luk, Mr. W. K. Lee, Mrs. Peggy Leung Lau, Mr. Y. W. Chung, Mr. Benny Sy and my colleagues in Department of Physiology, who gave me invaluable support.

ABSTRACT

Extracellular adenosine 5'-triphposphate (ATP) has been documented in a large number of cell types to elicit a variety of biological responses through binding to specific membrane receptors termed P_2 purinoceptors. In particular, stimulation of purinoceptor results in activation of transepithelial ion transport in many epithelia such as human airway and colonic epithelia. Earlier studies of cultured equine sweat gland epithelia have also demonstrated that extracellular ATP and uridine-5'-triphosphate (UTP) applied to the apical membrane of the epithelia are effective regulators of intracellular free calcium concentration ($[Ca^{2+}]_i$) and transepithelial anion secretion. This project aims to further characterize the various P_{2Y}-nucleotide receptor subtypes present on the apical membrane and its underlying mechanisms in activating the anion secretion across the epithelium.

In the first series of experiment, the effect of various nucleotides on ion transport across the epithelium was examined using the conventional short-circuit current (I_{sc}) technique. Cell monolayers were formed on permeable supports. When confluent, they displayed apical/basolateral polarity. The ATP-induced I_{sc} was found to be attributed to electrogenic transport of anions from the basolateral to the apical solutions which was sensitive to apical addition of chloride channel blockers: diphenylamine-2-carboxylate (DPC) or 4,4'-diisothiocyanatostilbene-2,2'-disulfonic acid (DIDS). Microspectrofluorimetric studies revealed that the ATP-activated Ca^{2+} signals could be attributed to the release of Ca^{2+} from internal stores and to Ca^{2+} influx from extracellular fluid. The Ca^{2+} influx pathway could be inhibited by Ca^{2+} channel blockers: lanthanum ions and flufenamate.

Apart from the well-documented P_{2Y2} receptors on the cultured equine sweat gland epithelial cell (Ko *et al.* 1994; Ko *et al.* 1997; Wilson *et al.* 1996; Wilson *et al.* 1998), our data from cross-desensitization experiments suggested that anion secretion in these cells could be activated by UTP and UDP (but not by ATP), which probably binds to a previously unidentified 'pyrimidinoceptors'. These cells only express such receptors when grown in permeable supports which favour the development of a polarized phenotype, but not in non-polarized cells. Therefore, using standard methods traditionally applied to single cells cannot reveal the means by which nucleotides activate anion channels in intact epithelia.

In order to further characterize the effects of nucleotides on $[Ca^{2+}]_i$ and anion secretion in polarized epithelia, a recently developed experimental approach was employed that could allow us to monitor short-circuit current (I_{sc}) and intracellular signaling events (*e.g.* $[Ca^{2+}]_i$) simultaneously in a functionally polarized monolayer. Sweat gland epithelial cells were grown on *Transwell*®-COL filters and mounted in a specially designed *Ussing* chamber that allows combined I_{sc} and $[Ca^{2+}]_i$ measurements. These data suggested that the nucleotide-evoked increases in $[Ca^{2+}]_i$ and I_{sc} have different pharmacological profiles.

Moreover, the changes in $[Ca^{2+}]_i$ and I_{sc} have shown different time courses. The increase in I_{sc} evoked by 100μM ATP preceded any discernible change in $[Ca^{2+}]_i$ by 5 sec. During prolonged stimulation, the I_{sc} fell back to its basal value more rapidly than did $[Ca^{2+}]_i$ suggesting that $[Ca^{2+}]_i$-independent processes may contribute to this response. Ionomycin or thapsigargin could increase both the I_{sc} and $[Ca^{2+}]_i$ but subsequent application of various nucleotides could only evoke an increase in I_{sc} but not $[Ca^{2+}]_i$. The ATP-induced I_{sc} persisted after depletion of internal stores by

thapsigargin in Ca^{2+}-free perfusate. These data further substantiate that the nucleotide-evoked increase in anion secretion involves a $[Ca^{2+}]_i$-independent component. One likely possibility is the direct coupling of P_{2Y} receptors to anion channels although the detail mechanism remains unknown.

簡述

在細胞外的腺甘三磷酸（ATP），能通過激活在細胞膜上的 P2-purinoceptors（嘌呤受體）而產生多種生物反應，這已在不同種類的細胞廣泛報道。例如在人類的氣管和腸道的上皮細胞，激活嘌呤受體能活化經上皮的離子輸送。在培養的馬汗腺上皮細胞，細胞外的 ATP 和尿甘三磷酸（UTP）加進向細胞頂膜上能有效地控制細胞內的鈣離子濃度 $[Ca^{2+}]_i$ 及增加經上皮的負離子分泌。這研究專題是希望能進一步分辨在頂膜上不同的 P2 受體與其活化負離子分泌的機理。

在第一批的實驗，利用短路電流 (I_{sc}) 方法，測試不同核甘酸的效力。在可滲透的表面上，細胞會逐漸形成平滑單層的上皮層，及頂和底的極性。ATP 引發的短路電流是歸因於負離子由底部到頂部的液體的主動運輸；而在頂部加進氯離子通道的阻遏劑，DPC 或 DIDS，均能阻遏這短路電流。顯微分光螢光學的研究發現 ATP-活化的 $[Ca^{2+}]_i$ 增加是歸因於鈣由內在釋放及細胞外流入。兩種鈣離子通道的阻遏劑：Lanthanum（鑭）和 flufenamate 也能抑制鈣的流入途徑。

在馬汗腺細胞上，除了之前已提及的 P_{2Y2} 受體外，我們從交叉脫敏感實驗的結果得知，UTP及UDP（不是ATP）能活化細胞的負離子分泌。而這分泌大概是激活一個之前還未辨認的嘧啶核甘酸 (pyrimidine nucleotide) 受體。這種受體只在適合極化顯性的生長環境，但這嘧啶核甘酸受體並不存在於生長在玻璃片上的非極化細胞。所以，傳統方法利用個別細胞去測量 $[Ca^{2+}]_i$ 的研究未能發現這些嘧啶核活化的負離子通道的途徑。

要進一步研究這些核甘酸如何引發細胞內鈣濃度的增加和負離子分泌，我們採用了一個能同步測量在功能上極化的上皮層的短路電流和細胞內鈣濃度 $[Ca^{2+}]_i$ 的嶄新實驗方法。汗腺上皮細胞生長在 *Transwell*-col 透明的滲透膜上，這滲透膜裝上於特別設計能同步量度 I_{sc} 和 $[Ca^{2+}]_i$ 的*Ussing* Chamber上。實驗結果顯示，核甘酸導致 $[Ca^{2+}]_i$ 和 I_{sc} 的增加有不同的藥理基礎。

此外，$[Ca^{2+}]_i$ 和 I_{sc} 在時間上的轉變也有差異。ATP引發的I_{sc}增加，往往先於 $[Ca^{2+}]_i$ 有任何明顯改變（大概五秒）。在延長激活下，I_{sc}也快於 $[Ca^{2+}]_i$ 回

落到基礎水平，這結果提示了非 $[Ca^{2+}]_i$ 依賴的過程也可能參與這 I_{SC} 的反應。Ionomycin 和 thapsigargin 也能增加 I_{SC} 和 $[Ca^{2+}]_i$，但其後加進不同的核甘酸只能引發 I_{SC} 的增加，但不是 $[Ca^{2+}]_i$ 的增加。當細胞內的鈣儲存被 thapsigarin 和不含鈣溶液耗盡之後，ATP依然能引致 I_{SC} 的增加。這結果進一步顯示這些核甘酸引起的負離子分泌增加含有一個非 $[Ca^{2+}]_i$ 依賴的成份。但詳細的機制還沒有清楚，其中一個可能性是 P_{2Y2} 受體直接與負離子通道偶聯。

Abbreviations

ap	apical/luminal
bl	basolateral/serosal
ADP	Adenosine-5'-diphosphate
ATP	Adenosine-5'-triphosphate
BAPTA/AM	1,2-bis (*o*-amino phenoxy)ethane-*N,N,N',N'*-tetraacetic acid (acetoxymethyl ester form)
$[Ca^{2+}]_i$	intracellular free calcium concentration
DIDS	4,4'-disothiocyanatostibene-2,2'-disulfonic acid
DMSO	dimethly sulfoxide
DPC	diphenylaminao-2-carboxylate
FBS	fetal bovine serum
G_i	inhibitory G-protein
I_{sc}, ΔI_{sc}	short-circuit current, change in I_{sc}
La^{3+}	lanthanum ion
Ptx	Pertussis toxin
R_t	transepithelial resistance
R_f, ΔR_f	fluorescence ratio, change in fluorescence ratio
S.E.M.	standard error mean
Tg	thapsigargin
$T_{lag(control)}$/ $T_{lag(BAPTA)}$	time difference between the peak of I_{sc} and R_f in control/BAPTA-treated epithelia respectively

$T_{Isc(control)}$/ $T_{Isc(BAPTA)}$	time required for I_{sc} to reach the peak after drug application in control/ BAPTA-treated epithelia respectively
UDP	Uridine-5'-diphosphate
5-Br-UTP	5-Bromo-uridine-5'-diphosphate
UTP	Uridine-5'-triphosphate

Table of Contents

Page no.

Chapter I. Literature Review

I.1. Structure, functions and general physiology of equine sweat gland

I.1.1. Ultrastructure of equine sweat gland 1

I.1.2. Functions and physiology of equine sweat gland 3

I.1.3. Experimental studies on equine sweat gland by functional approaches 4

I.1.4. Hormonal and neuronal regulation of sweat secretion in equidaes 5

I.1.5. Possible role(s) of extracellular ATP in equine sweat gland epithelia 6

I.1.6. Measurement of electrogenic anion secretion by short-circuit current (I_{sc}) technique 8

I.2. Classification of purinergic receptors and its existence in biological systems

I.2.1. Functional classification of purinergic receptors 13

I.2.2. Basic structure of G-protein coupled P_{2Y} receptors 17

I.2.3. Physiological function and significance of purinergic receptors 20

I.3. Objectives of study 22

Chapter II. Methods and Materials

II.1. Culture technique of the equine epithelial cells 23

II.2. Conventional short-circuit current (I_{sc}) measurement technique

II.2.1. Introduction 25

II.2.2. Preparation of permeable supports and electrodes 25

Page no.

II.2.3. Experimental set up and measurement of I_{sc} 28

II.2.4. Measurement of I_{sc} during experiment 30

II.3. Measurement of intracellular free calcium ($[Ca^{2+}]_i$) by microspectrofluorimetry

II.3.1. Preparation of cells 31

II.3.2. The set up and procedures for experiment 31

II.4. Simultaneous measurement of changes in $[Ca^{2+}]_i$ and I_{sc}

II.4.1. Experimental set up and manipulation 35

II.4.2. Other preparations before experiment 37

II.5. Material and solutions used for experiment

II.5.1. Culture media and enzyme 40

II.5.2. Chemicals and Drugs 40

II.5.3. Preparation of solution for experiments 42

II.6. Statistical analysis 44

Chapter III. Results

III.1. Effects of nucleotides on transepithelial ion transport

III.1.1. Basic electrophysiological properties of cultured equine sweat gland epithelia 45

III.1.2. Short-circuit current (I_{sc}) induced by nucleotides 45

III.1.3. Identification of ion species responsible for the change in I_{sc} 50

III.1.4. Effects of chloride channels blockers on the UTP-induced I_{sc} 51

Page no.

III.2. Signal transduction mechanisms of P_{2Y}-nucleotide receptors

III.2.1. The involvement of G_i-proteins 56

III.2.2. Effect of BAPTA on the increases in I_{sc} induced by nucleotides 58

III.2.3. Study of P_{2Y}-receptor mediated increase in $[Ca^{2+}]_i$ 62

III.3. Characterization of the P_{2Y} subtype(s) by cross desensitization experiments

III.3.1. Autologous desensitization experiments 70

III.3.2. Classical cross desensitization experiments 70

III.3.3. Characterization of the ATP-insensitive P_{2Y}-receptor 80

III.3.4. Interaction between ATP and bradykinin 87

III.4. Simultaneous measurement of $[Ca^{2+}]_i$ and I_{sc}

III.4.1. Effect of UDP and ADP 89

III.4.2. Correlation of I_{sc} and $[Ca^{2+}]_i$ 92

III.4.3. Cross desensitization experiments 97

III.5. Evidence of a $[Ca^{2+}]_i$-independent I_{sc}-component induced by nucleotides

III.5.1. The time course of the ΔR_f and ΔI_{sc} 102

III.5.2. Effect of ionomycin on the ΔI_{sc} and ΔR_f induced by nucleotides 110

III.5.3. Effect of thapsigargin on the ΔI_{sc} and ΔR_f induced by nucleotides 110

III.5.4. Effect of thapsigargin in nominal Ca^{2+}-free solution 115

Chapter IV. Discussion

IV.1. Role of extracellular nucleotides in epithelial tissues 119

IV.2. Characterization of an ATP-insensitive P_{2Y}-nucleotide receptor 120

IV.3. Expression of the novel ATP-insensitive receptor on a functionally polarized epithelia 122

Page no.

IV.4. Involvement of a $[Ca^{2+}]_i$-independent I_{sc} induced by nucleotides 124

Chapter V. References 128

Chapter I. Literature Review

I.1. Structure, functions and general physiology of equine sweat gland

I.1.1. Ultrastructure of equine sweat gland

An intact equine sweat gland can be morphologically divided into two parts, the duct body and the fundus, while the duct body can be subdivided into two portions:

(a) Intrafollicular region: The outermost part of the sweat gland, the lumen is lined with multi-layer of cornified cells, which are rich in keratohyalin. *Langerhans* cells are commonly found between cornified cells layers (Figure I.(a)).

(b) Intradermal region:

(i) Intradermal duct are enclosed with a fibrocyte sheath while the size of lumen and the layer of cells lining the lumen gradually reduced.

(ii) The fundus is composed of cuboidal secretory cells at the inner layer and the fundus are surrounded by connective tissues and fibrocyte sheath. Unmyelinated nerve fibres and blood vessels are commonly found between the fibrocyte sheath and the gland. The secretory cells are characterized by the numerous and long microvilli at the luminal side, and the junctional complexes between cells at luminal margin. Zonula occludens and desomosomes were also found at the junctional complexes. The secretory cells are interdigitated laterally and penetrated between the myoepithelial cells (Montgomery *et al.* 1982).

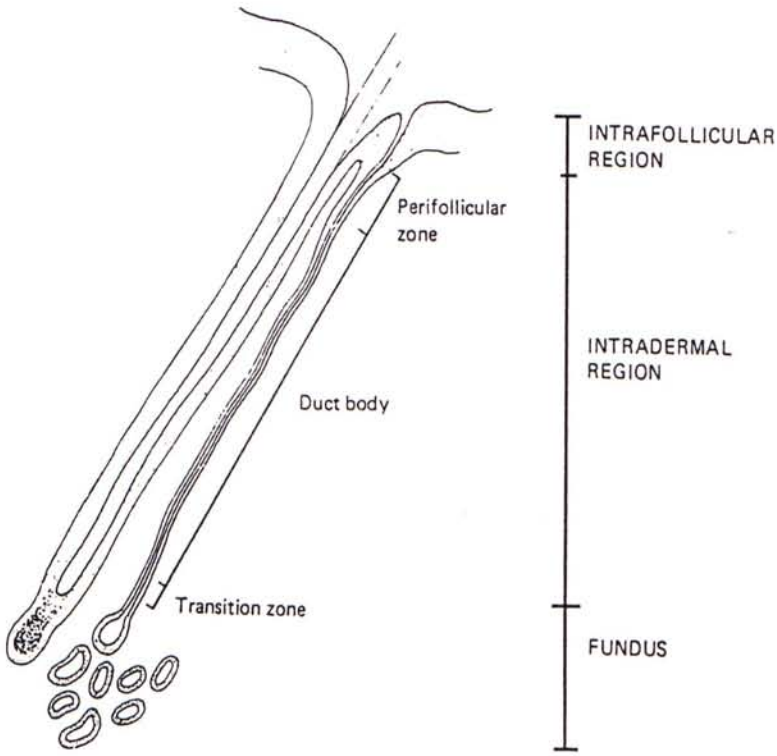

Figure I.(a)

Ultrastructure of an equine sweat gland from an intact horse skin. A diagram illustrating the fundus and different zones of the duct of the equine sweat gland and their situations with respect to the hair follicle.

I.1.2. Functions and physiology of equine sweat gland

In equidaes, thermoregulation is accomplished by sweating and respiratory heat loss. However, only primates and equidaes are predominantly regulating their body temperature through sweating (Wilson *et al.*1993) while respiratory heat loss only contribute to a substantial level (Kingston *et al.* 1997).

Apart from thermoregulation, the sweat gland of equidaes is also involved in the maintenance of electrolyte concentration in body fluid, plasma volume and the osmolality of plasma, especially during exercise and exposed to a hot environment (Kingston *et al.*1997).

Sweat formation in equidaes was postulated to be consisted of two components: (i) secretion (defined as exocytosis and fluid transport) and (ii) cell death. Fluid transport is achieved by an electrogenic anion secretion across a secretory epithelia, together with Na^+ ion and H_2O passively flow along the electrical/chemical gradient. Sweating in horses also induces a depletion of secretory vesicles in secretory cells by exocytosis. These vesicles were believed to be derived from golgi apparatus (Montgomery *et al.* 1982). Equine sweat contains the products of dead secretory cells, which is resulted from cell turn-over. The reabsorption of ions during thermal stimulation suggests that sweat secretion involved the modification of ionic composition of sweat (Wilson *et al.* 1988). Unlike human hypotonic sweat, horse sweat is slightly hypertonic (McConaghy *et al.*1995), with osmolality ranges from 290 to 320 mosmol/Kg (Kingston *et al.* 1997).

I.1.3. Experimental studies on equine sweat gland by functional approaches

Anhidrosis is the loss of the ability to sweat. The disease usually occurs in horses living in hot and humid climate like Hong Kong. Functional studies of the pathophysiological conditions of equine sweat gland were commonly based on the whole-animal experiments. These experiments were conducted through the administration of sudorfic drugs locally, or performing scheduled exercises. The measuring parameters included the ionic composition of sweat, osmolality, sweat rate and body temperature. Apart from whole-animal experiments, other researchers may prefer to investigate the physiology of sweating by using samples of skin biopsies (Bijman and Quinton, 1984) or isolated perfused skin (Johnson, 1975). Another earlier study performed by Montgomery (1982) employed a histological approach to study the morphological changes in different parts of sweat gland during sweat production.

In the present study, a cultured epithelial cell line derived from the secretory coil of the equine sweat gland (E/92/3) was employed. The cultured epithelial cells enable us to study the cellular mechanisms of sweat secretion in a more quantitative approach. Besides, it would reasonably provide an inexhaustible and reliable source for performing a quantitative study and exploring the mechanisms behind for stimulus-secretion coupling (Wilson *et al.*1993).

I.1.4. Hormonal and neuronal regulation of sweat secretion in equidaes

In human, the neural control of sweat production is primarily regulated through sympathetic nervous system, with acetylcholine as neurotransmitter. Unlike human, isolated equine sweat glands are unresponsive to acetylcholine, but are responsive to β-adrenergic agonists (Bijman and Quinton, 1984; Ko *et al.* 1994). However, noradrenaline, which predominantly act through α and β_1-adrenoceptor, was ineffective in *vivo* (Bijman and Quinton, 1984). In *vitro*, only extreme high concentrations of noradrenaline could induce the production of cAMP (Wilson *et al.* 1993). The study performed by Wilson (1993) also reported that adrenaline was more potent than noradrenaline in mediating the production of cAMP. Besides, butoxamine (β_2-antagonist) was more potent to inhibit the effect of adrenergic agonists than atenolol (β_1-antagonist). These findings strongly supported the adrenergic control in equine sweat gland belongs to β_2-subclass (Wilson *et al.* 1993). Similarly, β_2-adrenoceptor were also reported in another whole-animal study (Snow, 1977) as well as the isolated glands study performed by Bijman and Quintion (1984).

Apart from β_2-adrenergic control, extracellular ATP could also play a role in the regulation of sweating (Ko *et al.* 1994). ATP was once discovered to be released as co-transmitter with noradrenaline from sympathetic nerves endings to target tissues (Burnstock, 1990). The co-transmission model of ATP and noradrenaline was well-supported by the biochemical evidence of ATP and noradrenaline being costored in sympathetic synaptic vesicles. Thus it was suggested that ATP released from local sympathetic nerve endings of sweat gland may be capable of initiating signal transduction pathways in the sweat gland epithelium and regulating ionic secretion (Ko *et al.*1994).

Apart from the co-transmission model, extracellular ATP could also participate in the regulation of transepithelial ion transport *via* an autocrine control mechanism (Schwiebert *et al.* 1995; Wilson *et al.*1996). In the proposed autocrine mechanism, intracellular ATP was suggested to be released from cells to extracellular compartment and exerts its regulation through apically located purinergic receptors, although the detail transport pathway is still remained obscuse (Parr *et al.* 1994; Reisin *et al.* 1994; Schwiebert *et al.* 1995). Subsequently, nucleotides in the extracellular environment could activate the apically located P_2-nucleotide receptors and then these nucleotides in extracellular fluid would be eventually metabolized to nucleosides and inorganic phosphates or interconvert with other nucleotides by the action of multi-extracellular enzymes (*i.e.* ectonucleotidase and nucleoside diphosphokinase) (Harden *et al.* 1997).

I.1.5. Possible role(s) of extracellular ATP in equine sweat gland epithelia

In microspectrofluorimetric studies, extracellular ATP was able to elicit an increase in intracellular free calcium ($[Ca^{2+}]_i$) in the cultured epithelial cells (Ko *et al.* 1994). The increase in $[Ca^{2+}]_i$ was initiated by the stimulation of a functional purinergic receptor in the plasma membrane. The activated purinergic receptor coupled with G-proteins and then activate phospholipase C for the hydrolysis of a membrane phospholipid (phosphatidylinositol-4,5,-biphosphate:PIP_2) into inositol 1,4,5-triphosphate (IP_3) and diacylglycerol (DAG) (Dubyak *et al.* 1988) (Figure I.(b)). The accumulation of inositol triphosphate (IP_3) could activate the release of Ca^{2+} from internal stores. Subsequently, the increase in $[Ca^{2+}]_i$ due to internal releases would trigger the influx of Ca^{2+} from extracellular fluid (Dubyak *et al.* 1988). In a

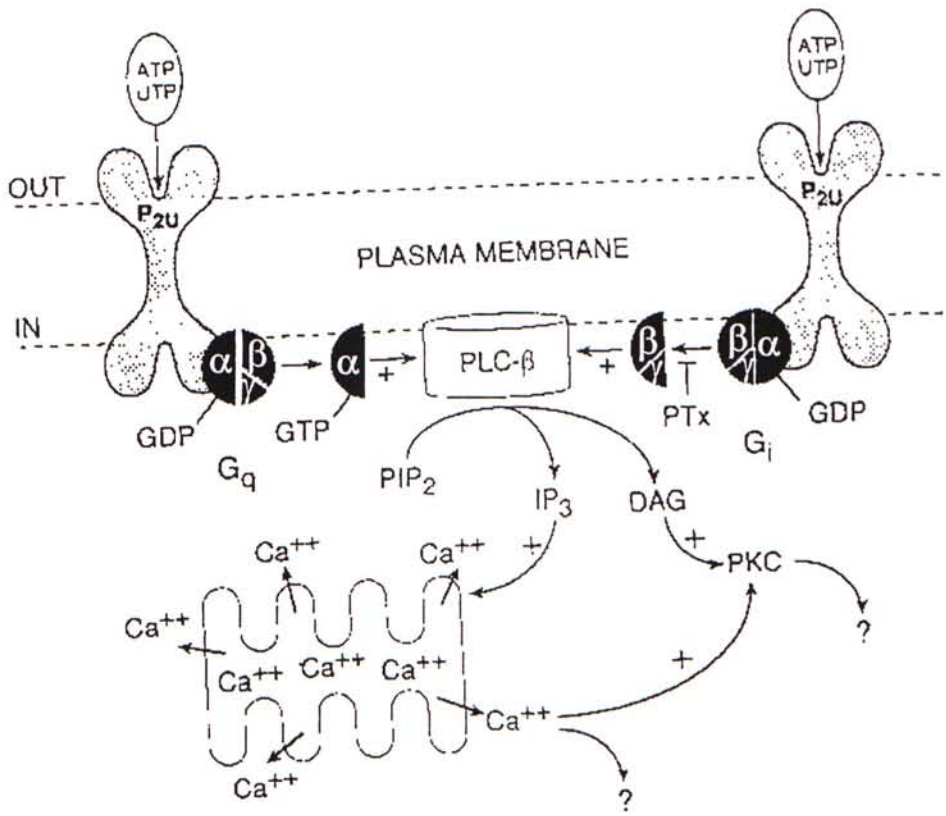

Figure I.(b)

A schematic diagram for the signal transduction pathway mediated by a subtype of P_{2Y} receptor (P_{2U}). PLCβ: phospholipase C β, PIP_2: phosphatidylinositol-4,5-bisphosphate, IP_3: inositol-1,4,5-triphosphate, DAG: diacylglycerol, PKC: protein kinase C $G_{q/11}$,G_i: G-proteins subunits coupled with P_{2Y2} receptor.

earlier $[Ca^{2+}]_i$ study on the same cell line, ATP and UTP were reported as effective regulators for $[Ca^{2+}]_i$. In contrast, the P_1-agonists: AMP or adenosine or other P_{2X} agonists were unable to elicit any change in $[Ca^{2+}]_i$ (Ko *et al.*1994). These data strongly indicated the purinergic control in equine sweat gland consists of a $P_{2Y2}(P_{2U})$ receptor population (Dubyak & El-Moatassim, 1993; Wilson *et al.* 1996).

I.1.6. Measurement of electrogenic anion secretion by short circuit current (I_{sc}) technique

To measure the transepithelial ion transport with a direct and quantitative approach, a short-circuit current (I_{sc}) measurement was employed. The transepithelial ion secretion across a cultured epithelial monolayer was measured by a change in I_{sc} (ΔI_{sc}) in a functionally polarized epithelia. The epithelial polarization was confirmed by a previous study in which the cross-section of the epithelial monolayer was examined with electron microscopy (EM). The EM pictures clearly displayed the apical/basolateral polarity as well as the possessing of junctional complexes and short and numerous microvilli at the apical side (Ko *et al.* 1996*a*). Therefore, all the sweat gland epithelial cells grown on permeable supports for subsequent experiments were adopted from this culturing technique (Ko *et al.* 1996*b*; Ko *et al.* 1997; Wilson *et al.* 1998). Previous studies revealed that the increase in I_{sc} could be activated by extracellular ATP, UTP and Ca^{2+} mobilizing agents, (*e.g.* thapsigargin and ionophores) (Wilson *et al.*1996; Ko *et al.*1996*a,b*; Ko *et al.*1997). The ΔI_{sc} is a direct evidence of electrogenic ion secretion.

The first ΔI_{sc} initiated by extracellular nucleotide on the cell line was discovered by the application of UTP to either apical (ap) or basolateral (bl) side of bathing solution. According to figure I.(c), apical application of UTP induced a clear

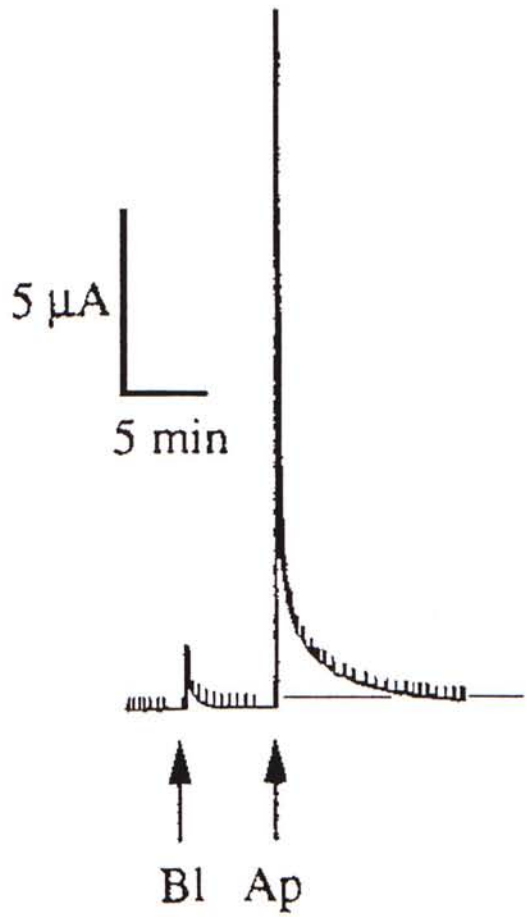

Figure I.(c)

Effects of UTP upon short-circuit current in cells grown on permeable supports. UTP at 100µM was added to the solution bathing the basolateral (bl) or apical (ap) side of the epithelium as indicated by the arrows. Upward deflections are defined as anions moving from basal to the apical compartments.

response, which was transient and returned to baseline regardless the present of stimulus. In contrast, the response to basolateral application was relatively small and variable (Wilson *et al.* 1996). These preliminary findings suggested that the functional P_{2Y}-nucleotide receptor were predominantly found on the apical membrane (Ko *et al.*1997).

The secretory model of $[Ca^{2+}]_i$-dependent ionic secretion of equine sweat gland was investigated in a previous study (Ko *et al.* 1996*a*). With the conventional I_{sc} technique, the secretory model was studied by using different pharmacological agents to inhibit various transporter proteins or ion channels.

In chloride secretion, three basolateral components were involved (Figure I.(d)); (i) Na^+/K^+ATPase, which pumps out Na^+ ion entering the cell for maintaining of low cytosolic Na^+ concentration. (ii) $Na^+/K^+/2Cl^-$ symport, which allows the accumulation of chloride ions for secretion; (iii) Basolateral voltage dependent K^+ channels, which allows the exit of K^+ from the cell for the recycling of K^+. The K^+ channels also facilitate the hyperpolarizing of the cell thus providing an electrical gradient favor for anion secretion.

In bicarbonate secretion, CO_2 and H_2O were catalyzed to H^+ and HCO_3^- by intracellular carbonic anhydrase. The produced H^+ ion would be transported out of the cell through the Na^+/H^+exchangers (Figure I.(e)). The entered Na^+ from Na^+/H^+ exchangers were also actively pumped out by Na^+/K^+ATPase located at basolateral side, whereas the K^+ level in the cell was also regulated by the K^+ channels. The HCO_3^- secretion was proposed to be transported through the apical Cl^- channels, as suggested in the rat epididymal epithelia (Wong, 1988).

Apical compartment

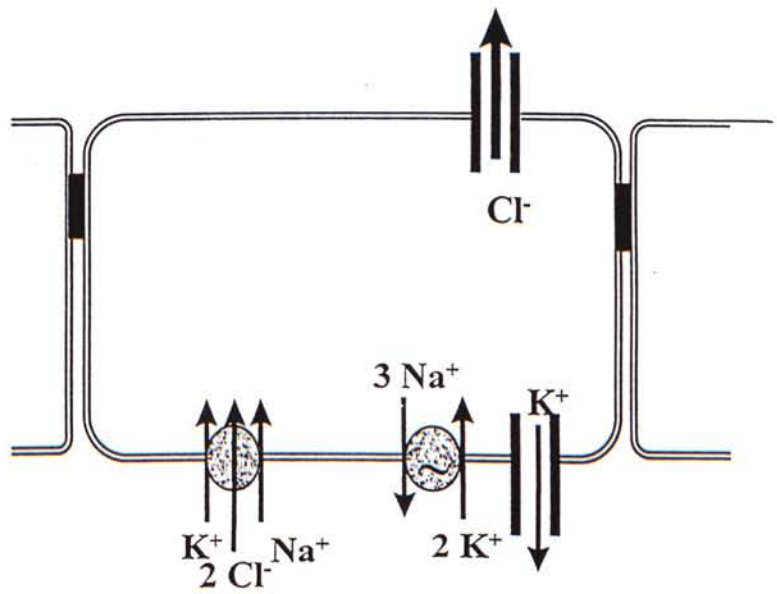

Basolateral compartment

Figure I.(d)

Proposed model of Cl^- secretion in cultured equine sweat gland epithelium.

Apical compartment

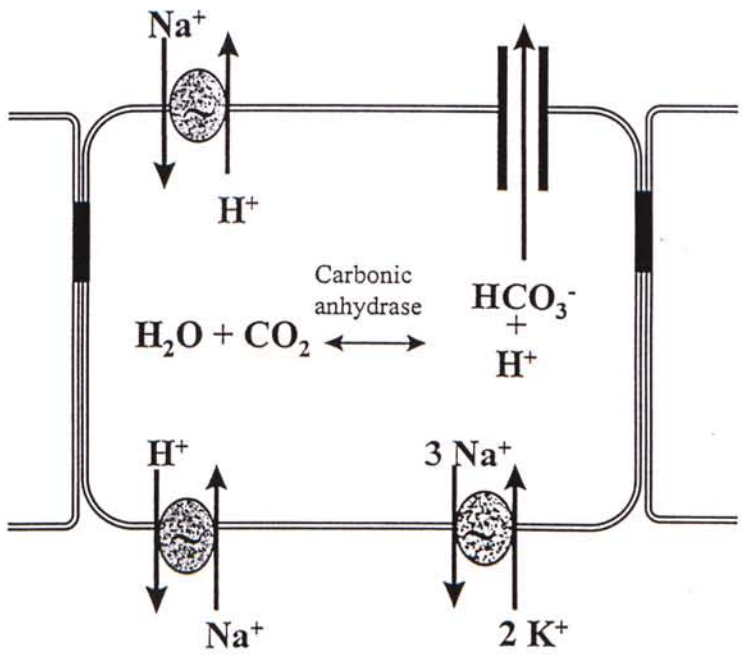

Basolateral compartment

Figure I.(e)

Proposed model of HCO_3^- secretion in cultured equine sweat gland epithelium.

I.2. Classification of purinergic receptors and its existence in biological systems

I.2.1. Functional classification of purinergic receptors

Adenosine and adenosine nucleotides (*i.e.* ATP, ADP & AMP) act on two distinct families of receptors: P_1-adeosine receptors and P_2-nucleotide receptors. P_1 receptors are preferentially activated by adenosine, methylxanthine analogues and to a less extent by AMP and ADP. P_1 receptors are basically divided into 3 classes: A_1 to A_3. The A_2 receptors could be subdivided into 2 subtypes: A_{2A} and A_{2B}. A_1 and A_2 receptors can either inhibit or activate the cAMP-mediated signal transduction pathway, whereas A_3 receptor can trigger the hydrolysis of phosphatidylinositol-4,5-bisphosphate (PIP_2) and the subsequent IP_3-mediated signalling pathway.

P_2-nucleotide receptors are functionally divided into 2 distinct families: P_{2X} and P_{2Y}. P_{2X} receptors belong to a ligand-gated ion channel receptors superfamily. Up to now, 6 subtypes of P_{2X} are cloned. In contrast to P_1-adenosine receptors, P_{2X} receptors are preferentially activated by adenosine triphosphate (ATP) or its analogue, such as: α,β-methyleneATP and 2-methylthioATP. ADP or adenosine are weak agonists or even unable to induce any activation in some subtypes. Generally speaking, P_{2X} subtypes regulate the opening of ligand gated cation channels, which allowed the entry of $Na^+/K^+/Ca^{2+}$ ions. The selectivity of cation entry mainly based on the structural difference of each subtype. All P_{2X} receptors are characterized by 2 membrane spanning segments, with both N and C termini inside the cytoplasm. The extracellular loops connecting two segments contain disulfide-bonded loops and N-linked glycosyl chains (Figure I.(f)). However, the structure of P_{2X} receptors is not

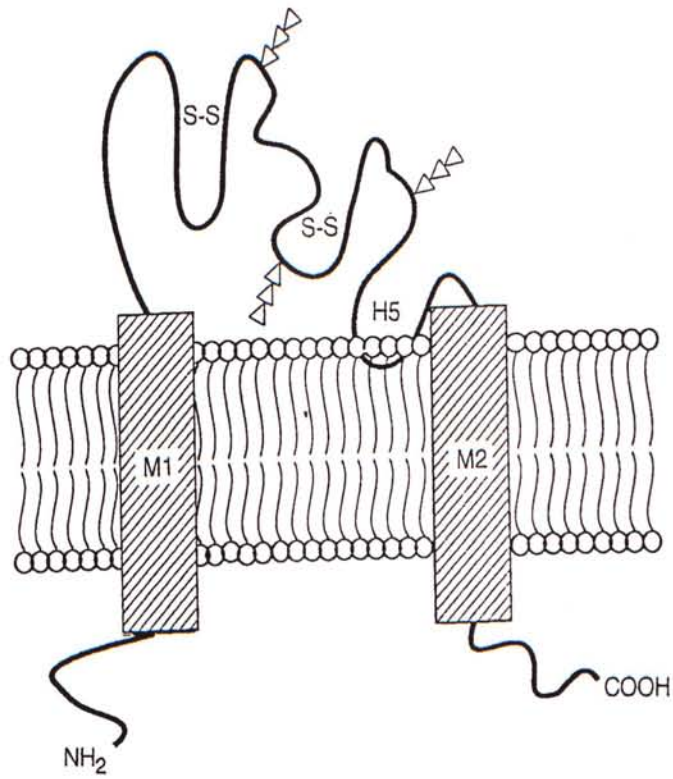

Figure I.(f)

Molecular structure of P_{2X} purinoceptor. Model depicting a proposed transmembrane topology for P_{2X} protein is shown with both *N*- and *C*- termini in the cytoplasm. Two putative membrane-spanning segments (M1 and M2) traverse in the lipid layer of the plasma membrane and are connected by a hydrophilic segment of 270 amino acids. This putative extracellular domain is shown containing two disulfide-bonded loops (S-S) and three *N*-linked glycosyl chains (Δ).

identical with other ligand gated cation channel receptors, which are characterized by the extracellular N-terminus and 3-5 membrane spanning segments.

P_{2Y} receptors belong to a G-protein coupled receptor superfamily. Up to now, at least 4 subtypes were cloned. The classification of different P_{2Y} subtypes were generally based on the pharmacological profiles of different nucleotides, as well as the amino acid sequences of cloned receptors. Typically, P_{2Y} receptors are characterized by the seven transmembrane domains. These receptors can couple with guanine binding proteins (*i.e.* G-proteins) which then dissociate into G_{α} and $G_{\beta\gamma}$ subunits. The dissociated G-protein subunits can activate phospholipase-C β-isoforms for phosphoinositol hydrolysis. The inositol triphosphate accumulation trigger the release of Ca^{2+} from internal stores. The depletion of Ca^{2+} in the internal stores and the elevated intracellular Ca^{2+} (*i.e.* $[Ca^{2+}]_i$) can then induce a Ca^{2+} entry. The increase in $[Ca^{2+}]_i$ can activate various specific cellular responses; such as the opening of $[Ca^{2+}]_i$-dependent chloride conductance for ionic secretion in epithelial tissues (Dubyak and El-Moatassim, 1993).

(i) P_{2Y1} subtype is only sensitive to adenosine nucleotides and it is more sensitive to 2-MeSATP than ATP. Besides, P_{2Y1} receptor is insensitive to pyrimidine nucleotides or α,β-methylene-ATP.

(ii) P_{2Y2} receptor was previously named as P_{2U} receptor, as it is the first P_{2Y} subtype sensitive to UTP. At P_{2Y2} receptor, UTP and ATP are equipotent, whereas UDP and ADP were initially reported as full agonists with lower potencies. However, these nucleoside diphosphates are ineffective after purification.

(iii) P_{2Y6} receptor, a novel pyrimidine-specific P_{2Y} receptor, is the third P_{2Y} subtype cloned and sequence published. P_{2Y6} subtype was first cloned from a rat aortic smooth muscle (Chang *et al.* 1995). And more recently, the cloning of a human

homologue of P_{2Y6} is also reported (Communi *et al.* 1996). At P_{2Y6} receptor, UDP and UTP are full agonists, although UDP is 100-fold more potent than UTP, while ATP and its analogs were ineffective (Nicholas *et al.*1996).

(iv) P_{2Y4} receptor, another novel pyrimidine-sensitive P_{2Y} receptors being cloned at the same time by Communi (1995) and Nguyen (1995). These two groups had isolated the partial sequences of P_{2Y4} and used the conserved sequences of other P_{2Y} subtypes to clone into a full sequence. However, the pharmacological profiles reported by these two groups were not consistent. Communi (1995) reported that UTP & UDP were equipotent at P_{2Y4}, while ATP & ADP were partial agonists. In contrast, Nguyen (1995) reported that UTP was the most potent agonist at P_{2Y4}, followed by UDP, while ATP was an antagonist of P_{2Y4} receptor. Until more recently, a detailed pharmacological study of P_{2Y4} receptor being expressed in a human astrocytoma cell line (1321N1) suggests that purified UDP is not an agonist, while ATP is a full agonist with a lower potency than UTP. ADP and 2-MeSATP are all unable to induce any effect. In other words, P_{2Y4} receptor is nucleoside triphosphate specific (Filtz *et al.*1997).

The characterization of P_{2Y} receptor was hampered for many years which was due to the lack of specific antagonists at subtype level. Another serious problem encountered was the ignorance of most researchers about the contamination of commercially available nucleotides. In fact, these nucleotides could be purified by hexokinase treatment or HPLC assay (Harden *et al.* 1997).

On the other hand, extracellular enzymes (*i.e.* ecto-nucleotidases and nucleoside diphosphokinase) can also affect the activity of a nucleotide on the cell surface. Ecto-nucleotidases can hydrolyze nucleoside triphosphates (*i.e.* ATP and UTP) rapidly to nucleoside diphosphates. Nucleoside diphosphokinase is another

common extracellular enzyme which can catalyze the transfer of γ-phosphate from nucleoside triphosphate to nucleoside diphosphate (*e.g.* ATP+UDP $\xrightarrow{\text{nucleoside diphosphokinase}}$ ADP+UTP) (Harden *et al.* 1997).

In addition, some cells natively expressed with a mixed population of P_2-receptors. Therefore, the isolation of a single subtype for mRNA expression or cloning from the mixed receptors population would be extremely difficult.

I.2.2. Basic structure of G-protein coupled P_{2Y} receptors

Like most other G-protein coupled receptors (*e.g.* thrombin receptor, angiotensin II receptor), P_{2Y} receptors are consisted of seven transmembrane domains. These domains are connected with extracellular and intracellular loops, an extracellular N-terminus for TM1 and intracellular C-terminus of TM7 were found (Figure I.(g)). In general, the extracellular domains 2 & 3 of P_{2Y} receptors are conserved as cysteine residues for the formation of disulfide bridge. With only exception of P_{2Y4}, other cloned P_{2Y} receptors possesses N-linked glycosylation at N-terminus. In addition, an Asp residue in TM2 is conserved in all G-protein coupled receptors. Among all the P_{2Y} receptors, an important common feature: a 'signature sequence' of "LFLTCIS" is conserved at the TM3 (Filtz *et al.* 1997; Communi *et al.* 1997). From a study of site direct mutagensis of P_{2Y2} receptor, the positive charged residues (His262, Arg265 in TM6 & Arg292 in TM7) were proposed to neutralize the negatively charged nucleotide phosphate (Erb *et al.* 1995) (Figure I.(h)). Interestingly, these charged residues were also conserved in P_{2Y4} receptor, which was consistent with its nucleoside triphosphate specificity. In the sequence of P_{2Y6} receptor, the residue of Arg265 was replaced by Lys259. In the sequence of P_{2Y2} receptor, the

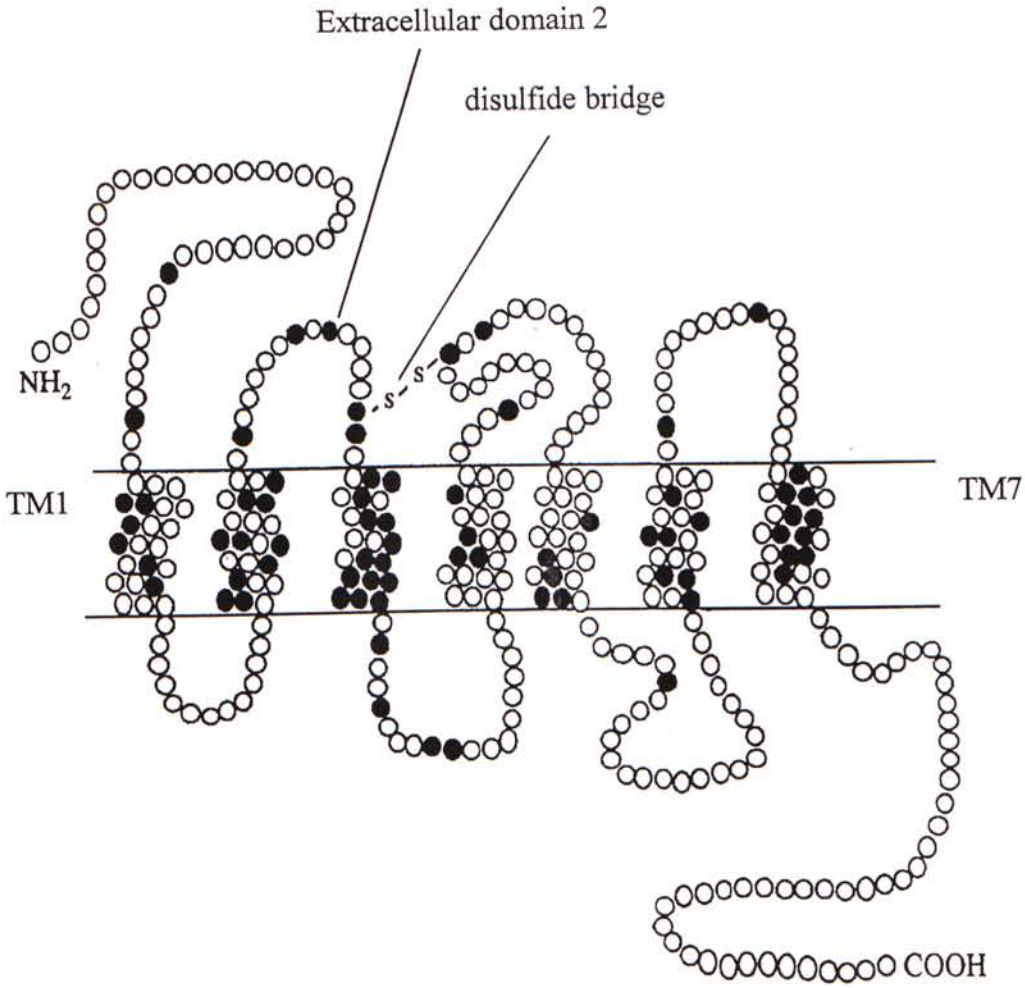

Figure I.(g)

Schematic diagram of the sequence of P_{2Y} receptor; filled circles represent residues that are known to be functionally important in other G-protein-coupled receptor.

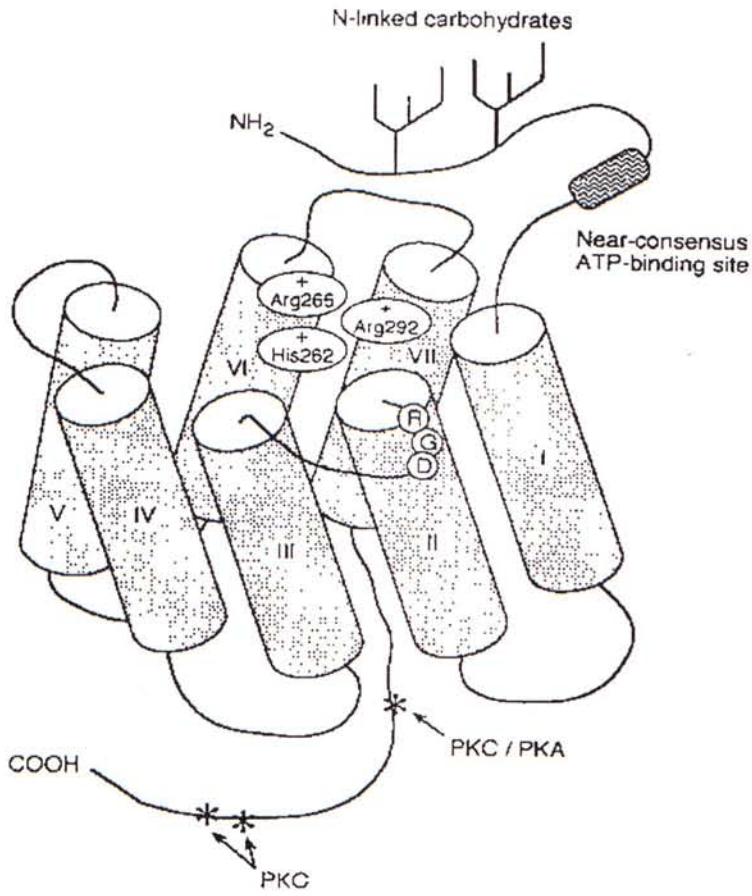

Figure I.(h)

Schematic diagram and proposed binding sites of P_{2Y2} receptor. Three positively charged residues (His^{262}, Arg^{265} and Arg^{292}) that are important for ligand binding and receptor activation are shown in transmembrane domains VI and VII. And a potential integrin binding motif (RGD) is shown in the extracellular loop between transmembrane domains II and III. * denote the location of several potential phosphorylation sites near the intracellular *C*-terminus. The two branched figures and the filled box near the *N*-terminus indicate the location of two consensus *N*-linked glycosylation sites and near consensus ATP-binding site, respectively.

residue of Lys289 also played a crucial role in the selectivity of nucleoside triphosphate over nucleoside diphosphate. At the junction between third intracellular loop and TM6, a Thr residue in the sequences of P_{2Y2} and P_{2Y4} is conserved in most G_i-coupled receptors, and this residue was proposed be related to pertussis toxin sensitivity of P_{2Y} receptor (Communi *et al.* 1997).

Regardless of the sources of cloned P_{2Y} subtypes, nearly 90% of homology was found in different species of same subtype. For example, a human cloned receptor P_{2Y1} could share a 93% homology with a turkey P_{2Y1} receptor (Schachter *et al.* 1996). However, the amino acid sequences of different P_{2Y} subtypes are largely variable. In human, the sequence of P_{2Y4} was only 55% homologous to P_{2Y2}, 38% to P_{2Y1} and 40% to P_{2Y6} (Filtz *et al.* 1997).

I.2.3. Physiological function and significance of purinergic receptors

Physiological function(s) of extracellular nucleotides on various biological systems

Although the pharmacological effects of extracellular ATP were proposed as early as 1930's, the importance of ATP in signalling was neglected and the existence of a functional nucleotide receptor for regulating different cellular responses was only realized in the last 25 years (Burnstock,1980).

The study of extracellular ATP was one of hottest topics in the past decade, and the action of extracellular ATP had been widely reported. For example, extracellular ATP was widely reported in regulatory of the contractions of cardiac, vascular and visceral smooth muscle. Extracellular ATP can also regulate the excitatory and inhibitory effects on neurons. In non-excitable tissue, ATP can

regulate of hormone secretion, exocrine gland secretion, inflammatory actions and many other well-documented cellular effects (Harden *et al.* 1995).

Instead of extracellular ATP, the identification of pyrimidine-selective P_{2Y} receptors, (*i.e.* P_{2Y4} & P_{2Y6}) could provide a strong evidence for the physiological significance of extracellular pyrimidine nucleotides. On the other hand, the detection of P_{2Y6} transcript in human spleen, thymus and leukocytes would suggest its possible role in immune system (Communi *et al.* 1997).

In general, the ATP-sensitive P_{2X} receptors are commonly involved in fast neuronal and muscle contraction response through its gated cation channel. Obviously, none of the P_{2X} subtypes are responsive to pyrimidine nucleotides. In contrast to ATP, extracellular pyrimidine nucleotides mainly participate in the metabotrophic role of regulation (Nicholas *et al.* 1996).

Physiological role(s) of extracellular nucleotides on epithelial tissues

Apart from the general physiological roles, the role of extracellular nucleotides in ionic secretion of epithelial tissues are essentially pronounced. Until recently, many evidences have emerged for the regulatory effects of nucleotides on ion secretion. In cultured human nasal tracheal submucosal glands, P_{2Y2} (P_{2U}) receptors was reported to regulate chloride secretion (Yamaya *et al.* 1996). Similarly, the existence of a UDP-selective receptor on human nasal epithelial cells would make this receptor a potential target for cystic fibrosis (CF) treatment (Lazarowski *et al.* 1997). Actually, the therapeutical action of uridine nucleotides together with amiloride was demonstrated by the enhancement of mucosal clearance in airway epithelial linings of CF patients (Bennett *et al.* 1996).

I.3. Objectives of study

The present study was carried out to investigate and characterize the P_{2Y}-nucleotide receptors present on the apical membrane of cultured equine sweat gland epithelia. This project also aimed to elucidate the electrolyte transport mechanisms of nucleotide-evoked anion secretion by I_{sc} technique.

The role of $[Ca^{2+}]_i$ in purinergic regulation of anion secretion in the cultured epithelia was also studied by microspectrofluorimetric technique. The measurement of $[Ca^{2+}]_i$ should be useful to explore the mechanisms underlying the increases in I_{sc} as well as the possible Ca^{2+} entry pathway(s) initiated by extracellular nucleotides.

Moreover, we aimed to establish a newly developed technique which can monitor the changes in $[Ca^{2+}]_i$ and I_{sc} simultaneously. The establishment of such technique would allow us to gain more informative data on how nucleotides could activate anion secretion in a polarized monolayer.

It was hoped that the information provided by this study would give some insights for the development of therapeutic agents in treatment of epithelial secretion disorders.

Chapter II Methods and materials

II.1 Culture technique of the equine epithelial cells

The cultured equine sweat gland epithelial cell line (E/92/3) was kept for experimental purposes within the range of 50 to 70 passages. For maintenance, it is necessary to thaw the cells routinely from liquid nitrogen storage. Rapid thawing was accomplished by melting the frozen cell suspension inside the cryogenic vial in a 40-50°C water bath. The melted cell suspension was then transferred to a 15ml centrifuge tube. 10ml of 10% fetal bovine serum (FBS) containing E/92/3 medium was added drop wise into the centrifuge tube. The cells were resuspended and transferred into two culture flasks for incubation. Cells were incubating in culture flasks for the attachment onto cells to the bottom of flask. After 12 hours, the culture medium in culture flasks was replaced. Subsequently, the culture medium was replaced again after 24 hours in order to promote the growth of the cells.

For freezing the cell line, epithelial cells were first harvested by trypsinizaton. The cells suspension were then centrifuged into pellets and resuspended in 3ml freezing medium. The freezing medium was prepared from adding 0.5ml dry dimethylsulfoxide (DMSO) into 9.5ml E92/3 medium with 10% FBS. Cells suspended in the freezing media were transferred into cryogenic vials, which were then embedded in a cotton-insulated box and cooled down stepwise to -70°C for 7-8 hours. Finally, the frozen cells were put into the *Nalgene® CANISTER* in liquid nitrogen tank for permanent storage.

The medium used for the culturing of the E/92/3 cell line was William's medium E, which was supplemented with 5% fetal bovine serum (FBS) , L-glutamine (1mM), penicillin (100i.u./ml), streptomycin (100μg/ml), hydrocorticone (10ng/ml), bovine insulin (100μg/ml), transferrin (10μg/ml), epidermal growth factor (0.1μg/ml) and sodium selenite (10ng/ml).

After culturing for 3 days, the cells in flasks would reach confluency and sub-culturing is essential. Media in culture flasks were discarded and another aliquots (1ml) of 0.25% trypsin/EDTA were added. Culture flasks were shaken gently for 1 minute to flush away any residual medium in culture flasks. After 1 minute, aliquots of trypsin/EDTA were discarded. Another aliquots (2ml) of trypsin were added and the flasks were stored at 37°C for 5-10 minutes. The detached cells in the flasks were transferred to centrifuge tubes. Then, 2ml 5% FBS containing E/92/3 medium was added to inhibit the further action of trypsin. In the same way, the remaining cells in the flasks were trypsinized until all the cells were removed from the flasks. The cell suspension in 15ml centrifuge tubes were spinned at 800X g for 3 minutes. Then, each pellet was disaggregated with 2 ml E/92/3 medium. The cell suspension was made up to 20ml with 5% FBS containing E/92/3 medium and splitted into 4 flasks for next passage.

II.2 Conventional short-circuit current (I_{sc}) measurement technique

II.2.1 Introduction

To study the active ion transport across the cultured equine sweat gland epithelia, conventional I_{sc} technique was employed. The technique was first developed by *Ussing* and *Zerahn* in 1951.

Under normal condition, when the equine sweat gland epithelia was bathing in a normal solution, a negative potential difference (*p.d.*) across the epithelia was detectd. The negative *p.d.* indicated the apical (luminial) side was more negative than the basolateral (serosal) side. This phenomenon was due to the active secretion of anion from basolateral to apical side. Besides, the presence of *p.d.* across the epithelia would provide an electrical gradient, which favoured the passive movement of Na^+ paracellularly to the apical side. If an external e.m.f. was applied across the epithelia to clamp a zero *p.d.* across the epithelia (*i.e.* short-circuited), the driving force for passive transport of sodium ion would be eliminated. A short-circuit current (I_{sc}) is therefore an index of active transport of ions across the epithelia. In our configuration, an upward deflection in I_{sc} is corresponded to the movement of anions from basolateral compartment to apical side, or cations from apical to basolateral side.

II.2.2 Permeable supports and electrodes for I_{sc} measurement

The permeable support for I_{sc} measurement was made up of a millipore filter membrane (type HAWP, 0.45μM pore size, Millipore Corporation, MA 01730, USA) and a silicon ring, which was made from Sylgard 184 clastomer kit (DOW Corning

Corp., USA). Silicon rings confined the filter area to 0.45cm^2 and form a well for seeding of cells. Rings were cut from a silicon plate by a double-barrel cutter and the ring was stuck onto millipore filters using Silastic® 3140 RTV adhesive (DOW Corning Corp., USA). Before seeding of cells on permeable supports, filters were sterilized by irradiated in UV box for 20 minutes (see Figure II.(a)).

During cell culture, the harvested cell pellet was resuspended and disaggregated by repeatedly pipetting before cell counting. The cell suspension was diluted to a final concentration of $4x10^5$ cells ml^{-1}. Sterile petri dishes were filled with 12 ml 5% FBS containing E/92/3 medium and 7-8 sterilized filters were allowed to float on the medium. Aliquots (0.25ml) of $1x10^5$ cells containing suspension were seeded carefully onto each well. The epithelial cells were then grown in an incubator with the temperature and gases composition maintained at 37°C and 95%O_2 + 5%CO_2 respectively. After 3 days, the epithelia would form tight confluent monolayers and available for experiment.

The electrodes were purchased from World Precision Instruments, INC, USA. Electrodes type 'EKV' are used to measure the *p.d.* across the epithelia and electrodes type 'EKC' are used to apply an external e.m.f. during experiment. Before these electrodes could be used, they needed to be filled with agar. The agarose solution was prepared by dissolving 3% (w/v) agarose into 3M KCl boiling solution. The agarose solution was filled into electrodes by suction with syringe. Assembled electrodes were cool down immediately by placing them in 3M KCl solution.

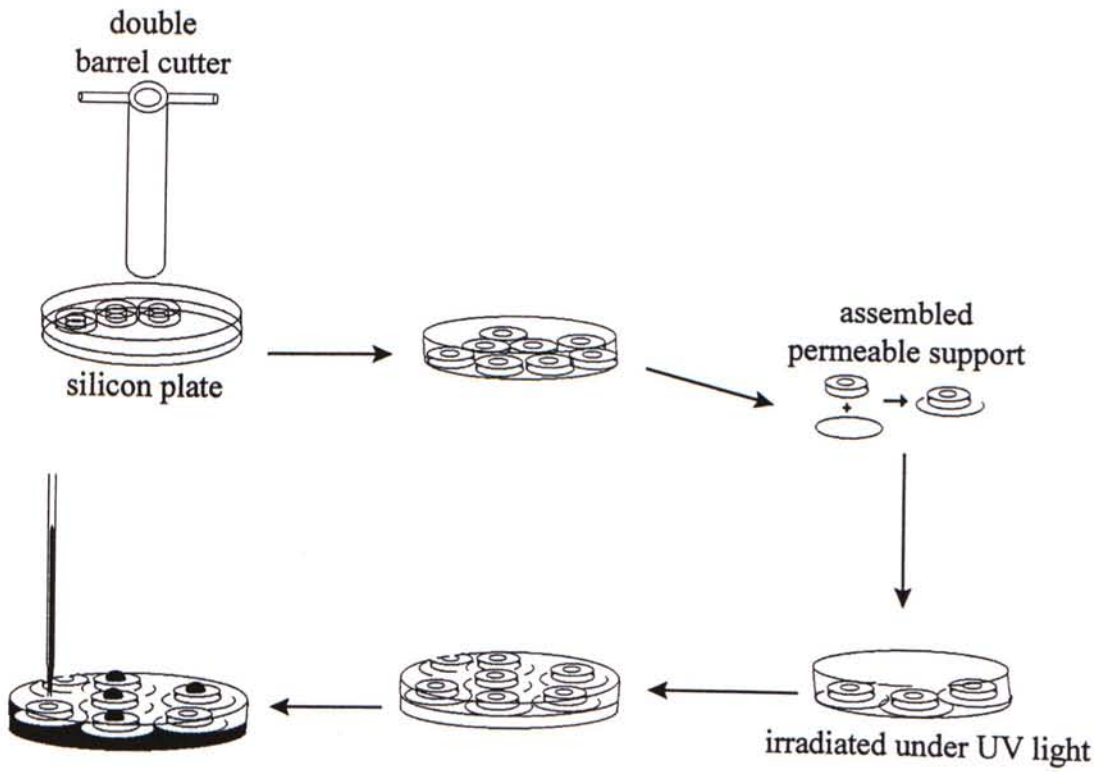

Figure II.(a)

Diagrammatic illustration for the preparation of permeable supports from adhesion of silicon ring and Millipore filter (0.45μm pore size) for conventional short-circuit current (I_{sc}) measurement and seeding of cells onto the permeable supports at $1X10^5$ cells/well. The cells were then allowed to grow for 3-4 days in incubator before experiment.

II.2.3. Experimental set up and measurement of I_{sc}

The set up of conventional I_{sc} measurement mainly comprised of 4 components (Figure II.(b)(A)).

(1). V/C amplifier (DVC-1000, World Precision Instruments Inc, USA) and preamplifier: They are used to amplify the *p.d.* across a monolayer by applying an external e.m.f. to clamp the epithelia at zero voltage. The change in I_{sc} was displayed continuously by an on-line chart recorder (Kipp and Zonen Delft, the Netherlands).

(2) *Ussing* chambers: The two halves of chambers were facilitated with insertions and pins/pinholes for inserting the electrodes and tubings and for mounting of the monolayer. During the experiment, the monolayer was placed on one halve of the *Ussing* chamber (C_2). The pins of another half (C_1) of the *Ussing* chamber pierced through the silicon ring of the filter and assembled with C_2 (Figure II.(b)(B)). The assembled chamber was then mounted on a stand and connected with electrodes and tubings before experiment.

(3) Apical and basolateral bathing solutions (Kreb's Henselnit solution (KH solution)) were maintained at 37°C by a water jacket and the solution was gassed with 95%O_2 + 5%CO_2 for maintaining a high O_2 content and a physiological pH (*i.e* pH=7.4). Drugs can also be added to the bathing solution of either side without affecting another side since the apical and basolateral solutions were well-separated.

(4) Electrodes: Type 'EKV' were used to measure the *p.d.*. Electrode connected to apical side was assigned as 'V_2', and basolateral side was assigned as 'V_1'. V_2 and V_1 were plugged into two insertions at a closer distance to the monolayer. Electrodes of type 'EKC' were assigned as 'I_2' and 'I_1'. I_2 and I_1 were

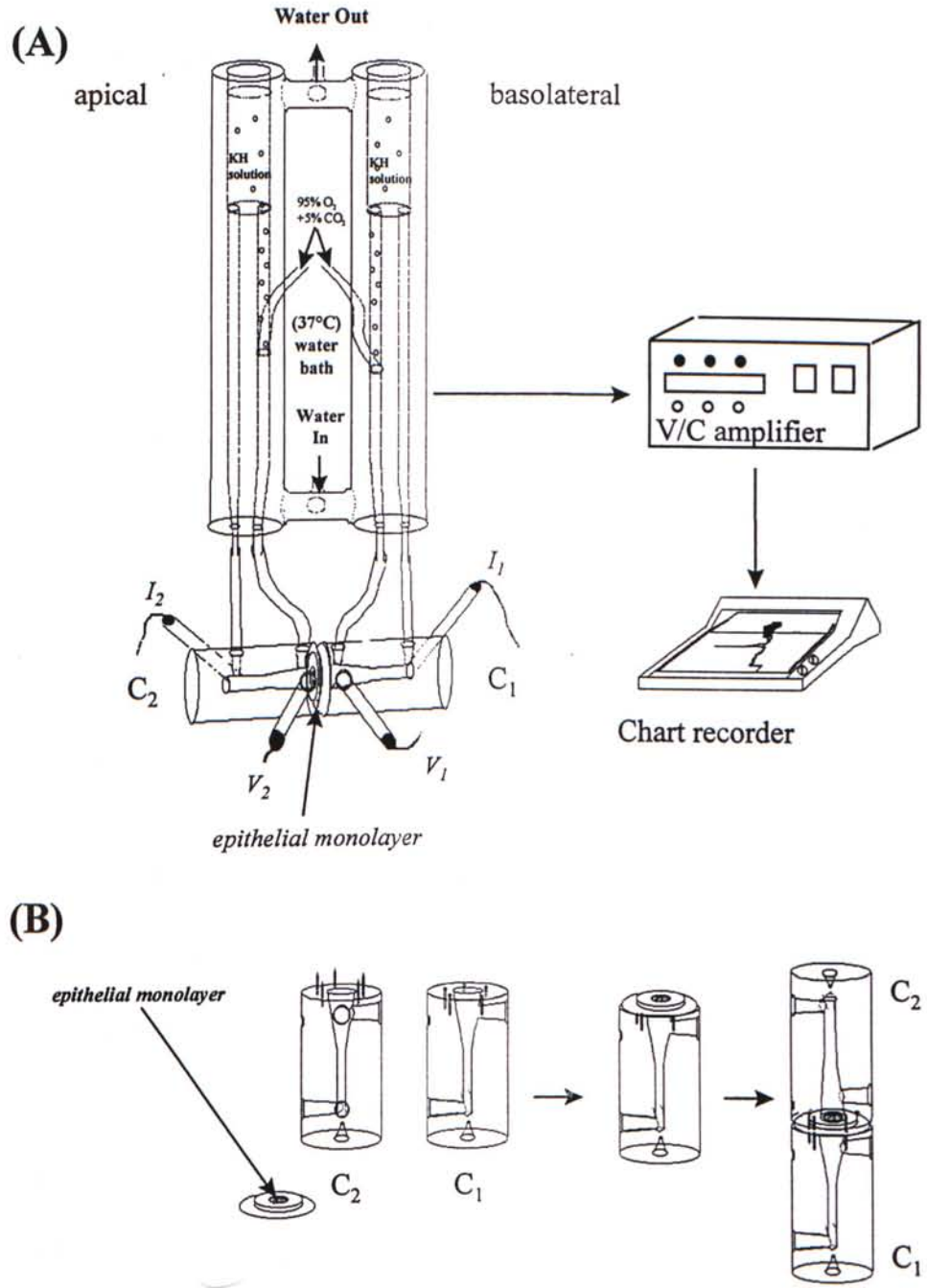

Figure II.(b)

(A) Diagrammatic illustration for the set up of I_{sc} measurement. The assembled chamber was then mounted horizontally on a stand and connected with electrodes (V_1 & V_2; I_1 & I_2) and tubings for experiment. The change in I_{sc} (ΔI_{sc}) was measured by the voltage/current clamp amplifier and recorded on the chart recorder. **(B)** Assemble of the epithelial monolayer between the two halves of *Ussing* Chamber (C_1 & C_2) during experiment. The position of the epithelial monolayer was fixed by the pins piercing through the silicon ring of the permeable support.

plugged into the insertions at the remote end for providing an evenly-distributed e.m.f. on the monolayer.

II.2.4. Measurement of I_{sc} during experiment

Prior to experiment, the intrinsic *p.d.* of electrodes and fluid resistance should be nullified. The *p.d* and fluid resistance were offset to zero by adjusting the knobs on the V/C amplifier. After 10-15 mins., the *p.d.* and fluid resistance would be steadily maintained at zero. Then, the two halves of chamber (C_2 and C_1) were disassembled for clamping of a monolayer between them before experiment.

During each experiment, transepithelial resistance (R_t) was strictly monitored. R_t can indicate the confluency and tightness of an epithelia (equation shown below). R_t was monitored by applying a small e.m.f. (*i.e.* 0.1-1mV) intermittently for 1 sec. The applied ΔV would induce a change in I_{sc} (ΔI_{sc}). Action of various drugs on a monolayer could be continuously displayed from the tracings on chart recorder. The change in I_{sc} measured from the V/C amplifier was showed as μA on the chart recorder. Practically, the unit of ΔI_{sc} was converted into $\mu A/cm^2$ for data input.

Equation: Transepithelial Resistance, (R_t) = e.m.f. applied (ΔV) / change in I_{sc} (ΔI_{sc})

II.3 Measurement of intracellular free calcium ($[Ca^{2+}]_i$) by microspectroflurimetic techniques

II.3.1. Preparation of cells

Before plating of epithelial cells on glass coverslips for $[Ca^{2+}]_i$ measurement, the coverslips were sterilized by dipping in 90% ethanol and flamed over a bunsen burner.

As described previously, cells suspension from cell culture were diluted and aliquots (0.8ml) of suspension containing $1x10^5$ cells were seeded onto a 25mm glass coverslip. After 6 hours, the culture medium droplet on the coverslips were replaced. Cells were then allowed to grow for 1-2 days before experiment.

II.3.2. The set up and procedures for experiment

Experimental set up for $[Ca^{2+}]_i$ measurement:

The set up for measuring $[Ca^{2+}]_i$ mainly comprised of the following parts:

(1). Xenon arc lamp, which can provide a continuous spectrum and high intensity light source;

(2). Chopping device, which can alternate the excitation light through two separate filters (*e.g.* 340nm and 380nm for Fura-2);

(3). Inverted microscope (Nikon ECLIPSE 300) equipped with fluorescent optics (20x and 40x Nikon Fluor objectives, extra long working distance);

(4). Dichroic mirror is used to reflect the short wavelength excitation light (340&380nm) into the objective. The emission light of longer wavelength (510nm) is allowed to pass through the mirror to eye piece or image detector;

(5). Photon Multiply Tube (PMT) is selected for the detection system, since it is cost effective, has highly sensitivity and has low background noise when compared with other detection systems. The measurement of fluorescent by PMT is achieved by summing and smoothing the photon currents detected from the PMT for producing a steady current, which is converted to voltage and digitized through an analog to digital (A to D) converter.

(6). Miscellaneous accessories include a software: ***FeliX***$_{\text{version 1.11}}$ (Photon Technology Internal Inc., NJ 08852, USA) and an interface card, (PTI RatioMaster Fluorescence System). The interface card is installed in the computer for data acquisition and data analysis. Others include an inline solution heater (Clark Electromedical Instruments, England) and heater controller (*TC-344A* Dual Heater Controller, Warner Instrument Corp., Hamden, CT 06514, USA). They are used to maintain the temperature of perfusing saline at 37°C precisely. The perfusion chamber (RC-21BR, Warner Instrument Corp.) uses coverslips at both the top and bottom to enclose the bath area. The distance between the top and bottom coverslips is 2.5mm and the bath volume is 260µl. The chamber have two inlet ports for perfusion and one outlet to drain away excess solution.

Procedures for $[Ca^{2+}]_i$ measurement during experiment:

During dye loading, the culture medium in petri dish was discarded and replaced with 2ml Ringer solution. Then, 6µl of 1mM Fura-2/AM was mixed with equal volume of pluronic acid (0.53mM) for better dispersion of the dye on cell's surface. The mixture was added into the solution and incubated for 40 minutes.

After dye loading, coverslips with cells was rinsed with normal ringer solution. Coverslip was adhered to the chamber by smearing small amount of 'Apiezon' Grease (M & I Materials LTD, Manchester, England). The sample containing coverslip was placed on the bottom and added with a droplet of saline. The top of chamber was enclosed by another coverslips and bubbles in the chamber were removed. The chamber was fixed and sealed by a plateform with clamping screws (Figure II.(c)). Under the view of microscope, cell patches with 4-5 cells were selected. The area of for measurement was confined by adjusting the diaphragm at the side port connected to photon multiply tube (PMT). Prior to experiment, background fluorescence was assessed by measuring an empty area on the coverslip. After deduction from the background fluorescence, the chamber was returned to the original position for experiment. Administration of drugs was accomplished by the combination of 3-way valves, a valve driver, perfusion tubing and a perfusion pump. During experiment, the intensities of emission from 340nm and 380nm excitations and the fluorescence ratio (R_f) were continuously displayed *via* the computer monitor. Event marks can be added for recording the change of perfusing solutions/drugs. A change in $[Ca^{2+}]_i$ could be reflected by a change in the R_f of Fura-2 (excitation wavelengths of Fura-2 = 340/380 nm; emmission wavelength of Fura-2 = 520 nm), which was detected from cells loaded with this dye and this allows changes in $[Ca^{2+}]_i$ to be measured.

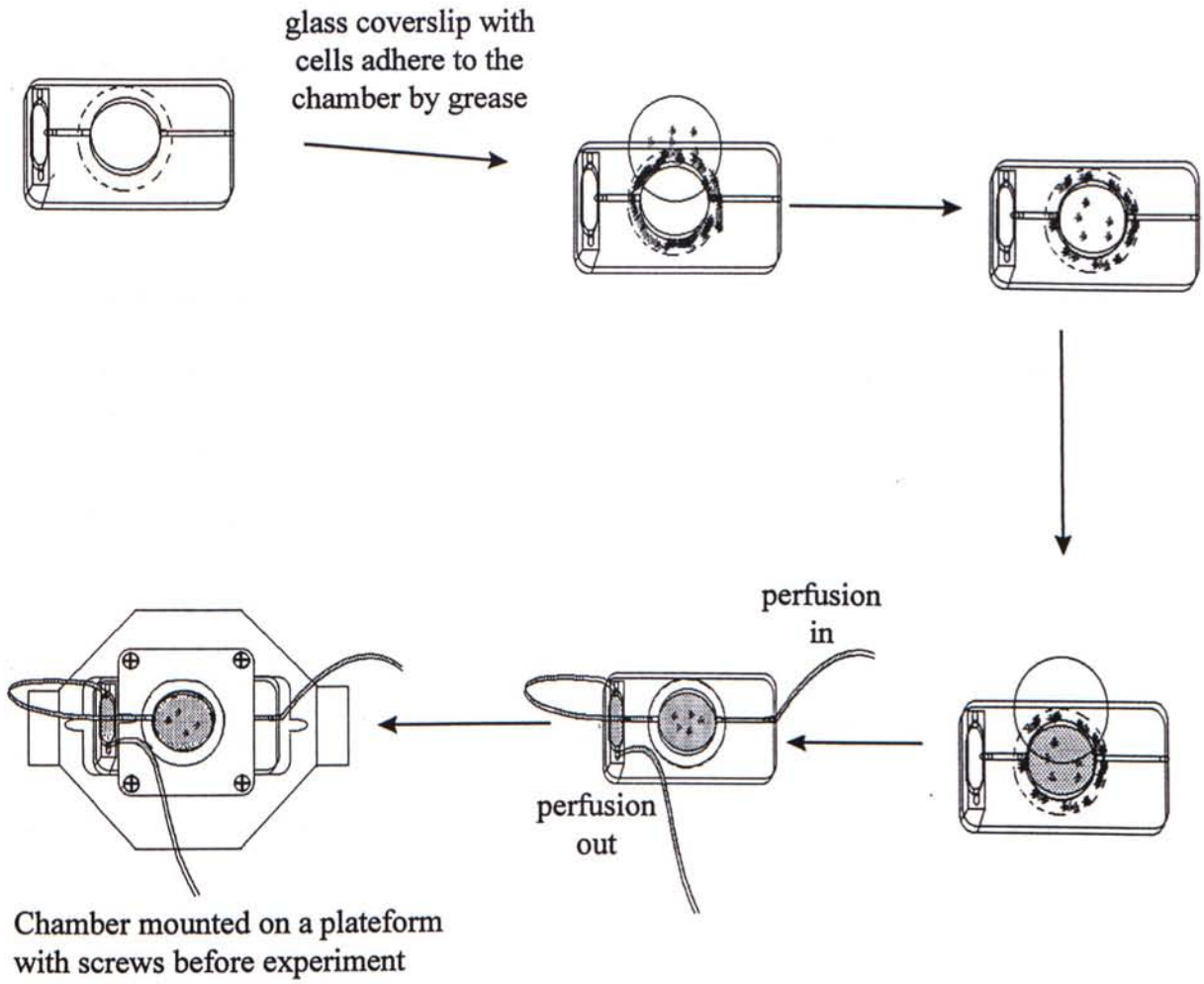

Figure II.(c)

Assemble of the perfusion chamber for microfluorometric study of cytosolic free calcium $[Ca^{2+}]_i$. Glass coverslip grown with patches of epithelial cells was adhered to the bottom of the chamber with grease, and the upper surface of the chamber was enclosed with another coverslip to confine the volume of perfusate (260μl). The assembled chamber was then fixed onto a platform with screws and connected with perfusion tubings prior to experiment.

II.4. Simultaneous measurement of changes in R_f and I_{sc}

II.4.1. Experimental set up and manipulation

Simultaneous measurement method was firstly developed in 1995 (Paradiso *et al.* 1995). This latest technique could simultaneously study two of the most important parameters of an epithelia (*i.e.*(i) ionic secretion and (ii) cytosolic Ca^{2+} level). In figure II.(d)(A), the simplified schematic diagram for the set up was illustrated.

As described previously, the measurement of R_f was achieved by the PTI RatioMaster Fluorescence System. Together with a special design miniature *Ussing* chamber (Zoophysiological Laboratory A, August Krogh Institute, Unversity of Copenhagen, Denmark), which allows bathing solutions to perfuse separately in apical and basolateral side. The chamber featured with mini-insertions of electrodes and salt bridges for I_{sc} measurement, together with inlets and outlets at both sides to facilitate the perfusing system (Figure II.(d)(B)). The bottom of chamber was water-sealed by adhering a 29mm diameter glass coverslip onto it with melted dental sticky wax. In a simultaneous measurement experiment, bicarbonate buffered KH solution is used. Therefore, the perfusing solution should be constantly bubbled with 95% O_2 & 5% CO_2 to maintain the pH at 7.4. For better conductance of electrodes, agar bridges were inserted into openings at basolateral side and were pumped gently with a syringe until small amount of agar was squeezed out from the opening. Excess agar was flushed away with deionized water, while another end was cut into a desirable length and connected with electrodes of V_1 and I_1 by means of saturated KCl solution. Agar bridges of apical side (V_2 & I_2) were simply dipped into the apical surface of the bathing solution. Similar to previous procedures in conventional I_{sc} ,

(A)

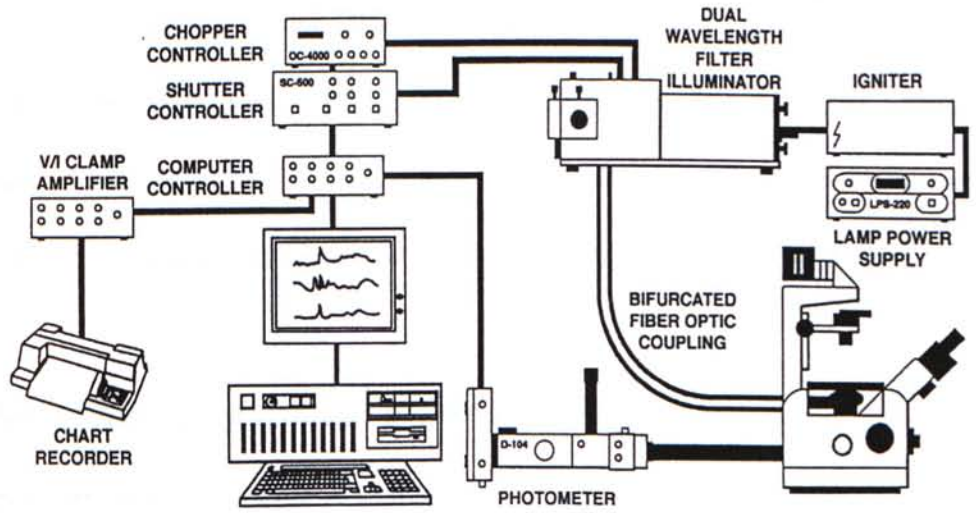

(B)

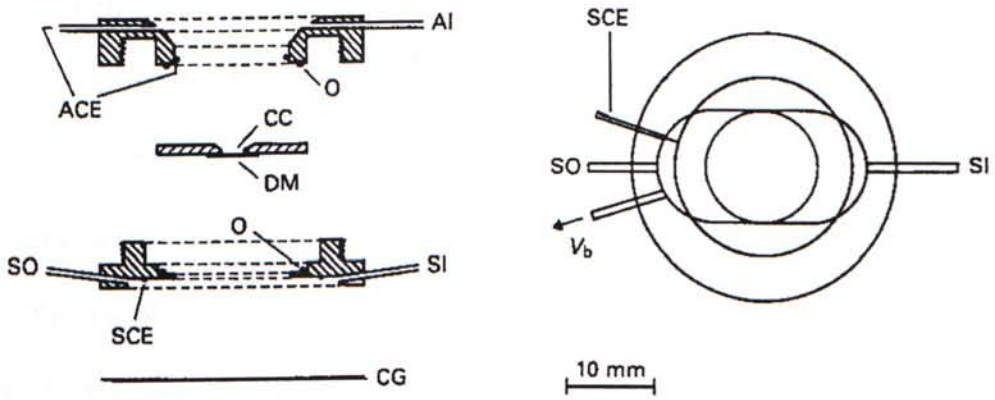

Figure II.(d)

(A) Set up modified from conventional I_{sc} method and microspectrofluorimetry for simultaneous measurement. Signals from V/C amplifier and PMT were simultaneously captured and digitized *via* an analog/digital converter, which were then continuously monitored by the computer. **(B)** Diagrammatic illustration of the miniature *Ussing* chamber used in the simultaneous measurement. (AI, apical inlet; O, O-ring; SI & SO, serosal inlet and outlet respectively; CG, coverglass; ACE & SCE, apical/serosal current electrode; CC, culture wafer for growth of epithelial cells; V_b, electrode for measuring (*p.d*).(Adopted from Larsen *et al.* 1989)

the *p.d.* and fluid resistance across electrodes V_2 & V_1 were offset to zero. Prior to experiment, background fluorescence of a blank filter needed to be estimated. For background correction, the intensities of emission from 340 and 380nm measured from a filter loaded with 3μM Fura-2 was subtracted before experiment.

II.4.2. Other preparations before experiment

Preparation of permeable supports

The permeable support used was made up of a *Transwell*® -COL membrane (24mm diameter, 0.4μM pore size, Corning Costar Corp., Cambridge) and a plastic wafer with 3.4mm internal diameter. The *Traswell*®-COL membrane was cut from its plastic support with scalpel and was divided into 4 pieces (Figure II.(e)(A)). The filter was stuck onto a wafer by Silastic® 3140RTV adhesive (Dow Corning., USA). Filters were then allowed to dry and were coated with 1% (v/v) collagen (VITROGEN (3mg/ml) 100®, Collagen Biochemicals, CA 94303 USA) for better attachment of epithelial cells. The coated filters were irradiated under UV light for sterilization. The sterilized filters were then rinsed with culture medium thoroughly to neutralize the acidity remained on filters after treated with collagen. Filters were then placed in 6-well plate with sterilized 'V-shaped' glass rods as support. Subsequently, each well were filled with 3ml E/92/3 medium and metal rings were placed above the filters to confine the area for cell seeding (Figure II.(e)(B)).

Seeding of cells

Cell suspensions were diluted to $2x10^5$ cells/ml and aliquots (100μl) of cell suspensions were seeded carefully onto each filter membrane through the metal ring. After 24 hours, the metal rings and glass supports were removed from the wells and culture media were replaced. Due to the transparent properties of the filter, the

(A)

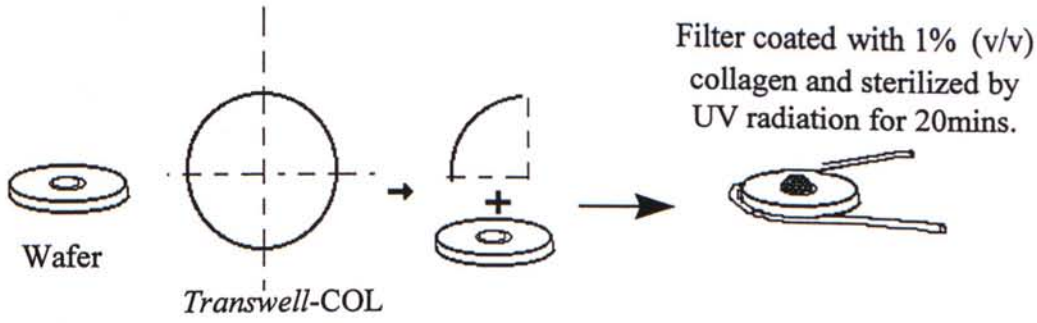

(B)

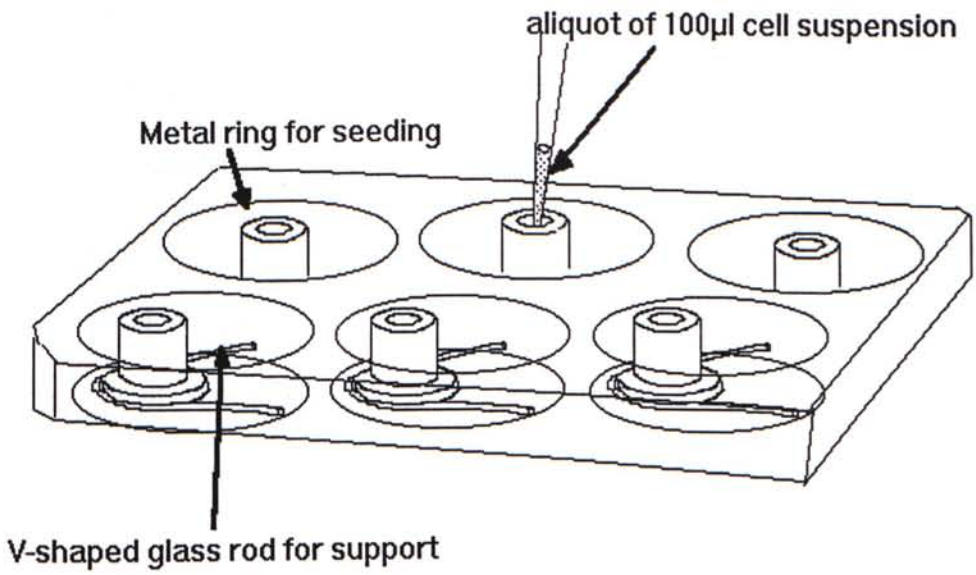

Figure II. (e)

(A) Diagrammatic illustration for the preparation of permeable support for simultaneous measurement. *Transwell*®-Col membrane (24mm diameter, 0.4µM pore size) were cut into four smaller pieces and carefully stuck onto a wafer (inner area: 0.091cm^2). The assembled wafers were then coated with collagen (1% v/v) and irradiated under UV light for sterilization. **(B)** V-shaped glass rod was used to support the wafer in the culture medium, with metal rings used to confine the area for seeding. Aliquots (100µl) of 2X10^4 cells containing cell suspension was added onto each wafer. The metal rings and glass rods were removed and culture media were replaced in each well after 24 hours. Monolayer reached confluency after culturing for 3 days.

confluency of cells could be monitored under an conventional inverted microscope. After 3-4 days culturing, the epithelial cells would form a confluent monolayer and ready for experiment. The formation of a tight and confluent monolayer would be a crucial step for measurement.

Dye loading

Similar to cells grown on glass coverslip for $[Ca^{2+}]_i$ measurement, 3μM of Fura-2/AM, together with 1.6μM pluronic acid (F-127) were loaded into the cells by incubating for 60 minutes in a incubator maintained at 37°C. Unfortunately, Fura-2 molecules would be continuously leaked out from cells at highest rate when cells were superfused in 37°C saline during experiment (Kao, 1994). To circumvent this problem, 2.5mM probenecid (an inhibitor of uric acid transport) was added during dye loading, in order to minimize the leakage of Fura-2 from cells (Kao, 1994). Probenecid was prepared by dissolving in a alkaline solution (0.5M NaOH) and then titrated with phosphate buffer (pH 5.7) until the pH had reached 7.4.

After dye loading, the filter membrane was rinsed with KH solution and the filter membrane was then placed on the basolateral half of the miniature *Ussing* chamber. Apical half of the chamber was assembled carefully until a water sealed compartment was formed in the basolateral side. The chamber was facilitated with O-rings to ensure bathing saline of both side was superfused separately. Subsequently, the assembled chamber was mounted on the stage of the inverted microscope, with the perfusing tubings and agar bridges connected. Meanwhile, the bathing solutions of both sides began to superfuse, and the change in I_{sc} was measured by a V/C amplifier (VCC600; Physiological Instrument, San Diego, USA). The output signal from V/C amplifier was diverted to a chart recorder and the inputs terminal of an

analog to digital converter. The PTI RatioMaster Fluorescence System digitized the input signals captured from V/C amplifier and the PMT tube. The fluorescence signals emitted from cells was detected by a Fluor objective (40X extra long working distance), from a area containing 40-50 cells.

II.5. Material and solutions used for experiment

II. 5.1. Culture media and enzyme

The cultured equine sweat gland cell line's (E/92/3) medium was prepared from William's medium E, and the supplement were indicated as followings: fetal bovine serum (FBS) (5% v/v), L-glutamine(1mM), penicillin (100i.u./ml), streptomycin (100μg/ml), bovine insulin (100μg/ml), hydrocortisone (100ng/ml), transferrin (10μg/ml), epidermal growth factor (0.1μg/ml) and sodium selenite (5ng/ml). The enzyme used for trypsinization was 0.25% trypsin/EDTA (0.05mM). All of these chemicals were supplied by Gibco Laboratories (N.Y., U.S.A.).

II.5.2. Chemicals and Drugs

The following drugs were supplied by Sigma Chemical Co. (St. Louis, MO, USA): 4,4'-disothiocyanatostibene-2,2'-disulfonic acid (DIDS), bumetanide, bradykinin, ADP, 5-Br-UTP, ionomycin, pertussis toxin (Ptx) and probenecid.

ATP, UTP were purchased from Pharmacia Biotech as Ultra-pure 100mM stock solution.

UDP and hexokinase (15,000u/5ml) were obtained from Boehringer (Mannheim, Germany).

Hexokinase treatment:

In order to remove the contaminating nucleoside triphosphates from nucleoside diphosphates, hexokinase treatment was necessary to purify these commercially available UDP and ADP (Nicholas *et al.* 1996; Harden *et al.* 1997).

Reaction:

nucleoside triphosphate + glucose $\xrightarrow{\text{hexokinase (10 i.u./ml)}}$ nucleoside diphosphate + glucose-6-phosphate

Hexokinase (10 i.u./ml) was used to catalyze the above reaction using glucose (22mM) as one of the substrates. Subsequently, nucleoside diphosphates were prepared as 10mM stock solution and were stored at -20°C.

The fluorescence probes (Fura-2/AM (acetoxymethyl ester form) Fura-2 (free acid form) and pluronic acid (P-127) were supplied by Molecular Probes (Eugene, OR, USA).

Thapsigargin *(Tg)*, 1,2 - bis (*o*-amino phenoxy)ethane-*N,N,N',N'*-tetraacetic acid (acetoxymethyl ester form) (BAPTA/AM) and 4-Br-A23187 were ordered from Calibiochem (CA, USA).

Diphenylamino-2-carboxylate (DPC) was purchased from Riedel-de Haen Chemicals, D-30926 (Seelze, Germany).

Sodium chloride, potassium chloride, sodium hydrogen phosphate, and potassium dihydrogen phosphate were obtained from Merck, (Darmstadt, Germany). Sodium bicarbonate, magnesium chloride and sodium dihydrogen phosphate were from BDH Limited (Poole, England). Sodium hydroxide from ProLabo, Paris. ADP, AMP, adenosine, D-glucose, N-methyl-D-glucamine (NMDG) and N-2-hydroxethypiperazine-N'-2-ethanessulfonic acid (HEPES) and choline were ordered from Sigma (St. Louis, MO, USA).

II.5.3 Preparation of solution for experiments

The composition of solution(s) used in short-circuit current (I_{sc}), $[Ca^{2+}]_i$ and simultaneous measurements were listed below:

(a) Normal Kreb's Henselnit solution (KH solution)(with Ca^{2+}/ nominal Ca^{2+} free KH*);
(b) Sodium free solution;
(c) Ringer solution (with Ca^{2+}/ nominal Ca^{2+} free*) (see Table II.5.(a) for detail)

Concentration in mM	Kreb's-Henseleit (KH)	Sodium free	Ringer solution
NaCl	117	-	130
$NaHCO_3$	24.8	-	-
$MgCl_2$	1.2	1.2	1
$MgSO_4$	-	-	-
KCl	4.7	4.7	5
KH_2PO_4	1.2	1.2	-
$CaCl_2$	2.56	2.56	2.5
D-glucose	11.1	11.1	10
NMDG Cl	-	117	-
Choline HCO_3	-	24.8	-
HEPES	-	-	20
Osmolality	283 mosmol/kg	283 mosmol/kg	280 mosmol/kg

(∗:nominal Ca^{2+}-free solution of KH solution and Ringer solution were prepared by omitting Ca^{2+} from the solution.)

Table II.5.(a). Composition of solutions used in conventional I_{sc} experiments and microfluorospectrometry

II.6. Statistical Analysis

The change in I_{sc} (ΔI_{sc}) was measured from the difference between the initial value and peak value of I_{sc} and was expressed as μA cm^{-2}. The change in $[Ca^{2+}]_i$ of microfluorospectrometric studies was expressed as fluorescence ratio (R_f). Cumulative concentration-response relations were analyzed with a non-linear curve fitting by a logistic equation (Grafit; Erithacus Software limited), and EC_{50} values were determined as the drug concentration causing a half-maximal response in I_{sc} or R_f. A level of probability of $p<0.05$ obtained from Student's unpaired *t*-test was considered as significant when comparing two groups. The means of more than two groups were compared by one way analysis of variance followed by Scheffe's multiple comparison test.

Chapter III Results

III.1. Effects of nucleotides on transepithelial ion transport

III.1.1. Basic electrophysiological properties of cultured equine sweat gland epithelia

Sweat gland epithelial cells grown on Millipore filters would reach confluency and form tight monolayers after culturing for 3-4 days. Under the light microscope, a confluent monolayered cells was observed. Apically located microvilli, junctional complexes, cytoplasmic filaments, mitochondria and the prominent nuclei were clearly observed in electron micrograph (Ko *et al.* 1996*a*). Transepithelial resistance (R_t = 421±16 Ωcm^2; N=150) of each epithelial monolayer was strictly monitored during experiment. A set-up potential difference of about -0.1 mV (apical side negative) and a small basal current of +0.3 $\mu A\ cm^{-2}$ was usually observed.

III.1.2. Short-circuit current (I_{sc}) induced by nucleotides

In order to establish the extent to which nucleotides are able to regulate ion transport in these epithelia, the I_{sc} technique was used. Each epithelial monolayer was only challenged once throughout the experiment unless otherwise stated. Change in I_{sc} (ΔI_{sc}) refers to the difference between the peak of a response and the basal I_{sc}. Each data point represented the means of ± S.E.M. for 4-10 separate epithelia.

Administration of ATP to apical bathing solution evoked a rapid and transient increase in I_{sc}, which returned to basal level gradually within 4-5 minutes (Figure

III.1(a)). The magnitude of the ATP-induced I_{sc} at apical side was found to be dose-dependent, with EC_{50} at 11.5±0.9μM (Figure III.1(c)). However, applications of ATP to basolateral side could only induce tiny and variable responses (Figure III.1.(a)& (b)). Obviously, these data strongly indicated that the P_{2Y}-nucleotide receptor(s) were predominantly located at the apical membrane. Due to this phenomenon, studies were focused on apically located P_{2Y}-nucleotide receptors.

A summary of dose-response curves were shown in figure III.1.(c). The EC_{50} of UTP was 2.2±0.3μM, while that of ATP was 11.5±0.9μM. These data suggested that the epithelia were approximately five times more sensitive to UTP than ATP. At maximal concentration tested, the magnitude of UTP and ATP induced I_{sc} were similar. Apart from ATP and UTP, the dose-response curves of 5-Bromo-UTP (an analogue of UTP) , ADP and UDP were also constructed. The estimated EC_{50} of 5-Bromo-UTP (2.8±0.3μM) was similar to that of UTP. ADP was a less effective nucleotide, and its EC_{50} could not be estimated. All the epithelia tested were insensitive to adenosine mono-phosphate (AMP) or adenosine (data not shown) which rules out the possibility of the existence of adeosine (P_1) receptors on the epithelia. According to this pharmacological profile, which strongly suggests P_{2Y2}(P_{2U}) receptors are expressed on the equine epithelia (Dubyak *et al.* 1993). In fact, the existence of P_{2Y2} (P_{2U})-receptor on the equine epithelia was already proposed in previous studies (Ko *et al.* 1994; Wilson *et al.* 1996; Ko *et al.* 1997).

On the other hand, UDP was also capable of evoking the increases in I_{sc} in a dose-dependent manner, with EC_{50} at 1.2±1.3μM. At 100μM, the magnitude of UDP-induced I_{sc} was found to be smaller than that of ATP or UTP (Figure III.1.(c)). In these experiments, we demonstrated that nucleoside diphosphates such as ADP and

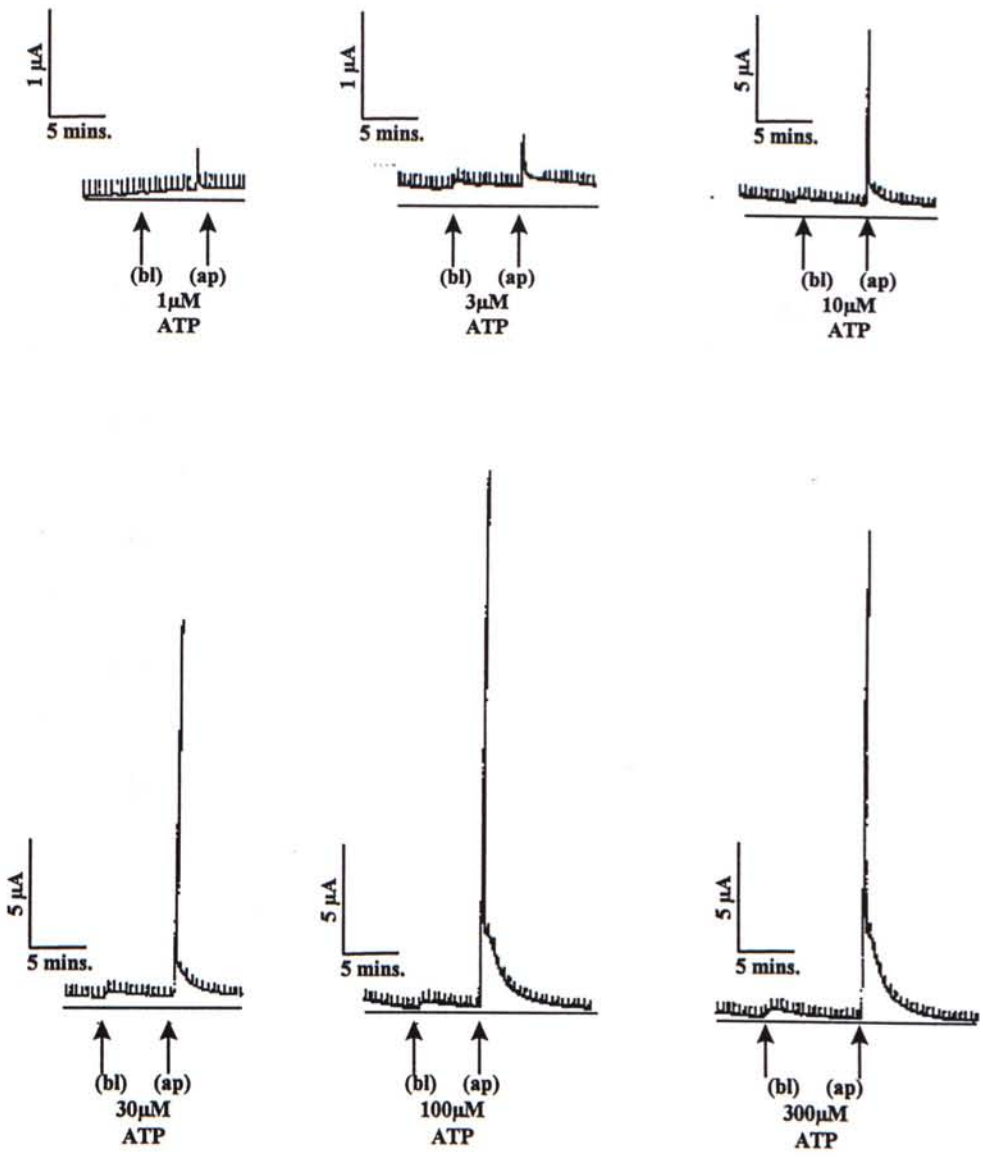

Figure III.1.(a)

Effects of ATP upon I_{sc}. Each panel shows a continuous record of I_{sc} made from a separate epithelial monolayer in which ATP was first added to the bathing solution of basolateral aspect of the cell layer (bl) and then to the apical side of the bathing solution. The final concentrations of ATP were 1µM, 3µM, 10µM, 30µM, 100µM and 300µM. The horizontal line in each record indicates the zero current. The current deflections in each tracing were result of intermittently clamping an external e.m.f. at 0.1-0.5mV. Calibration bars for 1µM and 3µM are obtained from higher gain.

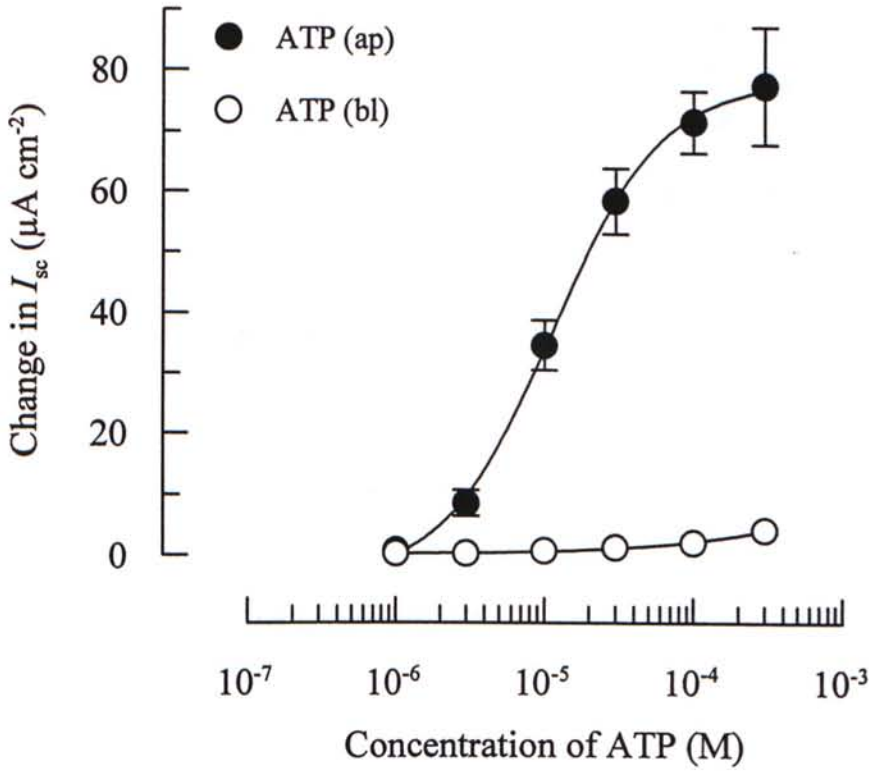

Figure III.1.(b)

Summarized dose-responses for the I_{sc} induced by adding ATP to apical (ap) or basolateral (bl) solution. Data are means ± S.E.M. for 4-6 separate epithelia.

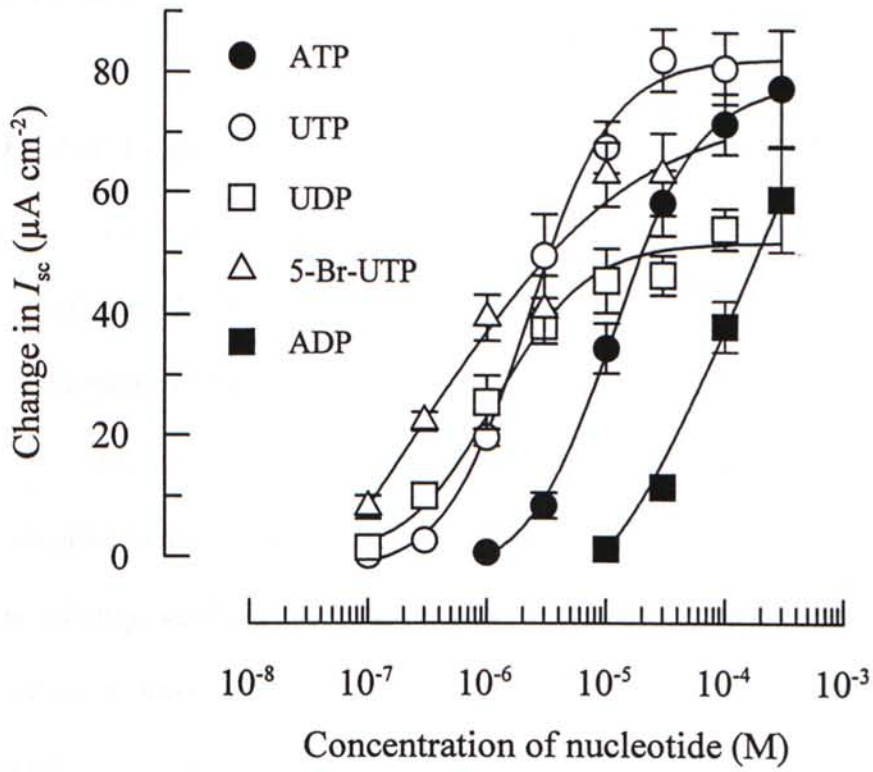

Figure III.1.(c)

Summarized dose-responses for the I_{sc} induced by adding different nucleotides to the apical bathing solution and the resultant increases in I_{sc} were quantified and plotted against the concentration of nucleotides used. Half maximal effective concentration (EC_{50}) of each agonist was estimated from the curve fitted above. Data are means ± S.E.M. for 4-8 separate epithelia.

UDP were able to mediate the cellular responses in the sweat gland epithelia. However, a previous $[Ca^{2+}]_i$ study had reported that UDP and ADP were unable to induce any detectable response (Ko *et al.* 1997). The contradictory findings between I_{sc} and $[Ca^{2+}]_i$ measurements would suggest the polarized cells grown on permeable supports may express different P_2-receptors.

III.1.3. Identification of ion species responsible for the change in I_{sc}

The previous I_{sc} experiments had demonstrated that the electrogenic ion secretion mediated by ATP in cultured equine epithelia was predominantly involved in chloride and bicarbonate secretion (Ko *et al.* 1997).

However, Na^+ reabsorption could not be excluded if the ion secretion is sensitive to amiloride: a Na^+ channel blocker (Kleyman *et al.* 1988). To rule out this possibility, epithelia were apically pretreated with 100μM amiloride, followed by apical addition of 100μM ATP. According to figure III.1.(d), pretreatment of amiloride (N=4) did not cause any significant (P>0.05) reduction to the ATP-induced I_{sc} (amiloride pretreated: 63.5±6.1μA cm^{-2} *Vs* control: 60.7±4.8μA cm^{-2}). The ineffectiveness of amiloride pretreatment could exclude the possibility of Na^+ reabsorption. Meanwhile, an ion substitution experiment was carried out to further confirm the ATP-induced I_{sc} was independence on extracellular Na^+. When apical solution was replaced with Na^+-free solution, the response of ATP (N=6) was unaffected (P>0.05) (control:56.1±4.1μA cm^{-2} *Vs* Na^+-free: 75.2±8.1μA cm^{-2}).

The involvement of other basolateral components of nucleotides-induced I_{sc} were studied by basolateral pretreatment of 100μM bumetanide ($Na^+/2Cl^-/K^+$ cotransporter inhibitor) or 5mM barium (K^+ channel blocker). Referring to figure

III.1.(d), basolateral pretreatment of the epithelia with 100μM bumetanide (N=4) could significantly ($P<0.05$) reduce the ATP-induced I_{sc} (bumetanide treated: 65.6±6.5μA cm^{-2} *Vs* control: 117.9±12.9μA cm^{-2}). Similarly, basolateral pretreatment of 5mM Ba^{2+} (N=9) could also significantly ($P<0.05$) reduce the ATP-induced I_{sc} (Ba^{2+} treated: 37.7±4.8μA cm^{-2} *Vs* control: 63.1±2.0μA cm^{-2}). These data suggests the basolaterally-located $Na^+/2Cl^-/K^+$ cotransporter and K^+ channels are responsible for the ATP-induced I_{sc}.

III.1.4. Effects of chloride channel blockers on UTP induced I_{sc}

To characterize the ion channels responsible for the nucleotides-induced I_{sc}, two chloride channel blockers (DIDS and DPC) were tested. The epithelia were first treated apically with one of the two blockers (DIDS or DPC) at the apical solution, followed by application of UTP at 100μM after 10 minutes. In control experiment, the epithelia were treated with essentially same volume of dimethyl sulfoxide (DMSO). The effectiveness of each blocker were calculated and expressed as percentage of inhibition to the UTP-induced I_{sc} (see Figure III.1.(f)).

As shown in figure III.1.(e), DIDS was a more effective compound to abolish the UTP-induced I_{sc} than DPC, with IC_{50} at 31.7±4.8μM. DPC was a less effective compound, and its IC_{50} could not be estimated since the highest dose tested (*i.e.* 3mM) could not completely inhibit the UTP-induced I_{sc}. The inhibitory profile suggested the Ca^{2+}-dependent chloride channels are predominantly responsible for the anion secretion initiated by P_{2Y}-nucleotide receptor (Yamaya *et al.* 1996).

In short, these data clearly demonstrated that ATP and related compounds were able to induce the increases in I_{sc} in the equine sweat gland epithelia. In the first

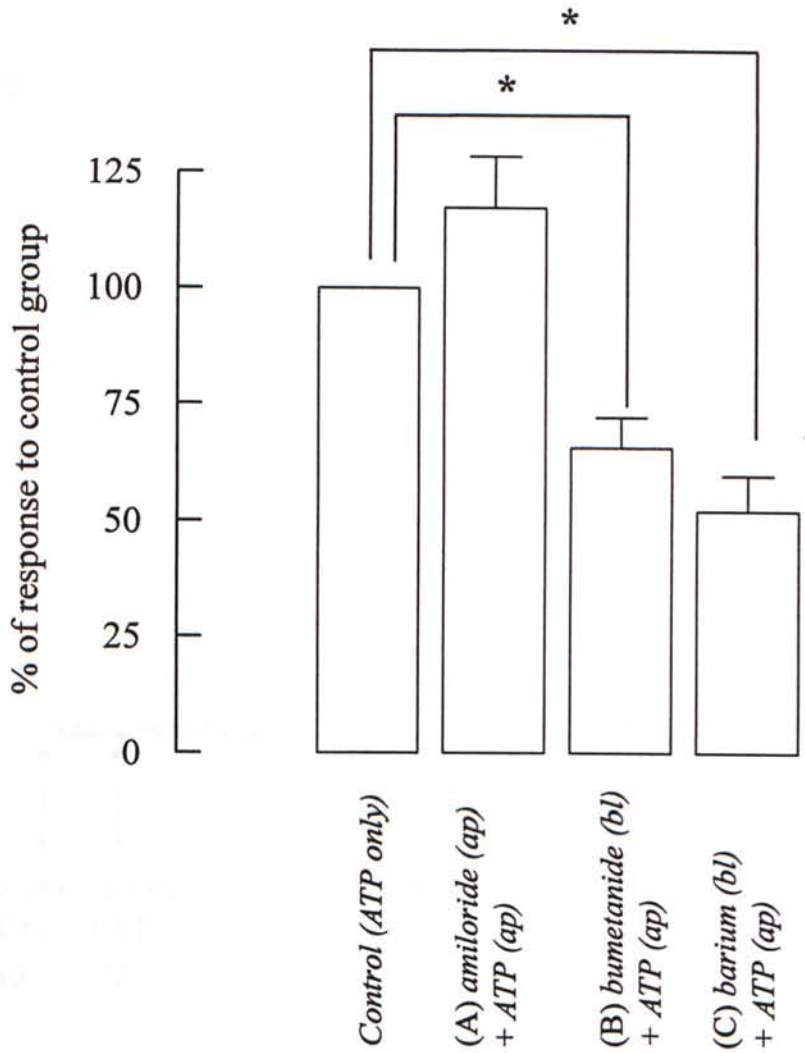

Figure III.1.(d)

Effects of pretreatment of **(A)** amiloride 100μM (ap); **(B)** bumetanide 100μM (bl) or **(C)** Ba^{2+} 5mM (bl) on the increases in I_{sc} induced by apical application of ATP at 100μM. Note the ineffectiveness of amiloride pretreatment on the ATP-induced I_{sc}. Columns and bars are means ± S.E.M. for 6-10 separate epithelia. * $P<0.05$ compared with control group.

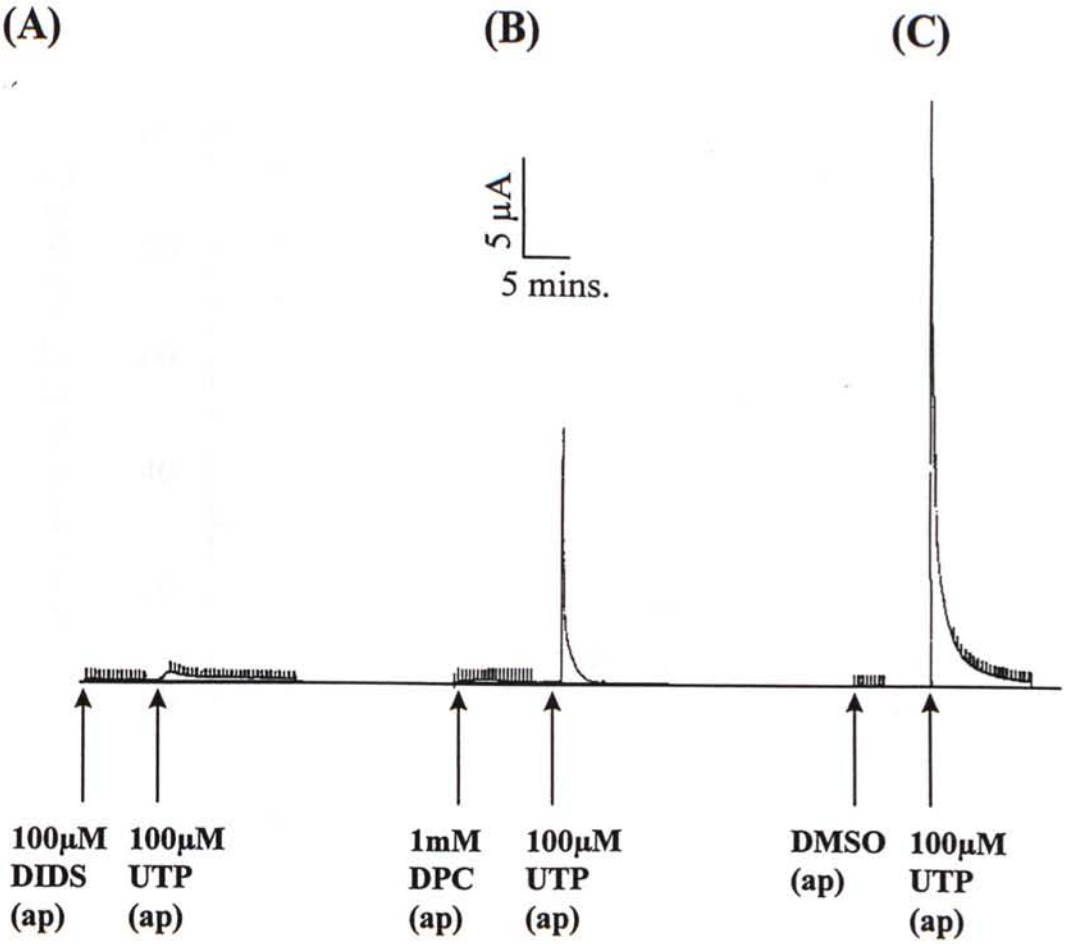

Figure III.1.(e)

I_{sc} recordings with arrow markings indicate the application time for the pretreatment of Cl^- channel blockers **(A)** 100μM DIDS, **(B)** 1mM DPC and **(C)** DMSO (control) on I_{sc} induced by apical (ap) application of UTP at 100μM. The horizontal line in each record indicates the zero current. Essentially identical responses were obtained in 4-6 epithelia.

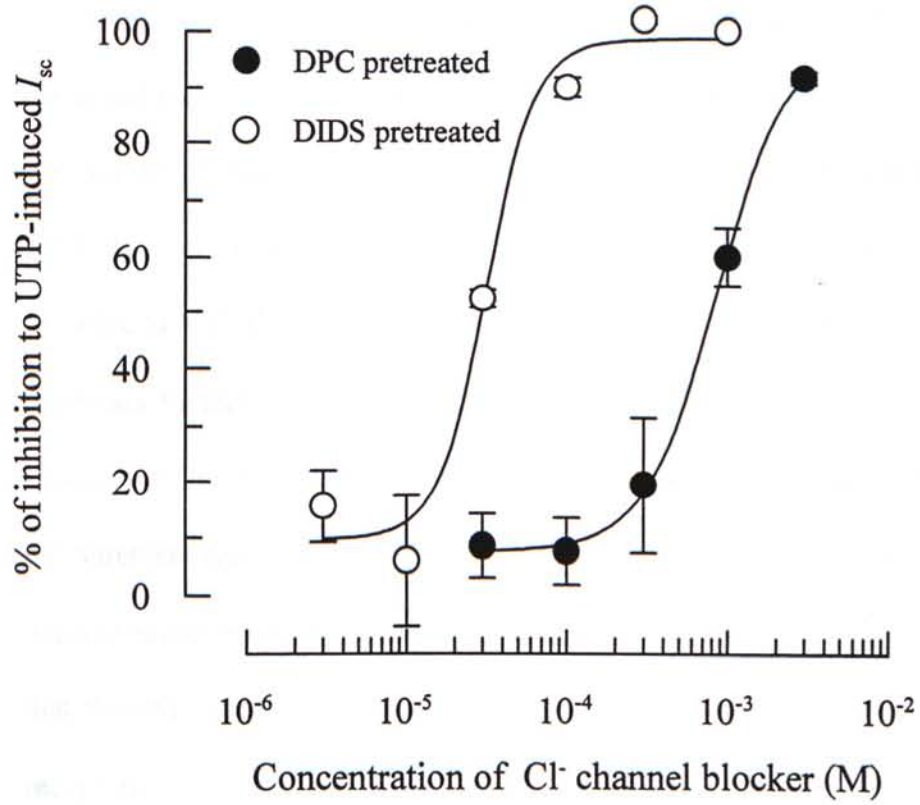

Figure III.1.(f)

Dose-dependent effects of apical addition of DIDS and DPC on the I_{sc} induced by apical addition of 100μM UTP. The percentage of inhibition to UTP-induced I_{sc} was derived from the formula $(I_{CONTROL}-I_{BLOCKER})/I_{CONTROL}$ X100%, where $I_{CONTROL}$ is the current response in control condition and $I_{BLOCKER}$ is the current magnitude obtained in the presence of a blocker. Half maximal inhibitory concentration (IC_{50}) for DIDS was estimated from the curve fitted above. Data are means ± S.E.M. for 4-6 separate epithelia.

set of experiments, we found that the nucleotides-induced I_{sc} were predominantly initiated by the apically confined P_{2Y}-nucleotide receptors. The activation of the P_{2Y}-nucleotide receptor would initiate the Cl^- secretion *via* the DIDS-sensitive, Ca^{2+}-dependent chloride channels. According to our data, ATP and UTP were able to initiate the increases in I_{sc}, thus suggesting that P_{2Y2}-receptor subtype is existing in the apical membrane (Dubyak and El-Moatassim, 1993). The expression of the P_{2Y2} subtype on this cell line was also consistent with other previous studies (Ko *et al.* 1994; Wilson *et al.* 1996; Ko *et al.* 1997). Of interest, the epithelia were more sensitive to UTP than to ATP. This is not entirely consistent with the hypothesis that responses to these nucleotides are simply mediated *via* P_{2Y2} receptors. Moreover, although ADP and UDP were unable to elicit any significant response in $[Ca^{2+}]_i$ measurement (Ko *et al.* 1997), these nucleoside diphosphates were able to elicit the definite responses during I_{sc} measurement. Such contradictory findings may indicate that the cells grown on glass coverslips and membrane filters may express different receptors.

III.2. Signal transduction mechanisms of P_{2Y}-nucleotide receptors

III.2.1. The involvement of G_i-proteins

P_{2Y} receptors belong to a structurally homologous group of receptors characterized by seven membrane spanning domains (Dubyak and El-Moatassim, 1993), which are all able to interact with a group of membrane proteins known as guanine-nucleotide-binding (G-proteins) for mediating different cellular responses. Previous studies in other cell types had revealed that $P_{2Y2}(P_{2U})$ receptors mediated responses could be inhibited by pertussis toxin (Ptx) (Cockcroft and Stutchfield,1989; Dubyak and El-Moatassim, 1993). An immunochemical study in the equine (E/92/3) cell line had detected the expression of two subunits of G_i-protein ($G_{i\alpha1}$ & $G_{i\alpha2}$) (Wilson *et al.* 1996). Meanwhile, the $[Ca^{2+}]_i$ study on the same cell line had demonstrated that the UTP-induced increases in $[Ca^{2+}]_i$ consisted of a Ptx-sensitive component and a Ptx-resistant component (Wilson *et al.* 1996).

In the present study, the inhibitory effect of Ptx was studied by replacing the culture media of the epithelial monolayers with 100ng ml^{-1} Ptx containing culture media for 24 hours prior to experiment. The effect of Ptx on ATP, UDP or UTP induced I_{sc} were assessed by comparing with control cells. For control group, the culture media were also replaced in the same manner to ensure that simply disturbing the cells did not affect their sensitivity.

Referring to figure III.2.(a), the ATP-induced I_{sc} was significantly reduced after the Ptx pretreatment. Data analysis showed that Ptx could significantly inhibit the increases in I_{sc} induced by ATP from 3μM to 300μM. Similar to ATP, the

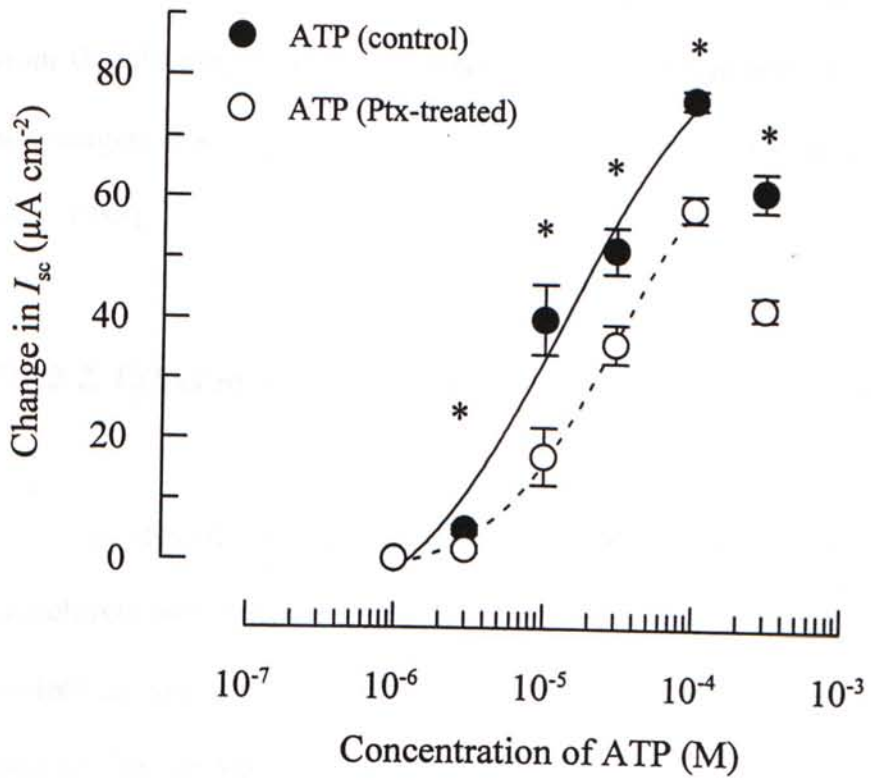

Figure III.2.(a)

Effects of pertussis toxin (Ptx)(100ng ml^{-1}) upon the ATP-evoked increase in I_{sc}. Responses of ATP were quantified and plotted against the concentration of ATP used. Data from both control (solid line) and Ptx-treated (broken line) cells at identical passenge are presented as means ± S.E.M. for 4-8 separate epithelia. * $P<0.05$ compared with control group.

increases in I_{sc} induced by UDP (Figure III.2.(b)) and UTP (Figure III.2.(c)) were also significantly reduced in the same fashion.

The inhibitory effect of Ptx on the nucleotide-induced I_{sc} was consistent with the previous $[Ca^{2+}]_i$ study which had demonstrated the involvement of G_i-protein subunits for the P_{2Y2} receptor coupled signalling pathway (Wilson *et al.* 1996). Apart from G_i subunits, the Ptx- insensitive I_{sc} components induced by these nucleotides was suggested to be predominantly mediated through the α-subunit of $G_{q/11}$ (Dubyak *et al.* 1988).

III.2.2. Effect of BAPTA on the increases in I_{sc} induced by nucleotides

To study the involvement of $[Ca^{2+}]_i$ in mediating the increases in I_{sc}, epithelial monolayers were pretreated with BAPTA/AM for 30 minutes before the addition of nucleotides into the apical solution. BAPTA/AM is a commonly used intracellular calcium chelator which can presumably abolish any cellular responses mediated by the $[Ca^{2+}]_i$-dependent pathway. The preliminary data revealed that the increases in $[Ca^{2+}]_i$ induced by ATP were essentially abolished by BAPTA/AM.

As shown in figure III.2.(d), the UDP-induced I_{sc} (N=10) (BAPTA-treated: 17.2±2.7μAcm^{-2} *Vs* control: 51.3±4.2μAcm^{-2}) and UTP-induced I_{sc} (BAPTA-treated: 9.3±0.7μAcm^{-2} *Vs* control: 31.6±3.0μA cm^{-2}) were both significantly reduced ($P>0.05$). The profound inhibitory effect of BAPTA on the increases in I_{sc} could provide a strong evidence for the involvement of $[Ca^{2+}]_i$. However, it still remained unclear for the mechanism underlying the increases in I_{sc} induced by UDP and UTP after treated with BAPTA.

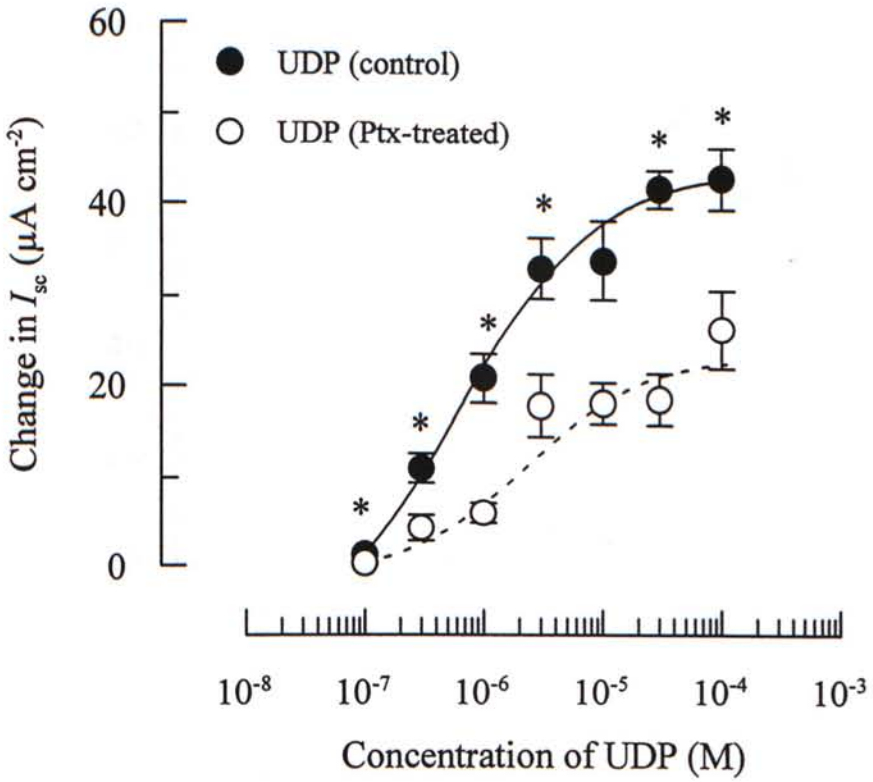

Figure III.2.(b)

Effects of pertussis toxin (Ptx)(100ng ml^{-1}) upon the UDP-evoked increase in I_{sc}. Responses of UDP were quantified and plotted against the concentration of UDP used. Data from both control (solid line) and Ptx-treated (broken line) cells at identical passenge are presented as means ± S.E.M. for 3-6 separate epithelia. * $P<0.05$ compared with control group.

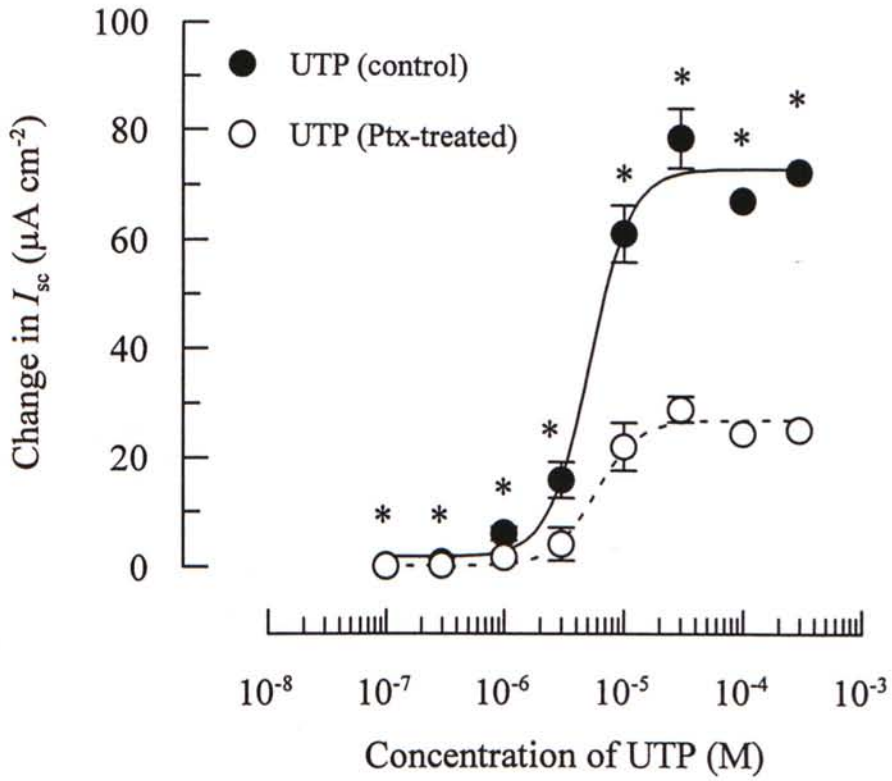

Figure III.2.(c)

Effects of pertussis toxin (Ptx)(100ng ml^{-1}) upon the UTP-evoked increase in I_{sc}. Responses of UTP were quantified and plotted against the concentration of UTP used. Data from both control (solid line) and Ptx-treated (broken line) cells at identical passenge are presented as means ± S.E.M. for 4-8 separate epithelia. * $P<0.05$ compared with control group.

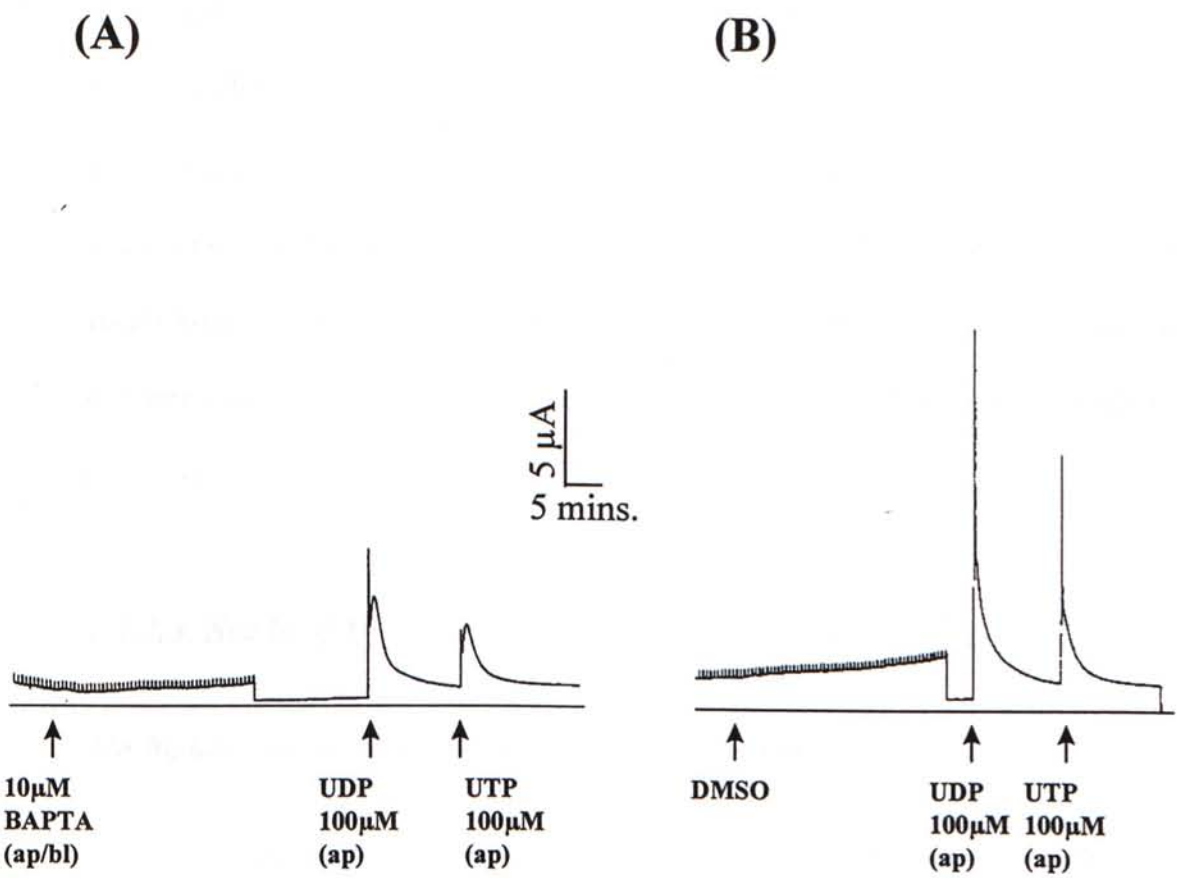

Figure III.2.(d)

I_{sc} recordings with arrows marking indicate the time of applications for the pretreatment of **(A)** 10μM BAPTA on apical and basolateral solutions (ap/bl) and **(B)** DMSO (control) on I_{sc} induced by apical (ap) application of UDP followed by UTP at 100μM. The horizontal line in each record indicates the zero current. Essentially identical responses were obtained in 10 separate epithelia. Calibration bar applied to both traces.

To further confirm the effect of BAPTA/AM, five-fold higher concentration (*i.e.* 50μM) was used, and similar findings were obtained. For epithelia treated with 50μM BAPTA, the ATP-induced I_{sc} (N=6) was reduced by 73.1±5.1% (from 65.1±6.9μA cm^{-2} to 17.5±3.3μA cm^{-2}). UDP-induced I_{sc} (N=6) was found to be more sensitive to BAPTA, which was reduced by 92.8±2.1% (control: 42.3±5.5μA cm^{-2} *Vs* BAPTA-pretreated: 3.1±0.9μA cm^{-2}) (Figure III.2.(e)). Data analysis found that the difference in sensitivities to BAPTA of ATP and UDP was statistically significant ($P<0.05$).

III.2.3. Study of P_{2Y}-receptor mediated increase in $[Ca^{2+}]_i$

The biphasic nature of Ca^{2+} response mediated by ATP

To investigate the nature of cellular responses activated by extracellular nucleotides, a microspectrofluorimetric technique was employed. In short, cells grown on coverslips were loaded with Fura-2/AM for the measurement of fluorescence ratio (*i.e.* 340nm/380nm (R_f)). R_f is an index which can reflect the $[Ca^{2+}]_i$ level. Under normal conditions, application of ATP could elicit a definite elevation in $[Ca^{2+}]_i$ level. The R_f rapidly shot up to a definite peak, which declined gradually to a sustainable plateau phase (Figure III.2.(f)). If external Ca^{2+} was removed, ATP could only elicit the initial transient increase in R_f. Once extracellular Ca^{2+} was replenished, ATP was capable of inducing another sustainable elevation in $[Ca^{2+}]_i$. This phenomenon strongly suggested that the ATP-induced R_f could be divided into two phases. The initial phase was attributed to the release of Ca^{2+} from internal stores, whereas the latter phase was due to the entry of Ca^{2+} from extracellular fluid (Boeynaems *et al.* 1996).

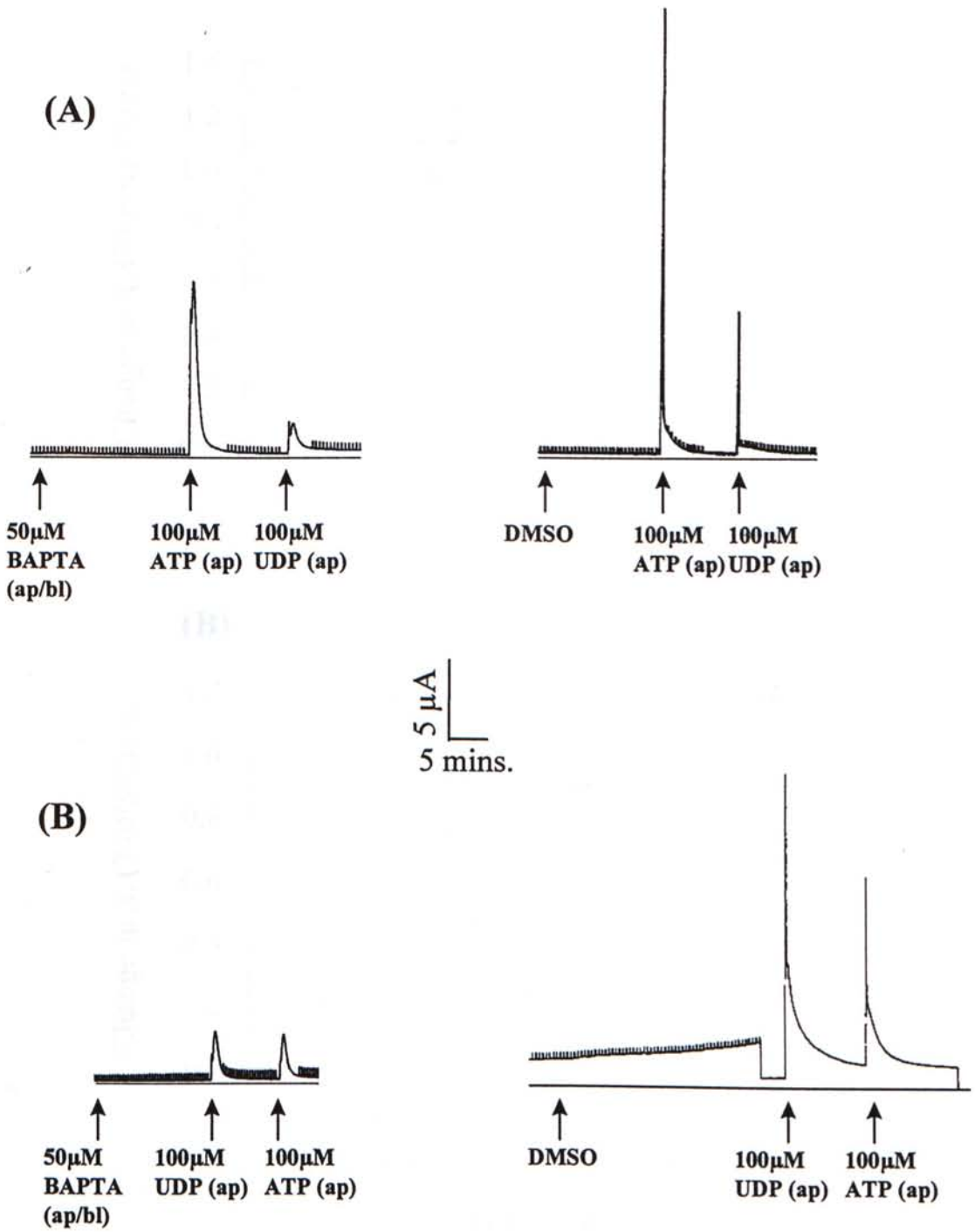

Figure III.2.(e)

I_{sc} recordings with arrows marking indicate the time of applications for the pretreatment of 50μM BAPTA or same volume of DMSO on **(A)** I_{sc} induced by apical (ap) application of UDP followed by ATP at 100μM or **(B)** *vica versa*. The horizontal line in each record indicates the zero current. Essentially identical responses were obtained in 6-8 separate epithelia for panel A and B respectively. Calibration bar applied to both traces.

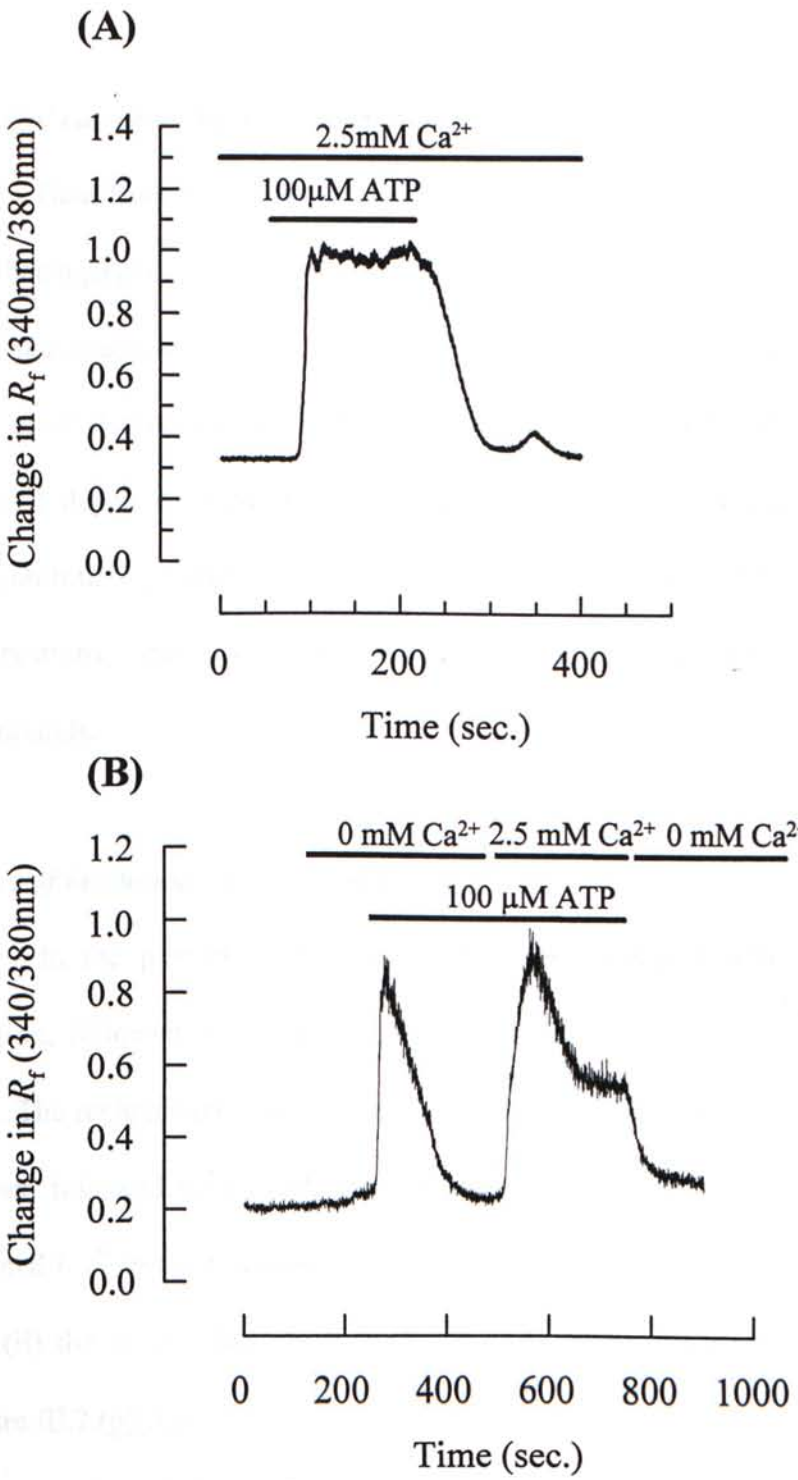

Figure III.2.(f)

Resolution of the increase in $[Ca^{2+}]_i$ induced by ATP into two phases. **(A)** Cells were perfused with normal Ringer solution and exposed to 100μM ATP. **(B)** Cells were initially perfused with Ca^{2+}-free solution and then exposed to 100μM of ATP until the R_f returned to basal level. Once $[Ca^{2+}]_i$ had returned to basal level, external Ca^{2+} was subsequently replenished (2.5mM) as shown. Essentially identical records were obtained in 4-6 separate experiments. Horizontal bars represent the duration of application of drugs/solutions.

Effect of calcium channel blockers on Ca^{2+} entry

Data from the previous experiments on the same cell line had demonstrated that thapsigargin (*Tg*) could induced a sustainable increase in I_{sc} (Ko *et al.* 1996*b*). *Tg* is a pharmacological tool which can inhibit the Ca^{2+}-ATPase of endoplasmic recticulum (Brayden *et al.* 1989). Unequivocally, the *Tg*-induced I_{sc} was attributed to a $[Ca^{2+}]_i$-dependent pathway. In the previous study, the increases in I_{sc} induced by *Tg* was inhibited by lanthanum (La^{3+}) or flufenamate (Ko *et al.* 1996*b*). Based on these observations, the nucleotide-induced Ca^{2+} entry was studied by these two compounds.

Effect of lanthanum on Ca^{2+} entry

In the present study, cells were first challenged with ATP in Ca^{2+} free solution, followed by replenishment of external Ca^{2+} together with applications of La^{3+}. The replenishment of extracellular Ca^{2+} would induce a second increase in R_f to a peak, followed by a steady plateau phase. The inhibitory effect of La^{3+} on ATP-induced Ca^{2+} entry was assessed by (i) the % of inhibition to the peak increase in R_f and (ii) the % of inhibition to increase in R_f during the steady plateau phase (see Figure III.2.(g)(A)).

At 0.1μM (N=3), the inhibitory effect of La^{3+} to the initial peak or the latter plateau were found to be statistically insignificant ($P>0.05$) (Figure III.2.(g)(B)).

At 1μM (N=3), the inhibitory effect of La^{3+} to the initial peak or the latter plateau were also statistically insignificant ($P>0.05$) (Figure III.2.(g)(C)).

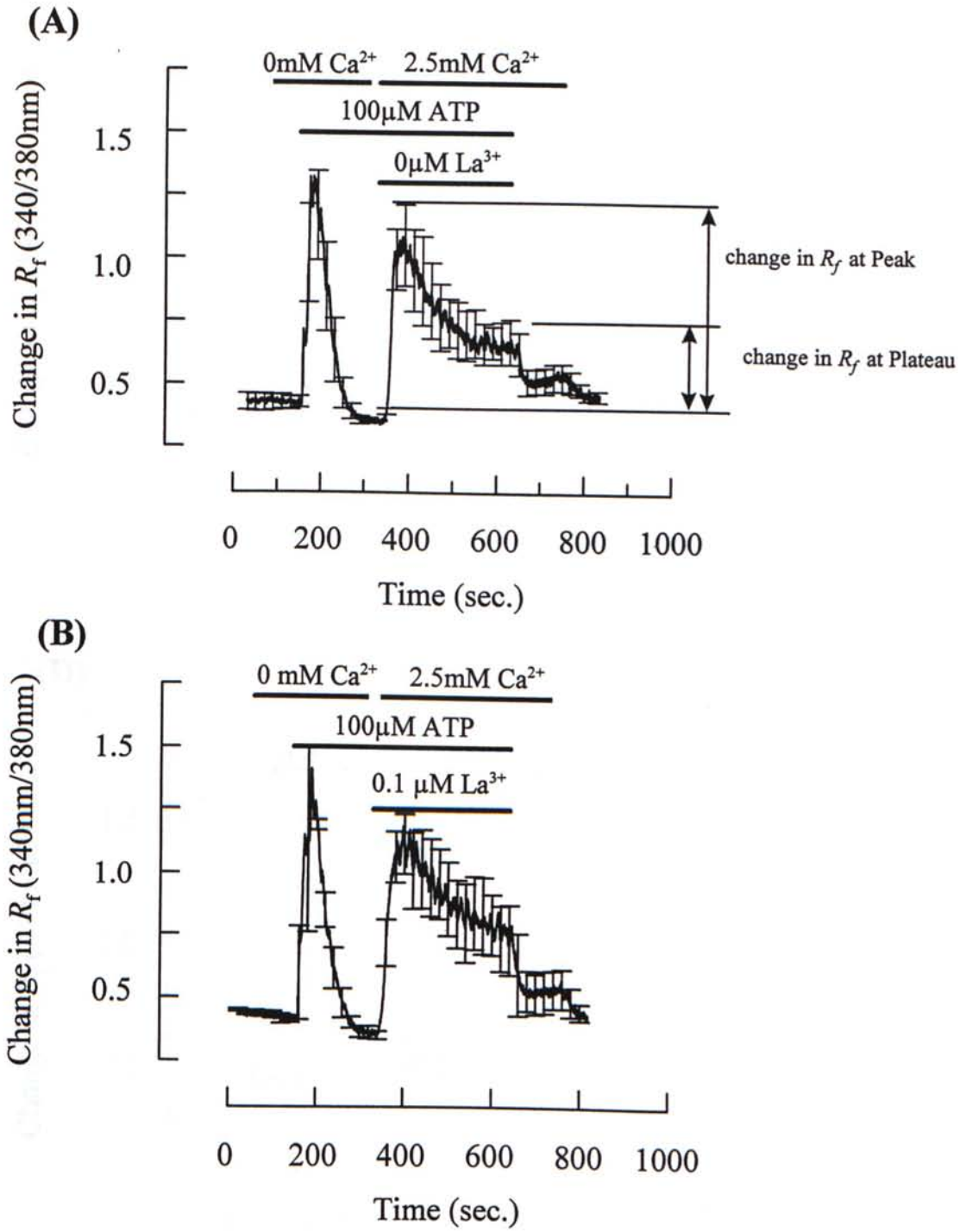

Figure III.2.(g)

Effect of lanthanum (La^{3+}) at **(A)** 0μM (control) and **(B)** 0.1μM on the Ca^{2+} entry induced by 100μM of ATP. La^{3+} was subsequently added together with external Ca^{2+} to the bathing solution after the initial increase in R_f returned to basal value. The percentage of inhibition to ATP-induced Ca^{2+} entry at *peak* and *plateau* were derived from the formula $(R_{CONTROL}-R_{lanthanum})/ R_{CONTROL}X100\%$, where $R_{CONTROL}$ is the fluorescence ratio (R_f) measured in control condition and $R_{lanthanum}$ is the R_f measured in the prescence of La^{3+}. Data are means of ± S.E.M. for three separate experiments. Horizontal bars represented the duration of application of drugs/solutions.

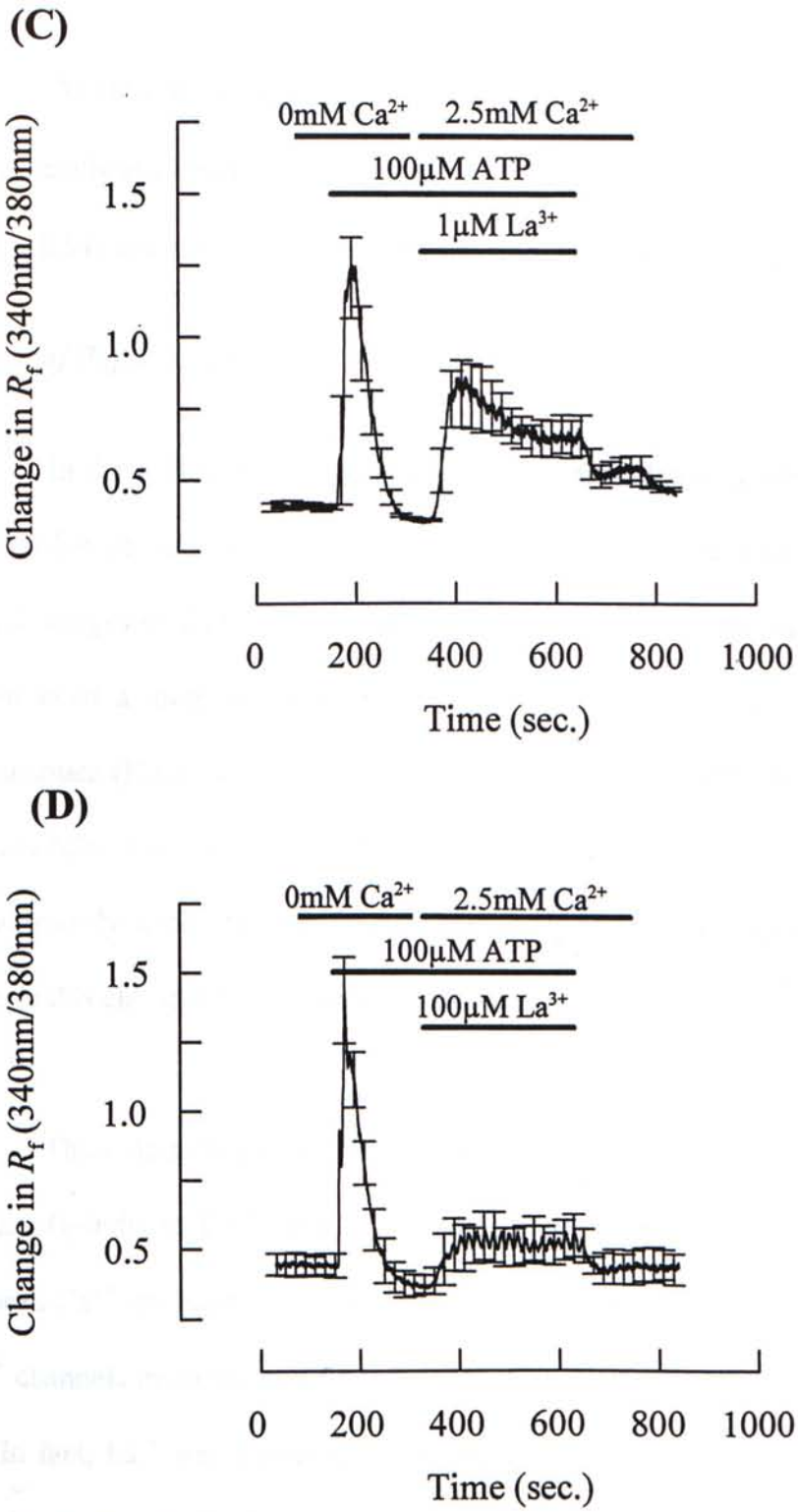

Figure III.2.(g)

Effect of lanthanum (La^{3+}) at **(C)** 1μM (control) and **(D)** 100μM on the Ca^{2+} entry induced by 100μM of ATP. La^{3+} was subsequently added together with external Ca^{2+} to the bathing solution after the initial increase in R_f returned to basal value. Data are means of ± S.E.M. for three separate experiments.

At 100μM of La^{3+}(N=3), the change in R_f (ΔR_f) at the peak (0.22±0.06) was significantly reduced by 71.7±7.4% (P<0.05). However, the ΔR_f at the latter plateau (0.15±0.04) was not significantly reduced (P>0.05) (Figure III.2.(g)(D)).

Effect of flufenamate on Ca^{2+} entry

In the following protocol, flufenamate was added only after the onset of the sustainable plateau phase. It was mainly based on the data from a previous study, which suggested that the application of flufenamate after the onset of a response could exert a more profound inhibitory effect than pretreating the epithelia with flufenamate (Ko *et al.* 1996*b*). Referring to figure III.2.(h)(B), the replenishment of extracellular Ca^{2+} would initiate the R_f increase by 0.70±0.15 to a peak level. Subsequently, application of 100μM flufenamate (N=4) could significantly (P<0.005) reverse this elevated $[Ca^{2+}]_i$ plateau by 69.8±3.0%.

These data from $[Ca^{2+}]_i$ measurement were consistent with the previous study of the *Tg*-induced Ca^{2+} entry (Ko *et al.* 1996*b*). The similar sensitivity of ATP-induced Ca^{2+} entry and *Tg*-induced I_{sc} to La^{3+} and flufenamate would suggest that the Ca^{2+} channels involved in ATP-induced Ca^{2+} entry are similar to those activated by *Tg*. In fact, La^{3+} was known to block many Ca^{2+} channels and had been shown to block capacitative Ca^{2+} entry in some epithelia (Bradyen *et al.* 1989), while the flufenamate sensitive component of Ca^{2+} entry may be attributed to some non-selective cation channels (Gögelein *et al.* 1990).

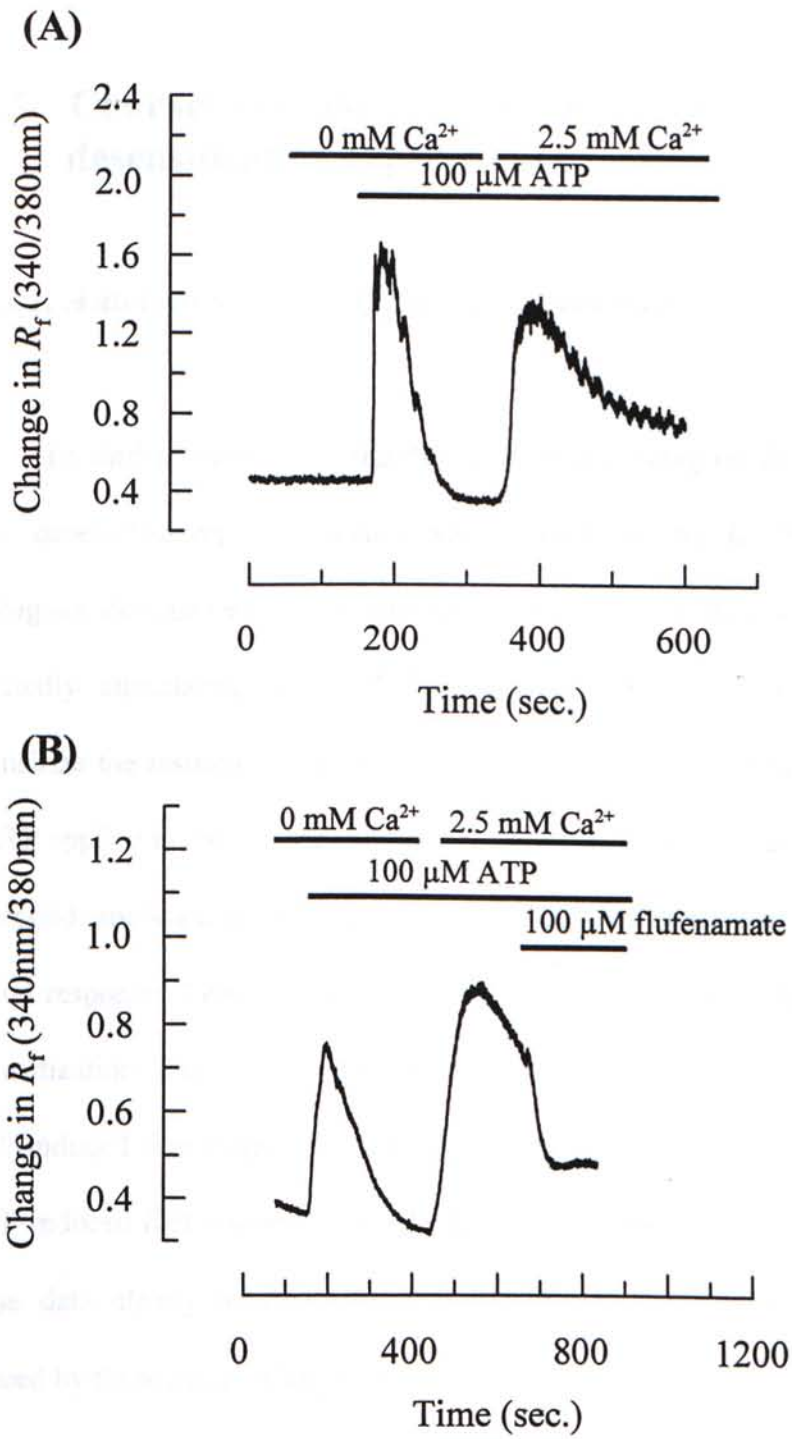

Figure III.2.(h)

Effect of flufenamate at **(A)** 0μM (control) and **(B)** 100 μM on the Ca^{2+} entry induced by 100μM of ATP. Flufenamate was subsequently added into the bathing solution during the onset of the *plateau*. The percentage of inhibition to ATP-induced Ca^{2+} entry at *plateau* was derived from the formula $(R_{CONTROL}-R_{flufenamate})/ R_{CONTROL}X100\%$, where $R_{CONTROL}$ is the fluorescence ratio (R_f) measured in control condition and $R_{flufenamate}$ is the R_f measured in the prescence of flufenamate. Essentially identical records were obtained in four separate experiments. Horizontal bars represented the duration of application of drugs/solutions.

III.3. Characterization of the P_{2Y} subtype(s) by cross desensitization experiments

III.3.1. Autologous desensitization experiments

To further characterize the P_{2Y} subtype(s) existing on the apical membrane, cross desensitization experiments were undertaken by I_{sc} technique. Initially, autologous desensitization experiments were done. As shown in figure III.3.(a), repeatedly stimulating the epithelia with the same agonist would drastically desensitize the response induced by second application. At 100μM, the first aliquot of ATP applied in the bathing solution (N=5) would severely desensitize the response of second application by 95.8±0.7% ($P<0.05$) (first response: 65.9±5.2μA cm^{-2}; second response: 2.8±0.4μA cm^{-2}). For UTP (N=5) and UDP (N=4), the % of self-desensitization were 98.5±0.0% ($P<0.05$) and 97.7±0.6% ($P<0.05$) respectively. (UTP-induced first response: 73.0±5.8μA cm^{-2}; second response: 1.1±0.0μA cm^{-2}) (UDP-induced first response: 53.3±11.8μA cm^{-2}; second response: 1.4±0.4μA cm^{-2}). These data clearly demonstrated the effectiveness of autologous desensitization induced by these nucleotides at 100μM.

III.3.2. Classical cross desensitization experiments

To explore the possibility of the existence of any separate pyrimidine nucleotide receptors on the apical membrane, cross desensitization experiments were carried out using ATP and UTP. Epithelia were first stimulated with 100μM UTP, then, 100μM ATP was added after ten minutes (FigureIII.3.(b)). Obviously, in the

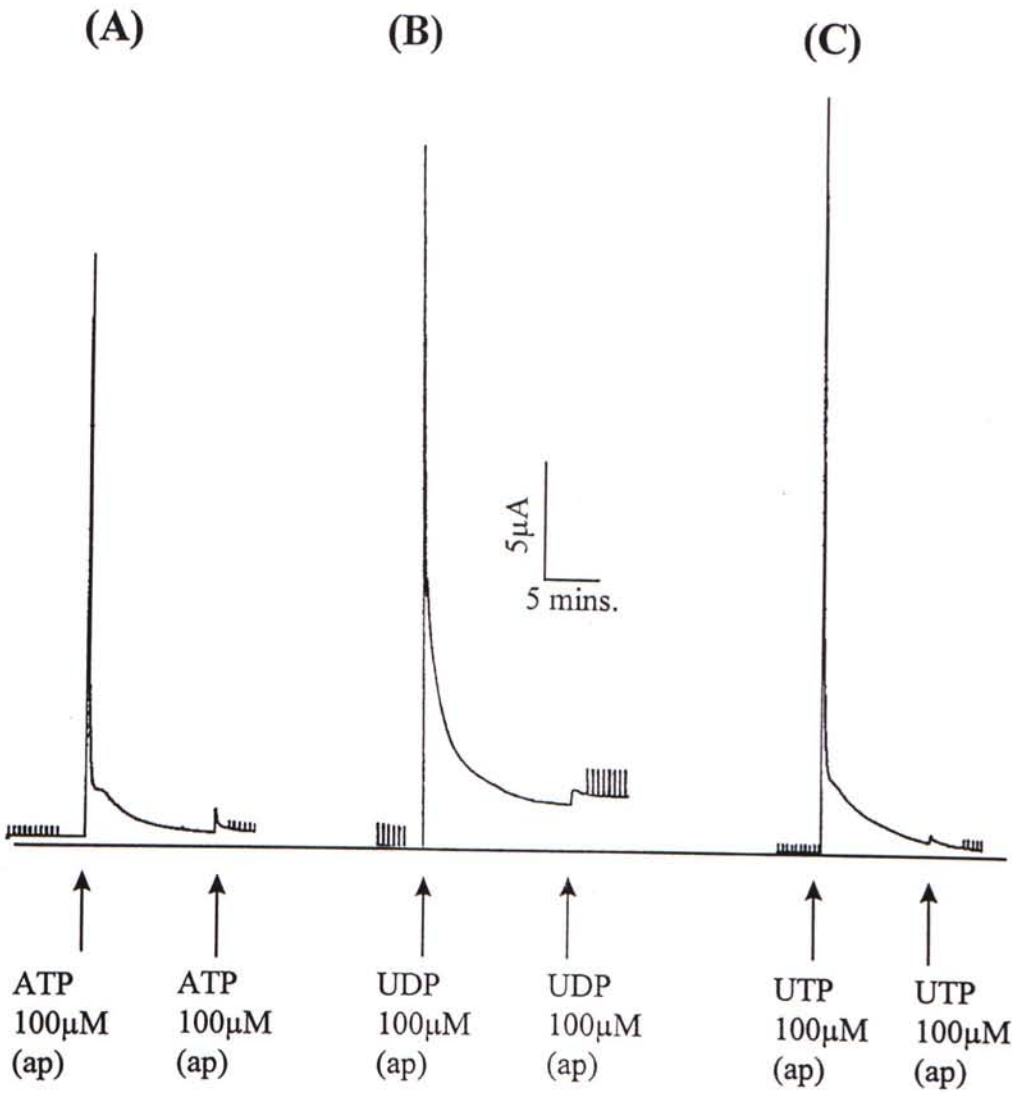

Figure III.3.(a)

Autologous desensitization of responses to apical nucleotides. Typical I_{sc} recordings showing the effects of repeatedly applications of aliquots of 100μM **(A)** ATP, **(B)** UTP or **(C)** UDP. Each I_{sc} recording are representative for 4-6 separate experiments. Calibration bar applied to all the three traces.

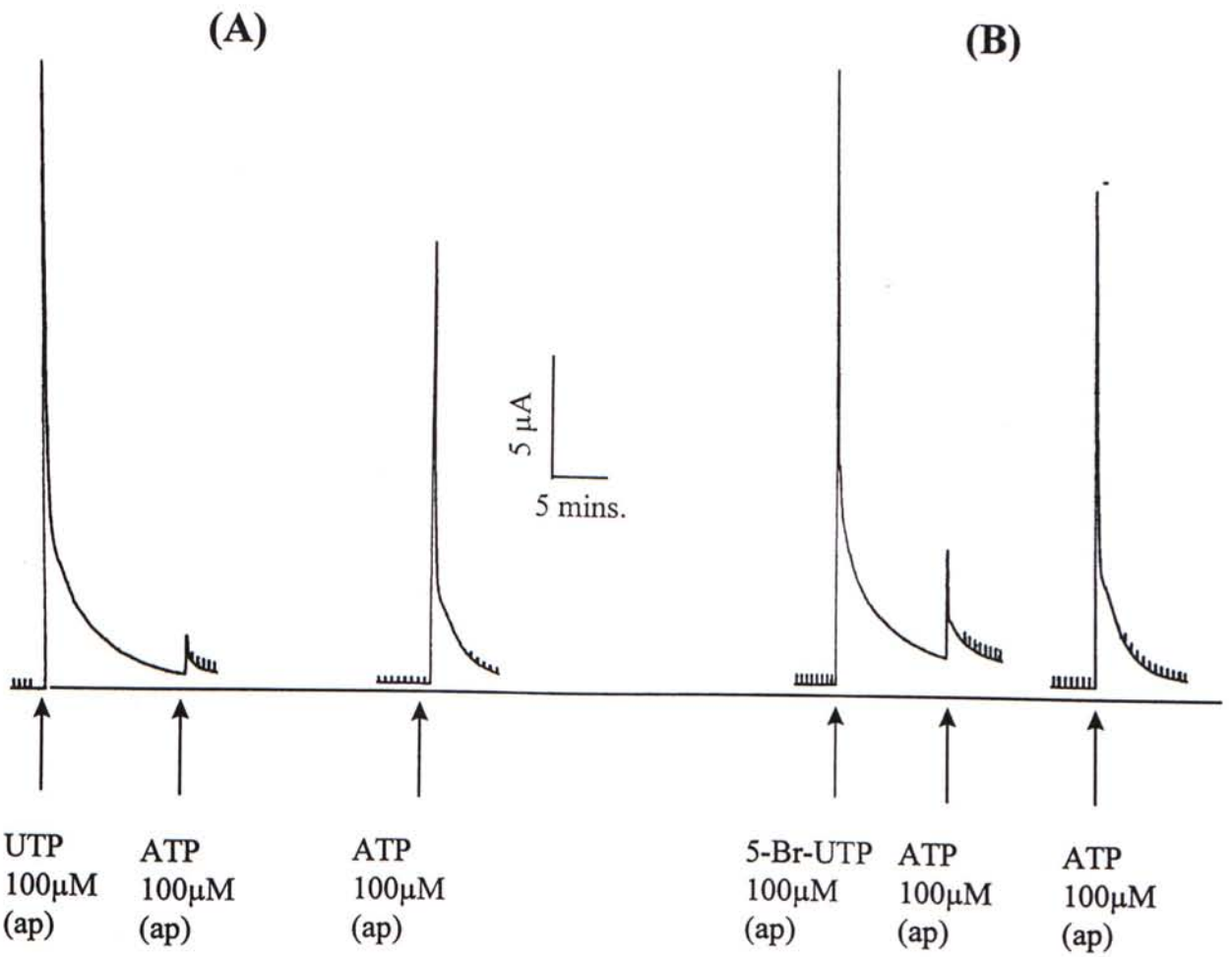

Figure III.3.(b)

Desensitizing effect on the ATP-induced I_{sc}. Typical I_{sc} recordings showing the changes in I_{sc} that occur when cultured epithelia are stimulated by **(A)** UTP or **(B)** 5-Br-UTP, followed by ATP to the apical (ap) solution. Notice the profound desensitization effect on ATP-induced I_{sc} after the applications of UTP or 5-Br-UTP is comparable to Fig.III.3.(a). Essentially identical responses are obtained in 4-6 separate epithelia. Calibration bar applied to all traces.

presence of UTP (N=4), the ATP-induced I_{sc} was significantly (P<0.05) desensitized by 93.1±0.7%. The magnitude of I_{sc} induced by ATP in control and UTP-prestimulated conditions were 52.5±6.3μA cm^{-2} and 3.3±0.4 μA cm^{-2} respectively. Similarly, 5-Br-UTP (N=6) could also significantly (P<0.05) desensitize the ATP-induced I_{sc} by 78.9±3.6%. The magnitude of I_{sc} induced by ATP in control and 5-Br-UTP-prestimulated conditions were 51.7±5.5μA cm^{-2} and 10.9±1.9μA cm^{-2} respectively.

Subsequent experiments were done with application of nucleotides in a reverse sequence. As shown in figure III.3.(c), either UTP (N=6) or 5-Bromo-UTP (N=5) seemed to be less sensitive to ATP and were capable of inducing another peak of I_{sc}. In the presence of ATP, the UTP and 5-Br-UTP induced I_{sc} was only partially desensensitized by 53.8±5.0% (P<0.05) and 51.2±6.9% (P<0.05) respectively. In control cells, the magnitude of UTP-induced I_{sc} was 80.7±5.9μA cm^{-2}, and 37.3±4.0 μA cm^{-2} in ATP-prestimulated cells. For 5-Br-UTP, the magnitude of I_{sc} was 63.1±6.9μA cm^{-2} in control cells, and 30.7±4.4μA cm^{-2} in ATP-prestimulated cells. Apparently, these results strongly suggested the existence of a separate receptor population which is insensitive to ATP and allows UTP and 5-Br-UTP to elicit another peak of I_{sc}.

To further characterize this ATP-insensitive receptor, cells were first challenged with UTP, followed by UDP or *vica versa*. Referring to figure III.3 (d), In the presence of UTP (N=3), the response evoked by second application of UDP could drastically be desensitized by 98.5±0.0% (P<0.05). The magnitude of I_{sc} induced by UDP in control and UTP-prestimulated conditions were 59.7±13.0μA cm^{-2} and 0.9±0.2μA cm^{-2} respectively. Conversely, prestimulation of UDP (N=4) could only

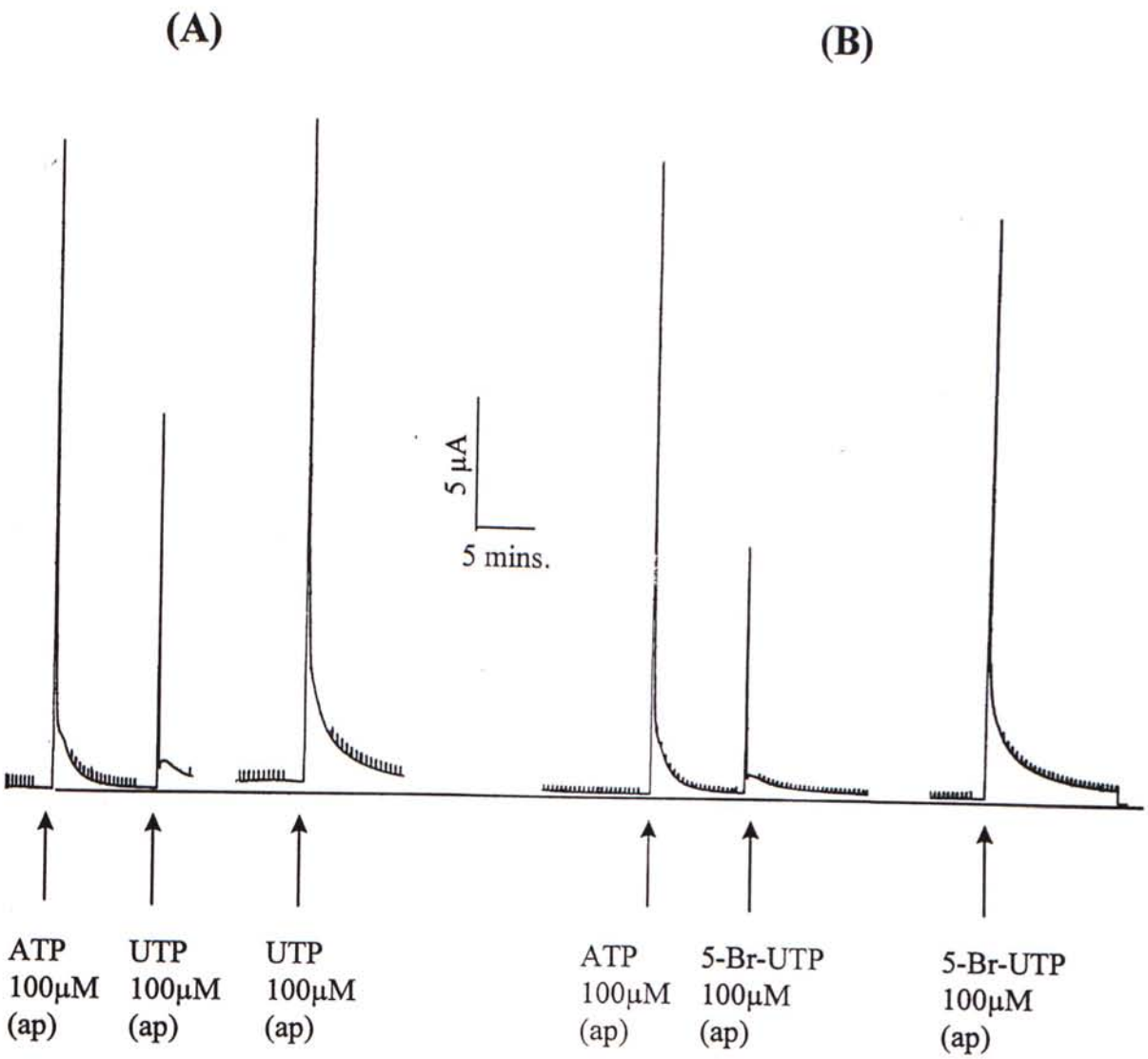

Figure III.3.(c)

Desensitizing effect on the **(A)** UTP or **(B)** 5-Br-UTP induced I_{sc}. Typical I_{sc} recordings showing the changes in I_{sc} that occur when cultured epithelia are stimulated by ATP, followed by UTP or 5-Br-UTP to the apical (ap) solution. Essentially identical responses are obtained in 4-6 separate epithelia. Calibration bar applied to all traces.

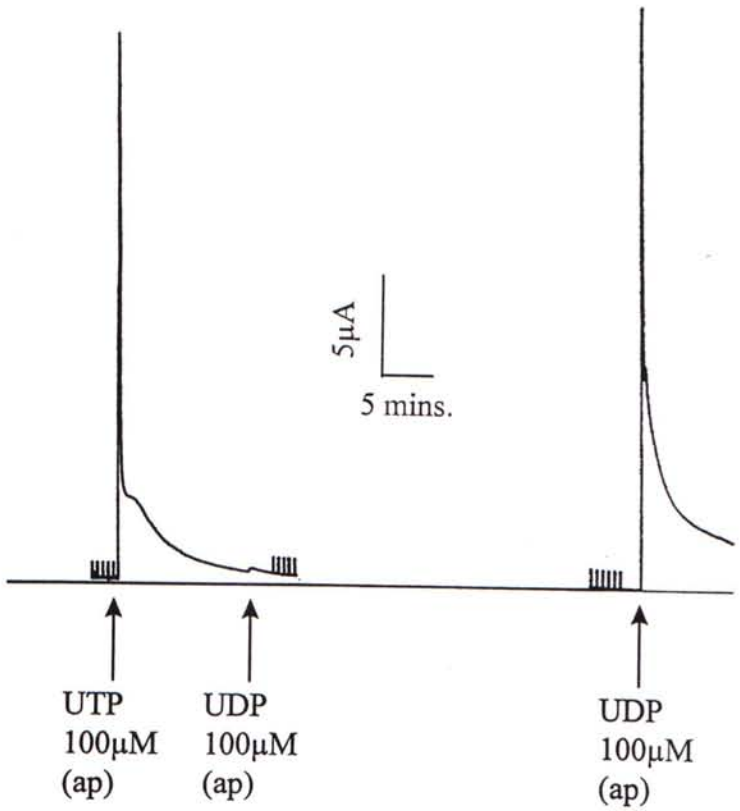

Figure III.3.(d)

Desensitizing effect on the UDP-induced I_{sc}. Typical I_{sc} recordings showing the changes in I_{sc} that occur when cultured epithelia are stimulated by UTP, followed by UDP to the apical (ap) solution. Essentially identical responses are obtained in 4-6 separate epithelia. Calibration bar applied to both traces.

partially desensitize the UTP-induced I_{sc} by 48.4±4.0% ($P<0.05$). The magnitude of I_{sc} induced by UTP in control and UDP-prestimulated conditions were 80±7.8 μA cm^{-2} and 41.3±3.2μA cm^{-2} respectively. (Figure III.3.(e)).

The interactions between ATP and UDP were also explored with this desensitization protocol. As illustrated in figure III.3.(f), in the presence of ATP (N=5), the response of UDP was partially desensitized by 37.8±8.8% ($P<0.05$). The magnitude of I_{sc} induced by UDP in control and ATP-prestimulated conditions were 56.7±6.0μA cm^{-2} and 35.2±5.0μA cm^{-2} respectively.

Similarly, in the presence of UDP (N=7), the response of ATP was partially desensitized by 46.4±5.3% ($P<0.05$). The magnitude of I_{sc} induced by ATP in control and UDP-prestimulated conditions were 71.5±5.1μA cm^{-2} and 38.3±3.8μA cm^{-2} respectively.

These findings strongly suggested the existence of an ATP-insensitive receptor population which allows pyrimidine nucleotides to elicit another discernible rise in I_{sc} after challenged with ATP. In the presence of UTP, the response of ATP and UDP were drastically reduced. This phenomenon suggested that UTP could effectively act on both a well-documented P_{2Y2}-receptor and an ATP-insensitive receptor. However, it is intriguing for the existence of partial desensitizing effects between ATP and UDP. The interaction may probably due to the depletion of common Ca^{2+} stores and/or another possibility that they were mutually interacting with each other at receptor level (Figure III.3.(g)).

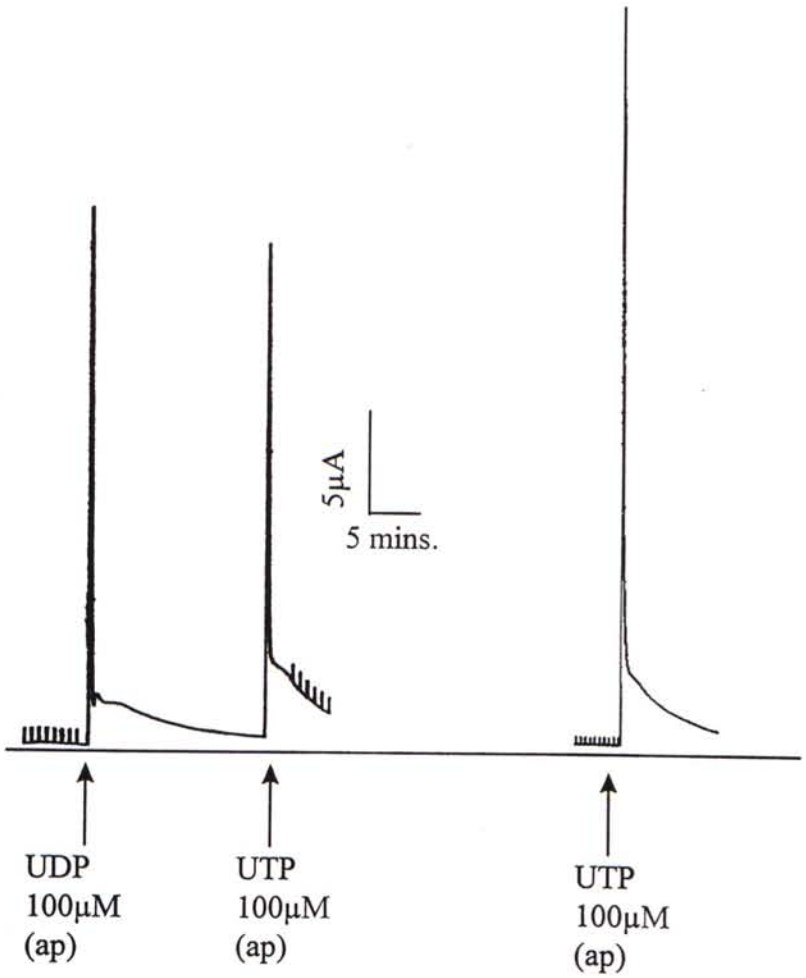

Figure III.3.(e)

Desensitizing effect on the UTP-induced I_{sc}. Typical I_{sc} recordings showing the changes in I_{sc} that occur when cultured epithelia are stimulated by UDP, followed by UTP to the apical (ap) solution. Essentially identical responses are obtained in 4-6 separate epithelia. Calibration bar applied to both traces.

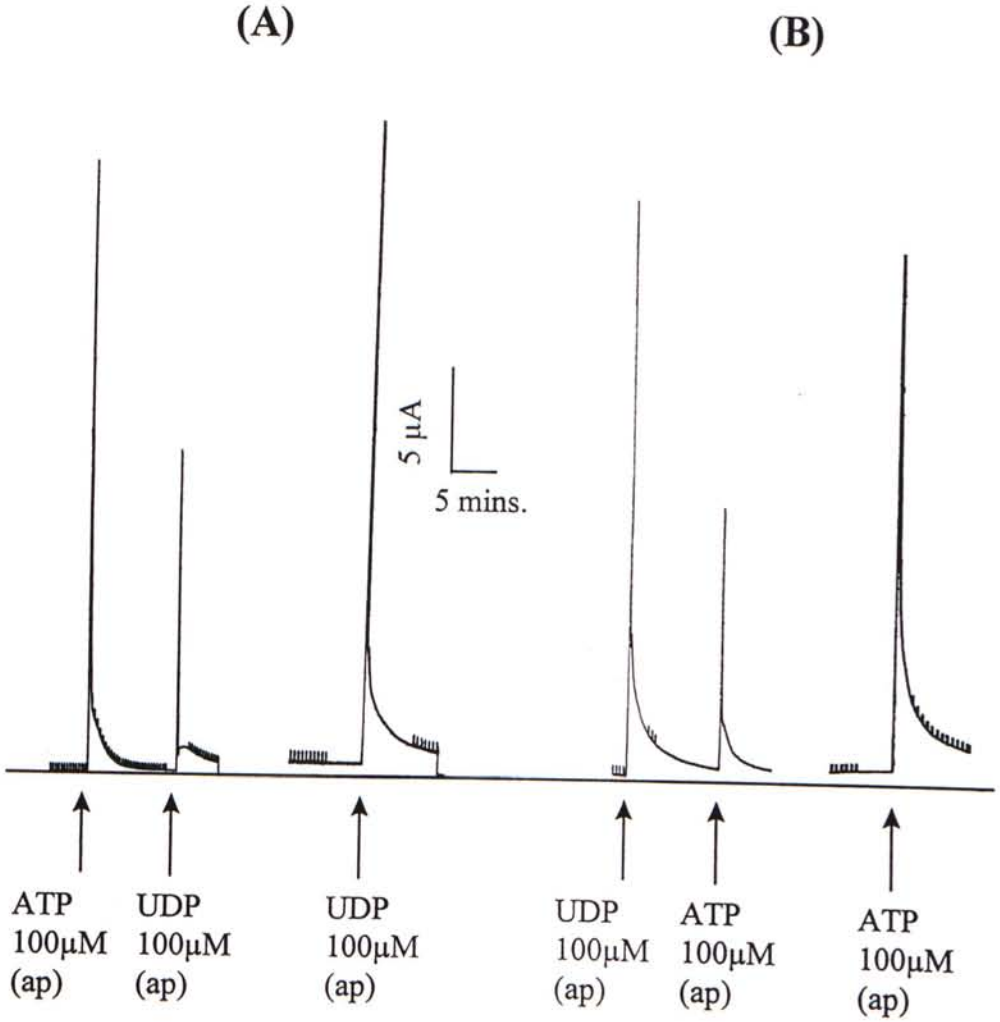

Figure III.3.(f)

Desensitizing effect on the **(A)** UDP-induced I_{sc} and **(B)** ATP-induced I_{sc}. Typical I_{sc} recordings showing the changes in I_{sc} that occur when cultured epithelia are stimulated by **(A)** ATP, followed by UDP or **(B)** *vice versa* to the apical (ap) solution. Essentially identical responses are obtained in 4-6 separate epithelia. Calibration bar applied to all traces.

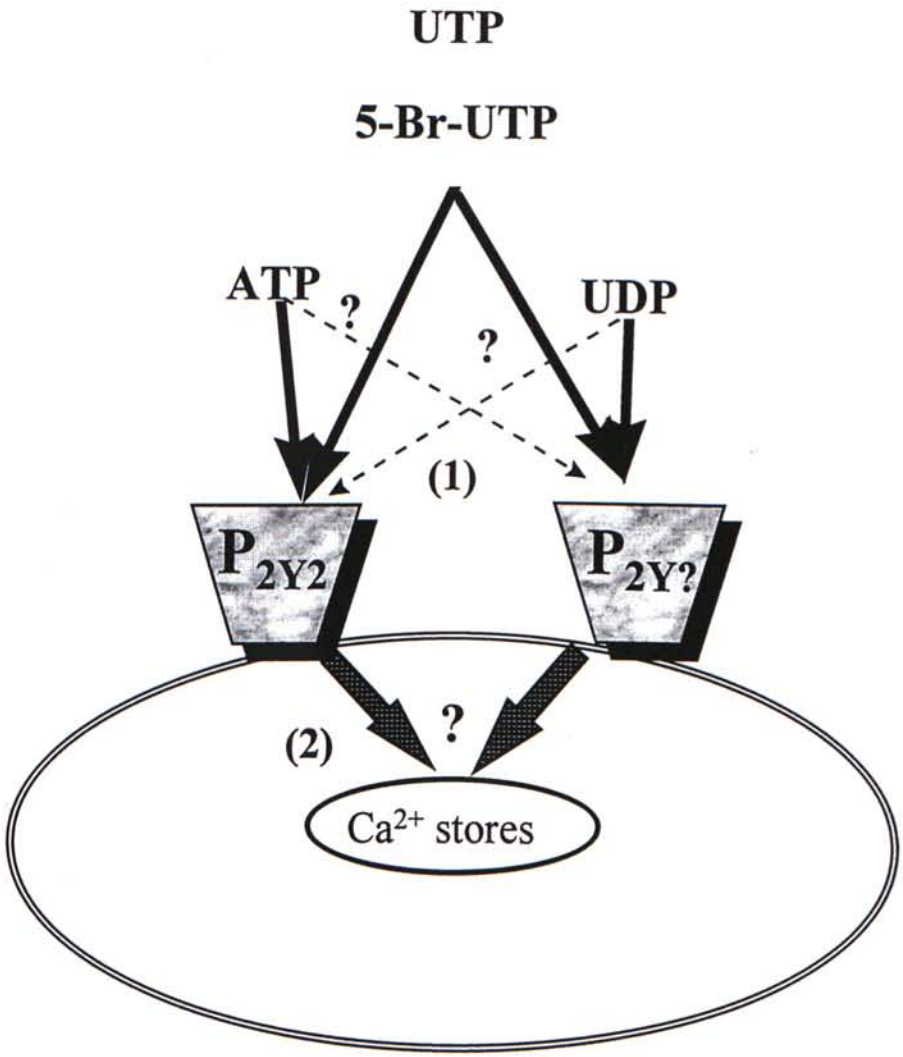

Figure III.3.(g)

Diagrammatic illustration for the proposed interactions between apical nucleotides during cross desensitization experiments. Among these nucleotides, ATP was suggested to preferentially bind to the P_{2Y2} receptor. UTP, 5-Br-UTP and UDP were capable of inducing another discernible responses after ATP application by acting on an ATP-insensitive receptor. In addition, UTP and 5-Br-UTP can effectively bind to the two different population of P_{2Y} receptors. However, ATP and UDP were interacting with each other *via* an unknown mechanism **(1)** interaction at receptors level; and/or **(2)** depletion of common Ca^{2+} stores.

III.3.3. Characterization of the ATP-insensitive P_{2Y} receptor

Studies of dose-responses relationship under ATP prestimulation

To study the pharmacological properties of this novel ATP-insensitive P_{2Y} receptor, cross desensitization experiments were undertaken. To knock-out the responses mediated through P_{2Y2}-receptors, nucleotides were added after the application of 100μM ATP. The rationale behind was due to the higher selectivity of P_{2Y2} to ATP than other nucleotides (Nicholas *et al.* 1996). Presumably, in the presence of ATP, the I_{sc} induced by other nucleotides should be predominantly mediated through the ATP-insensitive receptor population (Figure III.3.(h)).

A summary of dose-response curves was illustrated in figure III.3.(i). In the presence of ATP, 5-Bromo-UTP, UTP and UDP were all able to initiate the increase in I_{sc} definitely in a dose-dependent manner. ADP was less effective to induce the I_{sc} after the stimulation of ATP. In the presence of ATP, UDP was found to be the most effective to induce the I_{sc}, with EC_{50} at 2.4±1.9 μA cm^{-2}. The EC_{50} of 5-Bromo-UTP and UTP were 4.0±4.4 μA cm^{-2} and 10.9±0.1 μA cm^{-2} respectively. These data suggested us to speculate that the ATP-insensitive receptor is a pyrimidine selective P_{2Y} receptor. According to a latest pharmacological studies on different P_{2Y} subtypes (Nicholas *et al.* 1996), two novel pyrimidine sensitive receptors (*i.e.* P_{2Y4} & P_{2Y6}) were cloned and identified. P_{2Y4} is a nucleoside tri-phosphate specific receptor (*i.e.* UTP and ATP) and it only exhibits a low affinity to ATP. P_{2Y6} is more sensitive to UDP; UTP and ADP are only partial agonists and this subtype is insensitive to ATP (Nicholas *et al.* 1996). Therefore, it is tempting to speculate that this ATP-

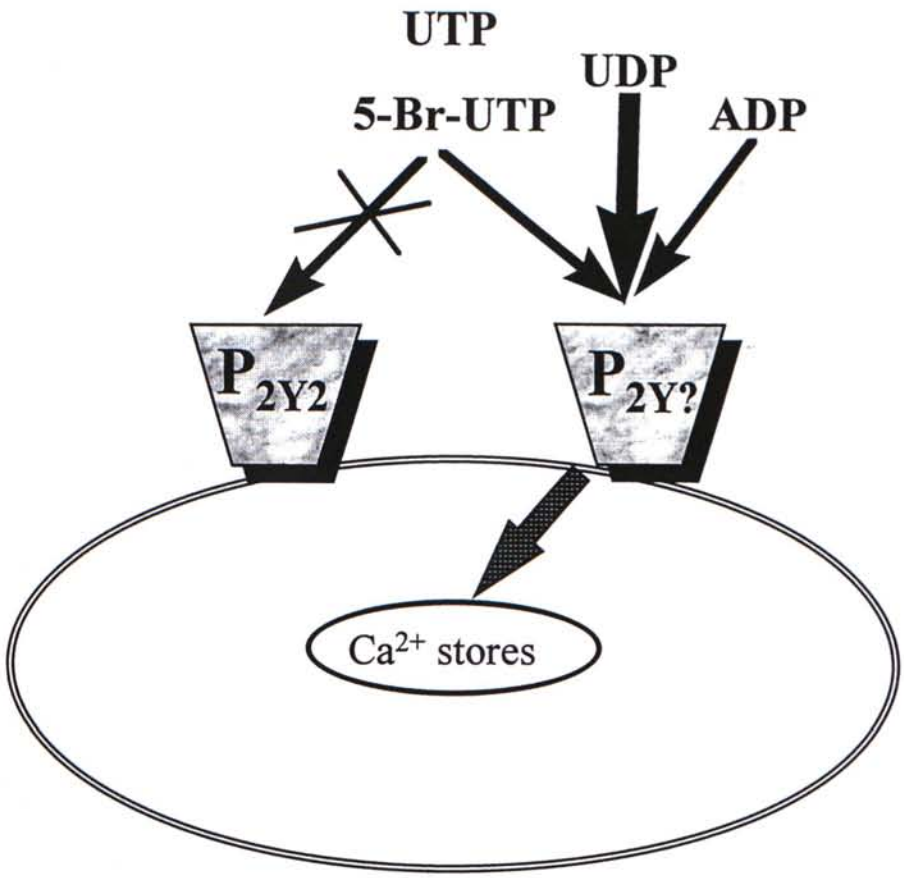

Figure III.3.(h)

Pharmacological studies of the ATP-insensitive receptor by prestimulating the epithelia with ATP (100μM). According to the profound effect of autologous experiments (fig.III.3.(a)), prestimulation of ATP would completely occupy the P_{2Y2} receptor. Under such circumstances, application of pyrimidine nucleotides as well as ADP as second agonists were presumably acted *via* the novel-P_{2Y} receptor population.

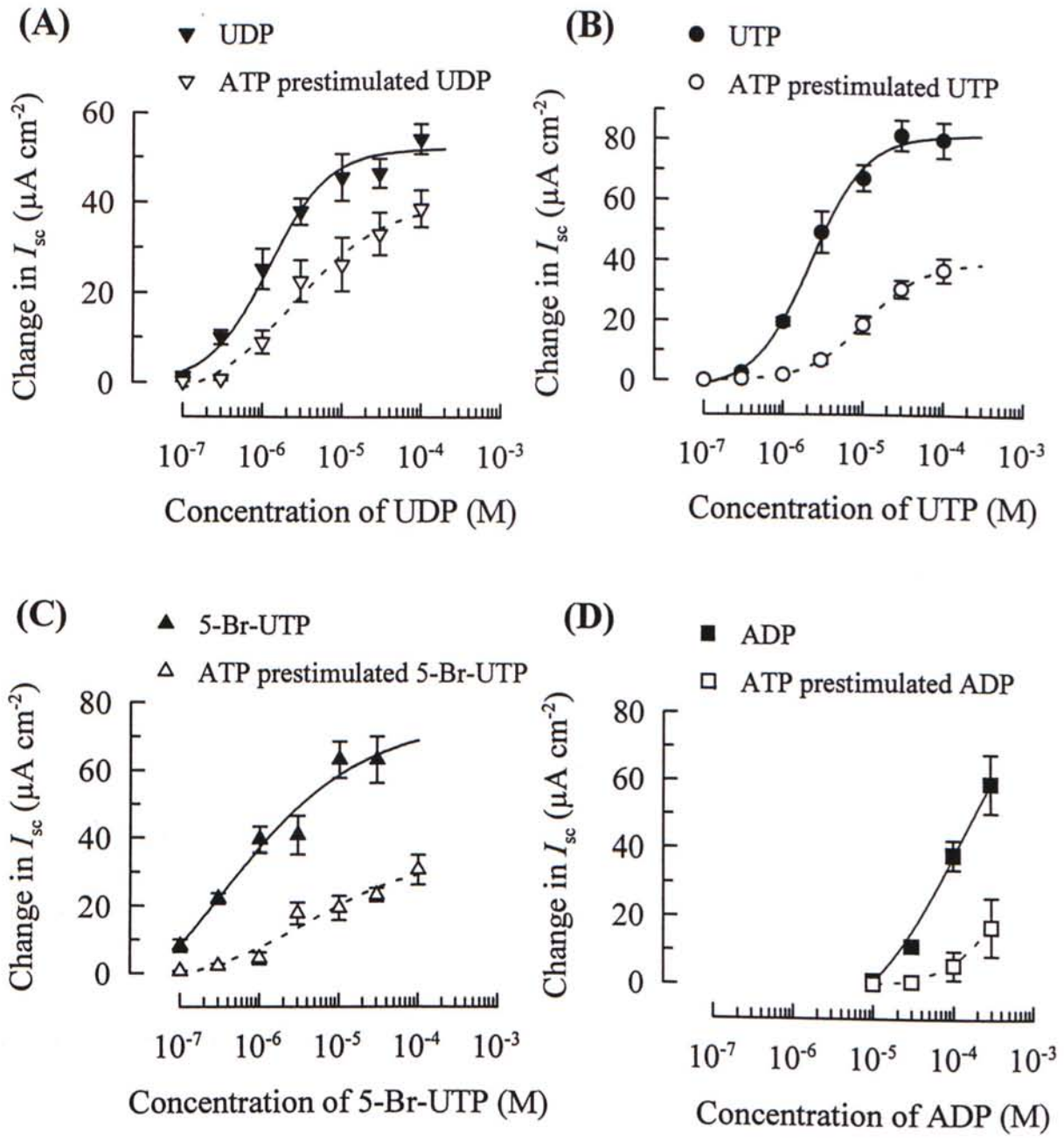

Figure III.3.(i)

Pharmacology of the ATP-insensitive receptor upon nucleotide-induced I_{sc}. Epithelial monolayers were stimulated by adding **(A)** UDP, **(B)** UTP, **(C)** 5-Br-UTP or **(D)** ADP to the solution bathing the apical sides of the cell layers. The resultant increase in I_{sc} were quantified and are plotted against the concentration of nucleotide used. Data are presented as mean ± S.E.M. of 4-8 separate experiments. In each figure, the data obtained from control epithelia are shown by the filled symbols and the open symbols indicate responses of age-matched epithelia that had been prestimulated with 100μM ATP.

insensitive receptor may be belonged to P_{2Y6} subtype although the identity of this receptor needed to be confirmed by molecular study.

Studies performed under UDP-prestimulation

In the presence of UDP (N=5), the response of 100μM ADP was drastically desensitized by 80.1±3.3% (control: 36.3±2.0 μA cm^{-2} *Vs* UDP-prestimulated: 7.2±1.2 μA cm^{-2}) (Figure III.3.(j)). The profound desensitizing effect of UDP may be due to the fact that ADP also predominantly binds to this novel P_{2Y}-nucleotide receptor.

As our findings in chapter III.3.2 suggested that the effects of UDP upon these cells were primarily mediated *via* an ATP-insensitive receptor, we undertook a more detailed study of the interaction between UDP and ATP by quantifying responses to ATP in a full dose range with the pretreatment of 100μM UDP (Figure III.3.(k)). This result confirmed that UDP reduced the cell's sensitivity to ATP and showed that this was associated with a shift in the EC_{50} value from 11.0±0.6μM to 30.6±1.1μM.

Studies performed under ADP-prestimulation

In the presence of 1mM ADP, the response of ATP (N=5) was desensitized by 82.8±3.1% (control: 51.7±5.5μA cm^{-2} *Vs* ADP-prestimulated: 8.9±3.1μA cm^{-2}).

Under the same condition, the response of UDP (N=5) was also desensitized by 45.0±4.5% ($P<0.05$) (control: 50.1±2.5 μA cm^{-2} *Vs* ADP-prestimulated: 22.6±3.3μA cm^{-2}) (Figure III.3.(l)).

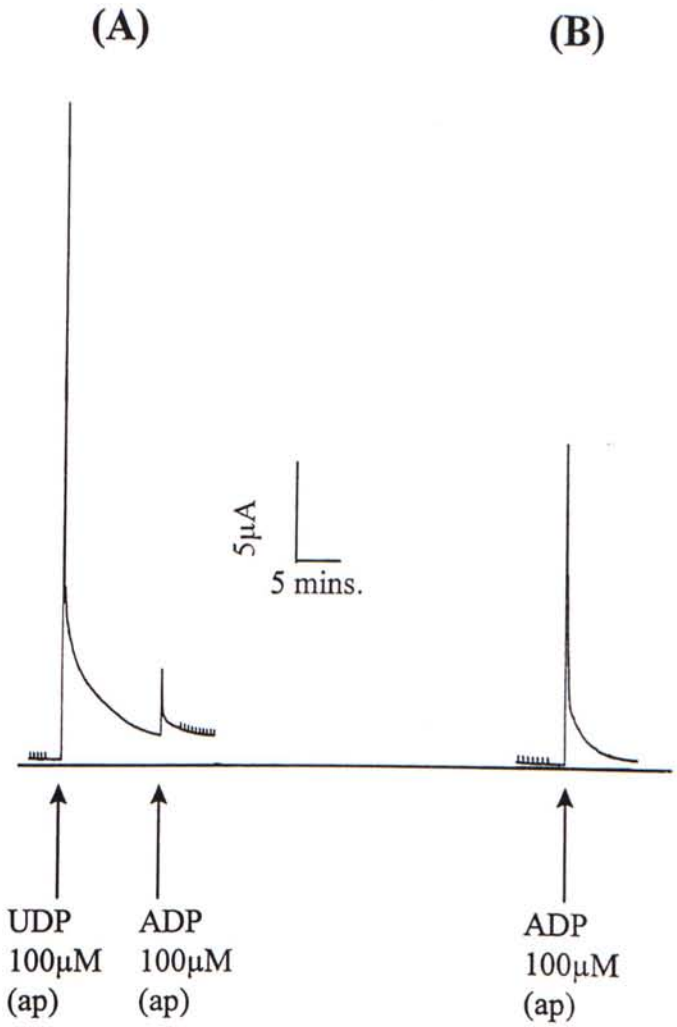

Figure III.3.(j)

Desensitizing effect on the ADP-induced I_{sc}. Typical I_{sc} recordings showing the changes in I_{sc} that occur when cultured epithelia are stimulated by **(A)** UDP, followed by ADP or **(B)** ADP to the apical (ap) solution. Essentially identical responses are obtained in 4-6 separate epithelia. Calibration bar applied to both traces.

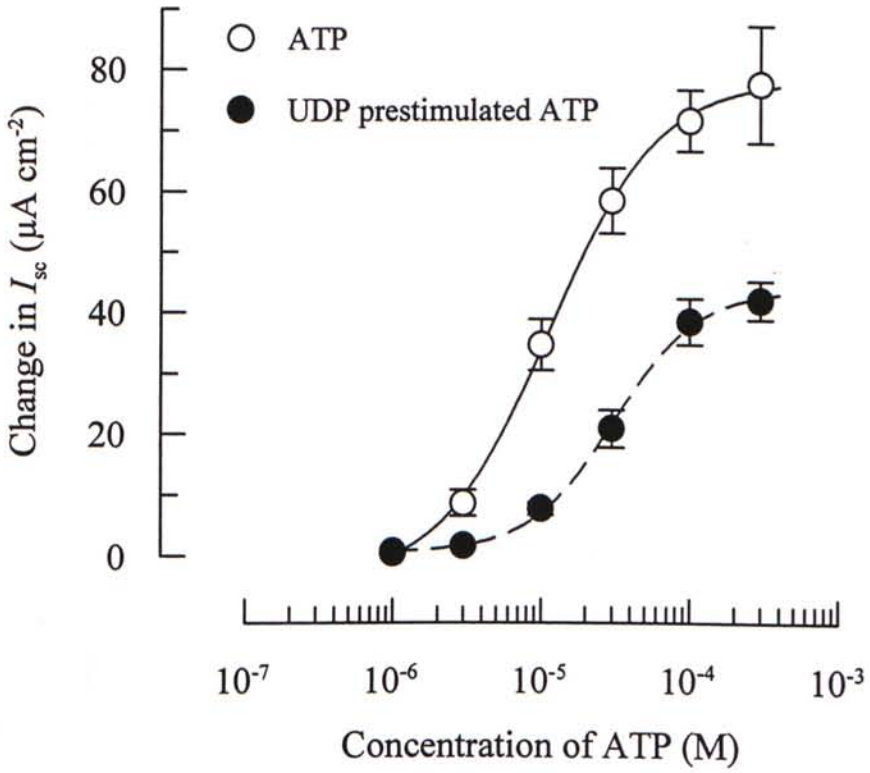

Figure III.3.(k)

Desensitizing effect upon ATP-induced I_{sc}. Epithelial monolayers were stimulated by adding ATP to the solution bathing the apical sides of the cell layers. The resultant increase in I_{sc} were quantified and are plotted against the concentration of nucleotide used. Data are presented as mean ± S.E.M. of 4-6 separate experiments. In each figure, the data obtained from control epithelia are shown by the filled symbols and the open symbols indicate responses of age-matched epithelia that had been prestimulated with 100μM UDP.

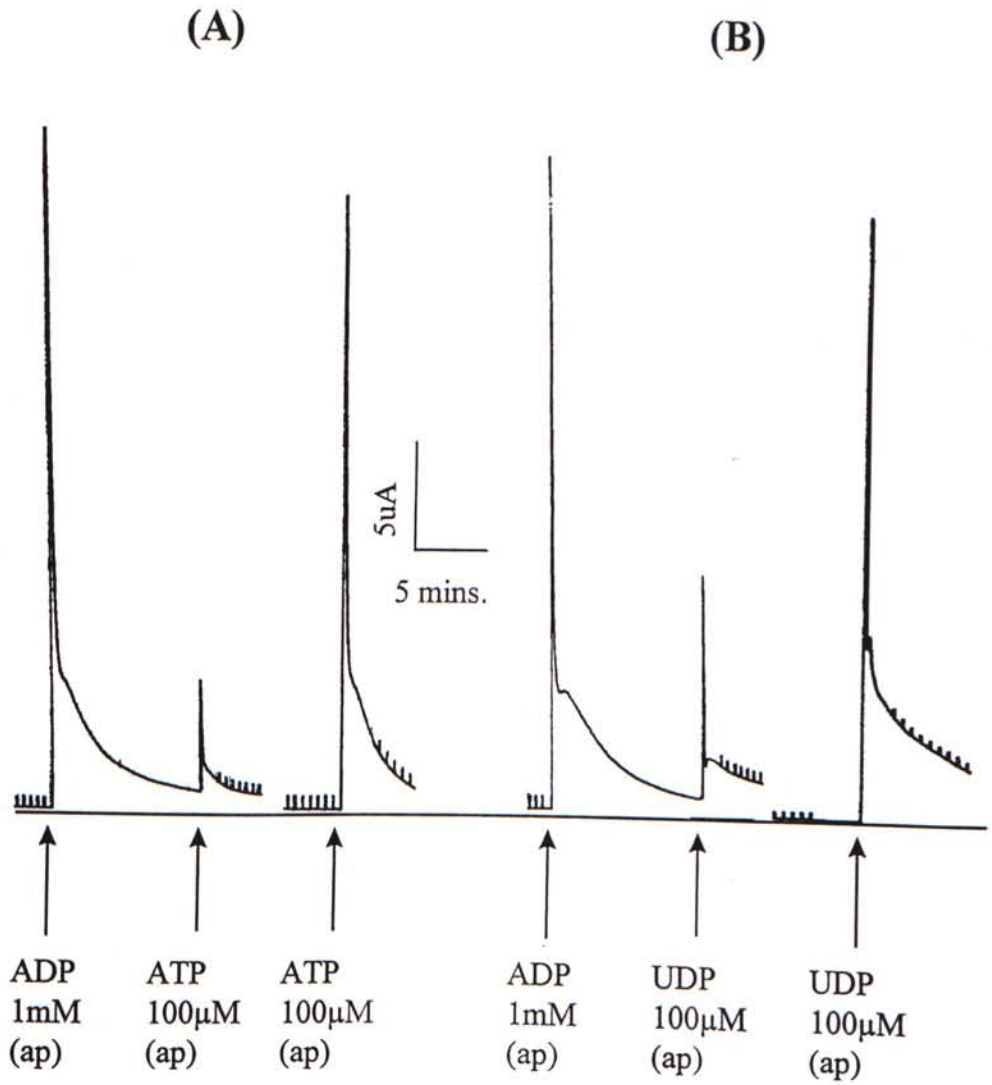

Figure III.3.(l)

Desensitizing effect on the **(A)** ATP or **(B)** UDP induced I_{sc}. Typical I_{sc} recordings showing the changes in I_{sc} that occur when cultured epithelia are stimulated by 1mM ADP, followed by ATP or UDP to the apical (ap) solution. Essentially identical responses are obtained in 4-6 separate epithelia. Calibration bar applied to all traces.

III.3.4. Interaction between ATP and bradykinin

Our findings in chapter III.3.2 showed that ATP could partially desensitize the 100μM UDP-induced I_{sc} by 37.8±8.8% and *vice versa* (46.1±4.2%). To investigate the possibility of their interactions, a non-purinergic agent: bradykinin (10μM) was employed. Bradykinin acts on functionally-expressed receptors which can induce an increase in $[Ca^{2+}]_i$ and I_{sc}, except that it activates a mutually independent receptor family.

In the presence of 100μM ATP (N=6), the bradykinin-induced I_{sc} was drastically desensitized by 75.0±6.7% ($P<0.05$) (control: 26.7±6.7μA cm^{-2} *Vs* ATP-prestimulated: 6.7±1.8μA cm^{-2}).

In the presence of 10μM bradykinin (N=6), the desensitizing effect of bradykinin on ATP-induced I_{sc} was statistically insignificant ($P>0.05$) (Figure III.3.(m)). The most likely possibility for the desensitizing effect of ATP on bradykinin-induced I_{sc} was due to the exhaustion of common Ca^{2+} stores. Moreover, this protocol could provide an indirect evidence that the interaction of ATP and UDP was due to depletion of common Ca^{2+} stores. However, the interaction of ATP and UDP at receptor level could not be excluded.

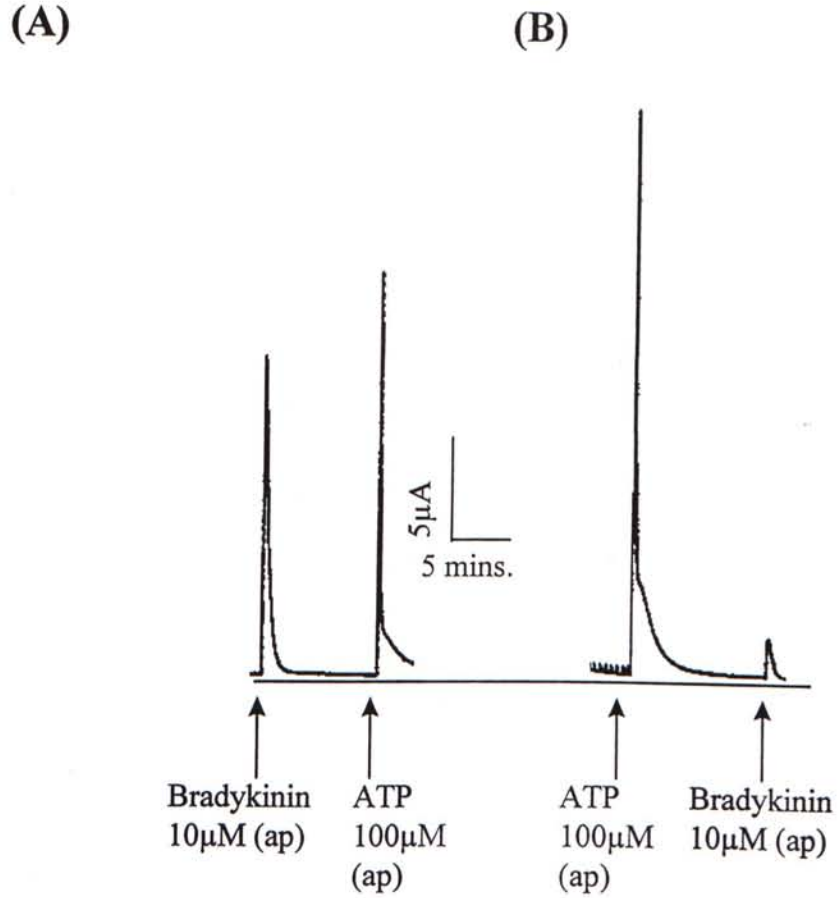

Figure III.3.(m)

Desensitizing effect on the **(A)** ATP or **(B)** bradykinin induced I_{sc}. Typical I_{sc} recordings showing the changes in I_{sc} that occur when cultured epithelia are stimulated by **(A)** bradykinin, followed by ATP or **(B)** *vice versa* to the apical (ap) solution. Essentially identical responses are obtained in 5-6 separate epithelia. Calibration bar applied to both traces.

III.4. Simultaneous measurement of $[Ca^{2+}]_i$ and I_{sc}

In the following study, epithelial cells were grown on *Transwell*®-COL filter for simultaneous measurement. After culturing for 3 days, the epithelial cells would form a confluent monolayer, which could be easily observed under an inverted microscope (Figure III.4. (a)(A)). A cross section of the membrane filter could also demonstrate the epithelia only consisted of a single layer of cells (Figure III.4. (a)(B)).

III.4.1. Effect of UDP and ADP

Earlier $[Ca^{2+}]_i$ studies on the same cell line had reported that ADP and UDP were unable to initiate any response (Ko *et al.* 1997; Wilson *et al.* 1998). In contrast, our experiments from conventional I_{sc} measurement found that ADP and UDP were able to mediate the increases in I_{sc}. Based on these contradictory findings, we were tempting to investigate the mechanism underlying the ADP and UDP-induced I_{sc}. Therefore, in the following experiments, a novel measurement technique was employed. This technique enables us to simultaneously measure the anion secretion and $[Ca^{2+}]_i$ on a functionally polarized epithelia.

As illustrated in figure III.4.(b), ADP and UDP were capable of evoking the increases in R_f accompanied with the increases in I_{sc}. Without doubt, this finding could directly illustrate that the ADP and UDP-induced I_{sc} were also $[Ca^{2+}]_i$-dependent. Such phenomenon also indicated that the epithelia cells only sensitive to UDP and ADP in a growth condition which favored the formation of polarized epithelia (*i.e.* permeable support).

(A)

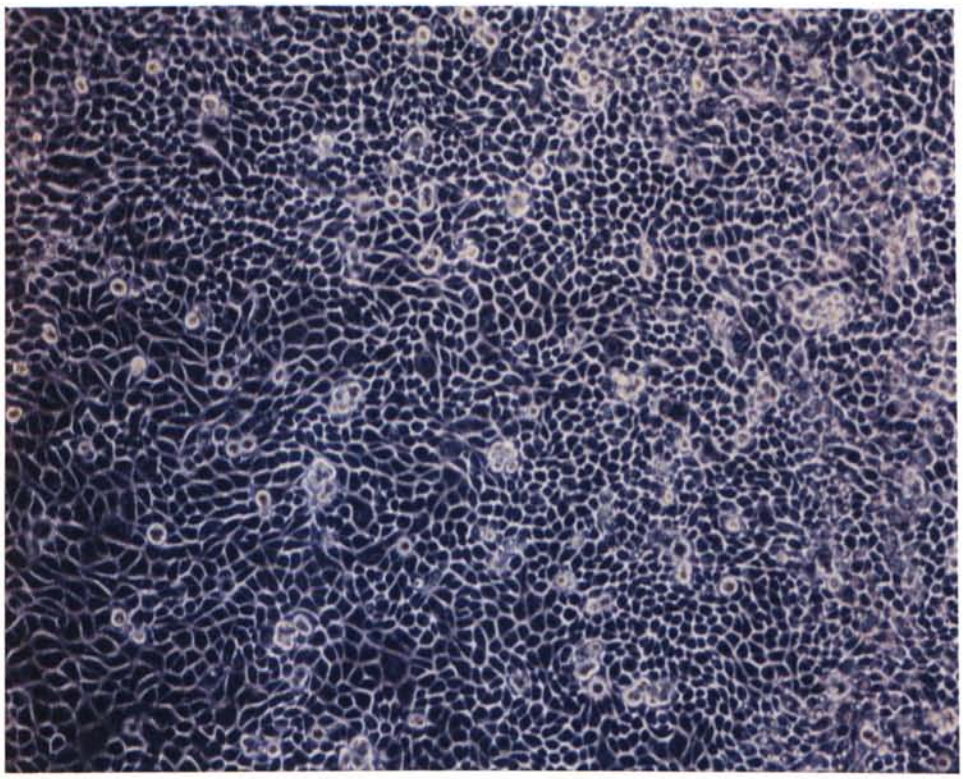

(B)

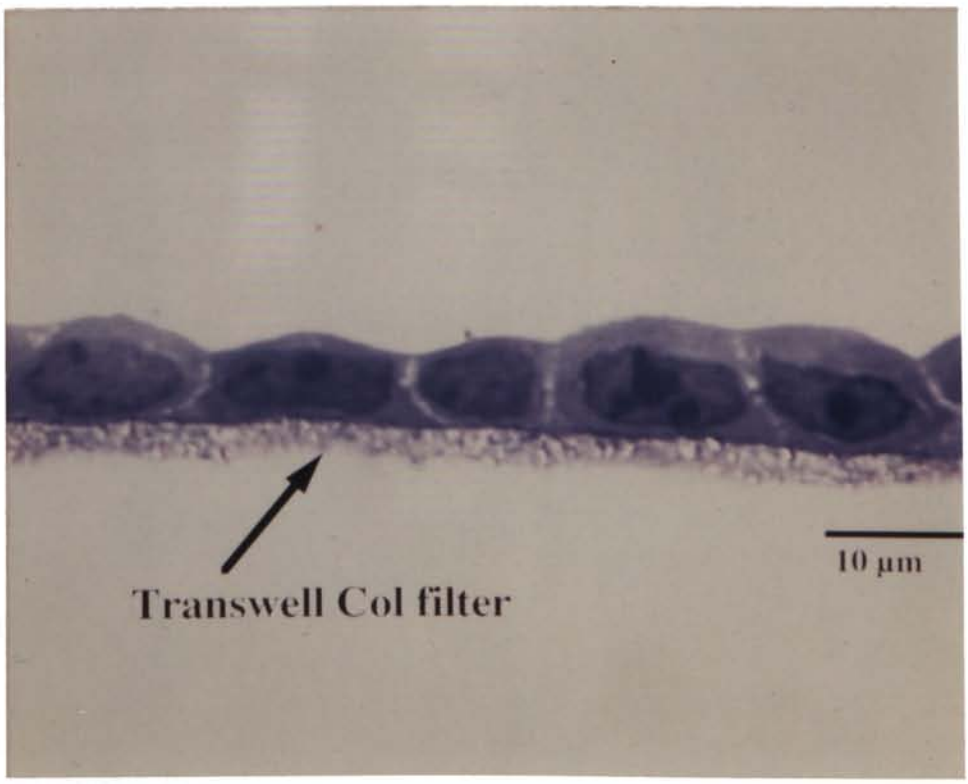

Figure III.4.(a)

(A) Epithelial cells grown on *Transwell*®-COL membrane filter and were viewed under an inverted microscope (10X10). **(B)** Cross section of the single layer of cells grown on the membrane filter.

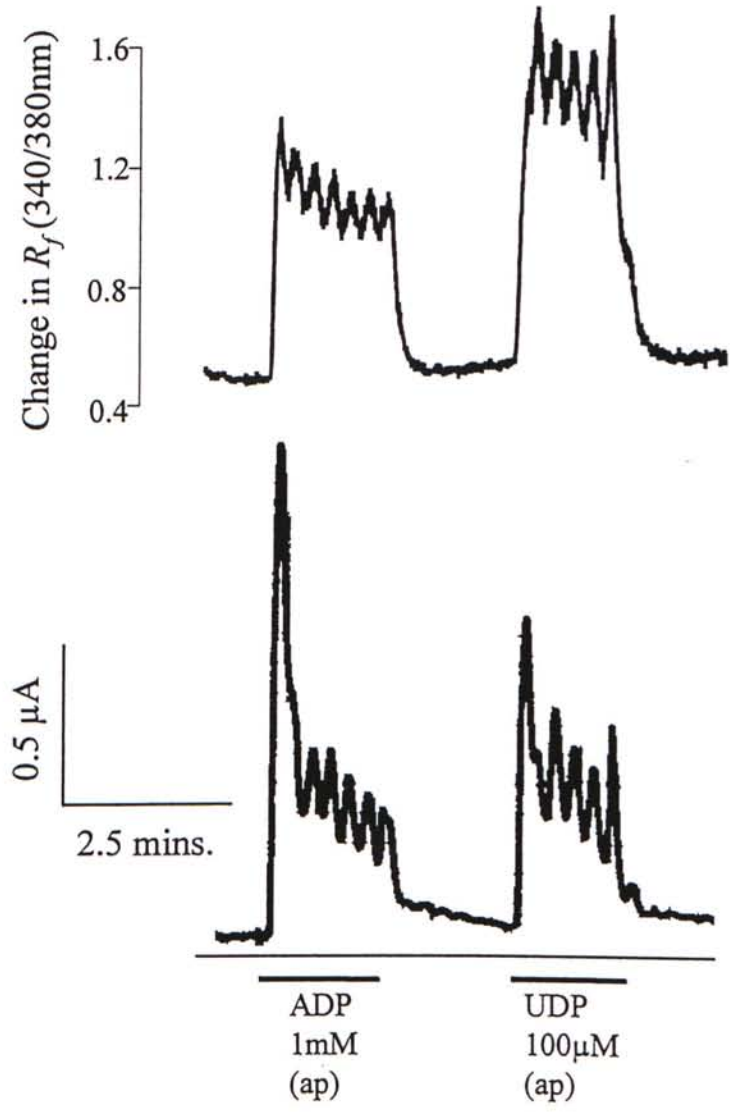

Figure III.4.(b)

I_{sc} and R_f recordings obtained by a simultaneous measurement method. The upper panel shows a continuous record of R_f *via* the computer interface. The lower panel shows the I_{sc} tracing obtained from a pen recorder with calibration bar indicates the magnitude of I_{sc}. ADP (1mM) and UDP (100μM) were added to the apical (ap) solution as indicated from the horizontal bars. Essentially similar results were obtained in 6 separate experiments.

III.4.2. Correlation between I_{sc} and $[Ca^{2+}]_i$

In the following study, the correlation between the changes in I_{sc} and R_f induced by nucleotides were studied by repeatedly challenged the epithelia monolayer with brief pulses (30 sec.) of increasing concentration of ATP, UDP or 5-Br-UTP at 2-3 minutes intervals. At the end of each experiment, 100μM ATP was added so that all these data could be expressed as fraction of response to this standard stimulus (Figure III.4.(c)). Subsequently, data were summarized and quantified as dose-response curves. The correlation between the changes in I_{sc} and R_f were demonstrated by plotting a linear regression line of change in R_f *versus* change in I_{sc}.

Referring to figure III.4.(d)(A), ATP (N=6) was an agonist with a similar effectiveness to elicit the increases in I_{sc} and R_f. The slope of the linear regression line was insignificantly different ($P>0.05$) from the hypothetical slope (*i.e.* 1), which suggested that the increase in R_f was directly proportional to the increase in I_{sc} (Figure III.4.(d)(B)).

UDP (N=10) was more effective to elicit the increases in R_f than I_{sc}. As shown in figure III.4.(e), the slope of the linear regression line was significantly greater than one ($P<0.05$), thus UDP was more effective to induce the increase in R_f than that of I_{sc}.

In contrast to UDP, 5-bromo-UTP (N=6) was more effective to elicit the increases in I_{sc} than that of R_f, since the slope of the linear regression line was significantly smaller than one ($P<0.05$) (Figure III.4.(f)).

In summary, these findings suggested that the I_{sc} induced by nucleotides were not necessarily to be closely associated with the increase in R_f. Such discrepancies

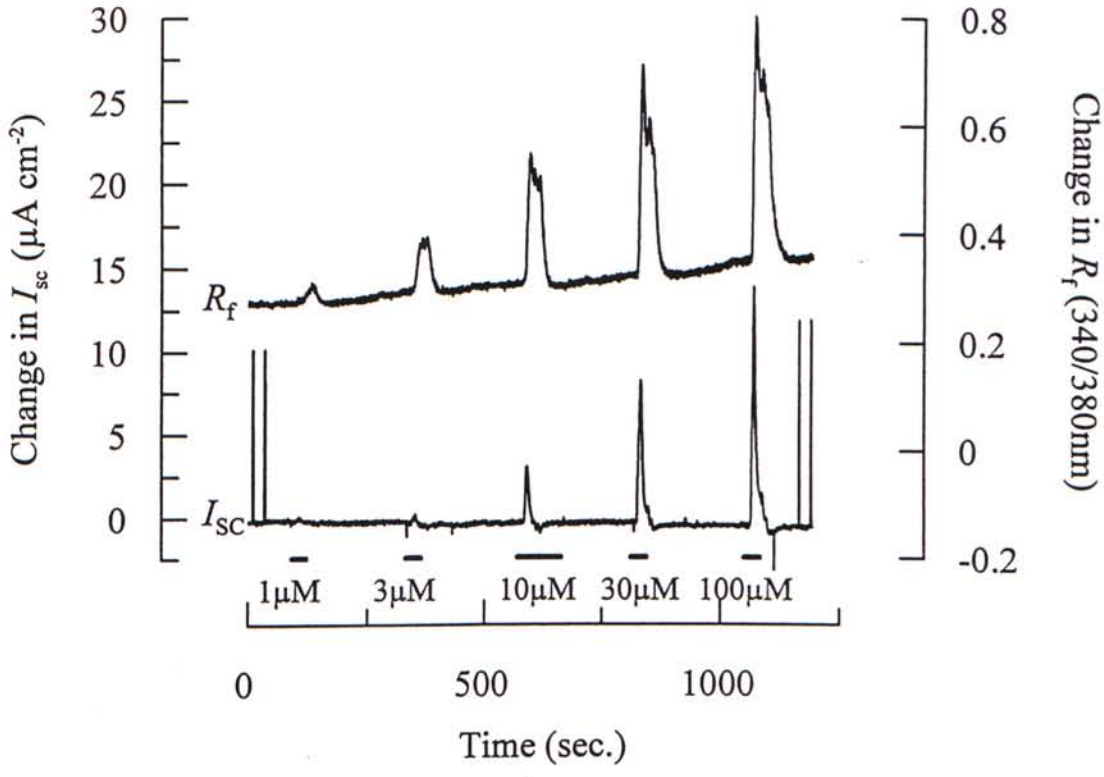

Figure III.4.(c)

Typical I_{sc} and R_f recording obtained from simultaneous measurement. The I_{sc} signals and R_f signals were synchronously digitized *via* an A/D converter. In this experiment, the monolayer was repeatedly stimulated with 30s. pulses of increasing concentrations of ATP delivered apically at a interval of 2mins. Essentially similar results were obtained in 6 separate experiments. Horizontal bars indicate the duration of applications.

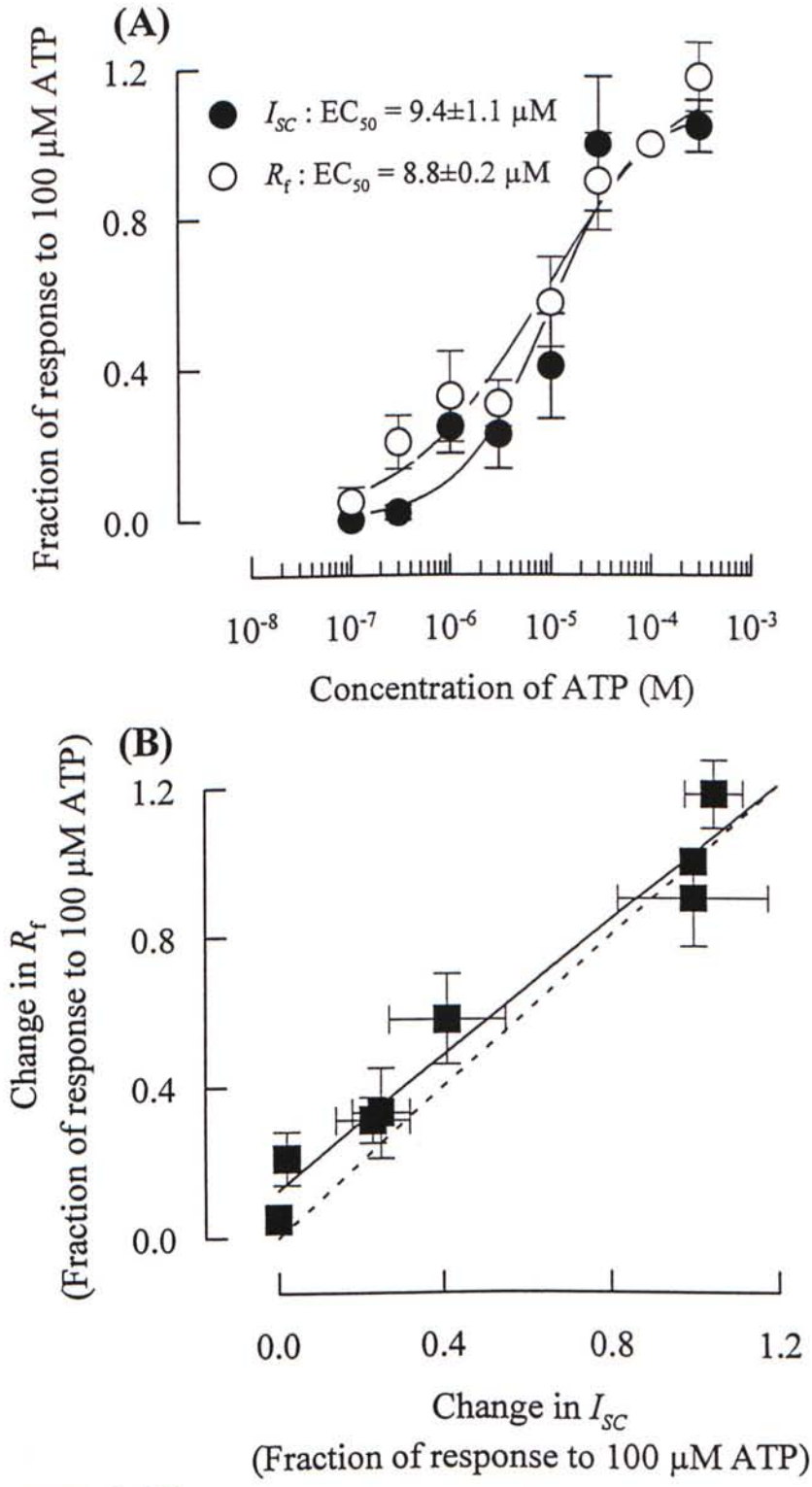

Figure III.4.(d)

(A) ATP-induced R_f (open circles) and I_{sc} (filled circles) were quantified as fraction of response to 100μM ATP and plotted against the concentration of ATP used. Data for each point are means of ± S.E.M. for 6 separate epithelia. **(B)** Correlation between the fraction of increases in R_f and I_{sc}. The dotted line shows the linear regression line with hypothetical slope of 1. Bars and columns of each data point are S.E.M. values.

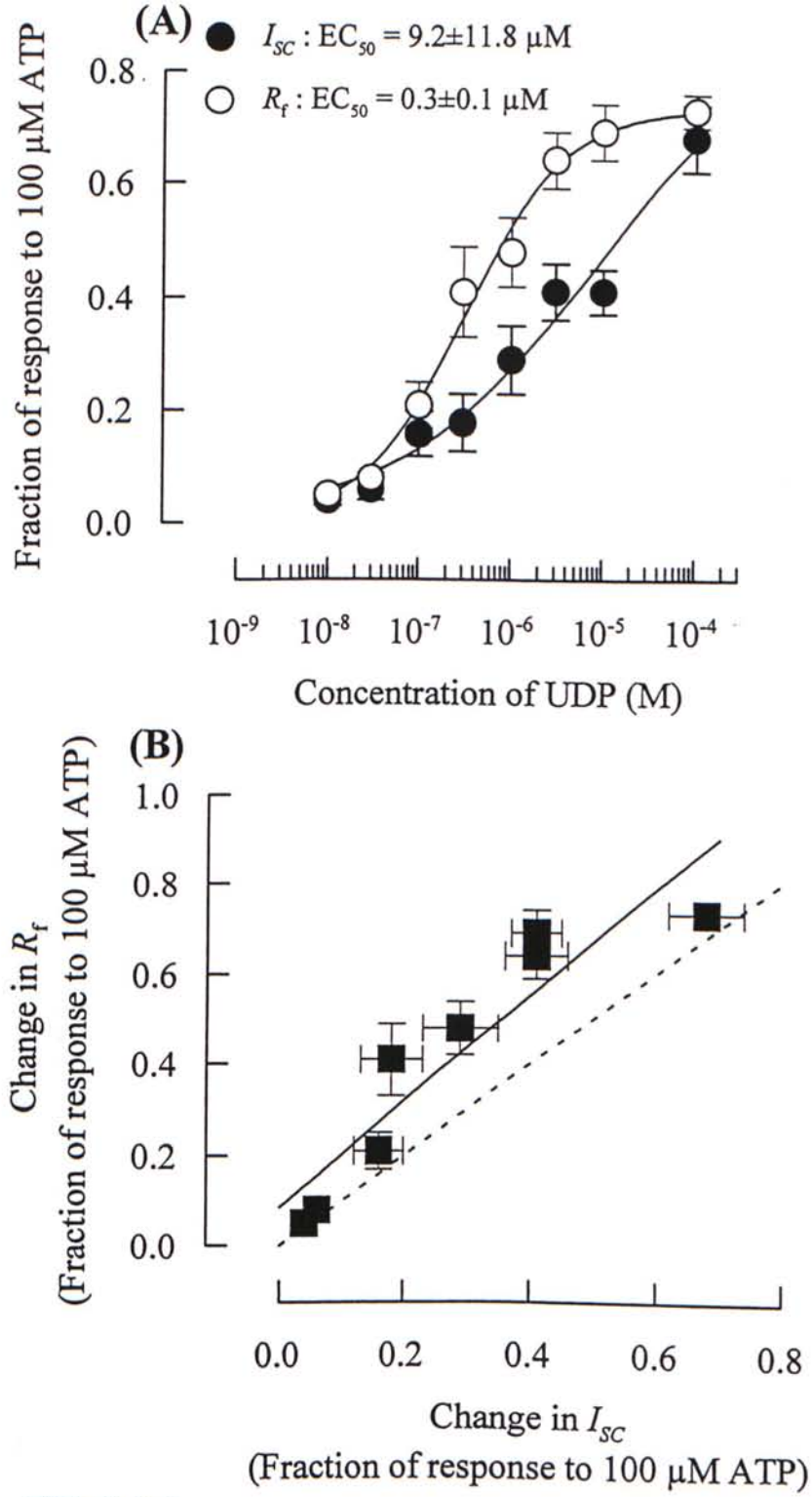

Figure III.4.(e)

(A) UDP-induced R_f (open circles) and I_{sc} (filled circles) were quantified as fraction of response to 100μM ATP and plotted against the concentration of UDP used. Data for each point are means of ± S.E.M. for 10 separate epithelia. **(B)** Correlation between the fraction of increases in R_f and I_{sc}. The dotted line shows the linear regression line with hypothetical slope of 1. Bars and columns of each data point are S.E.M. values.

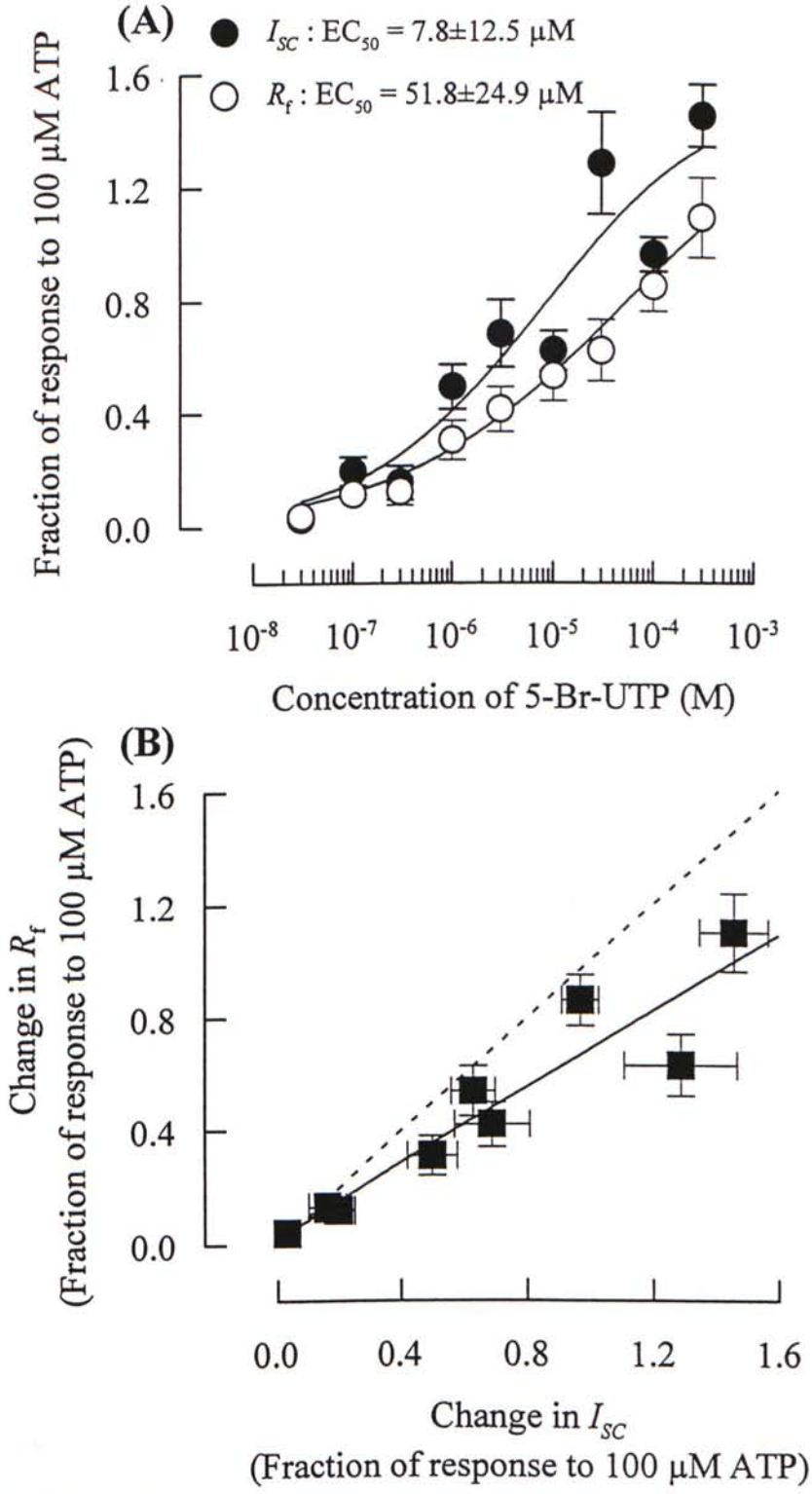

Figure III.4.(f)

(A) 5-Br-UTP-induced R_f (open circles) and I_{sc} (filled circles) were quantified as fraction of response to 100μM ATP and plotted against the concentration of 5-Br-UTP used. Data for each point are means of ± S.E.M. for 6 separate epithelia. **(B)** Correlation between the fraction of increases in R_f and I_{sc}. The dotted line shows the linear regression line with hypothetical slope of 1. Bars and columns of each data point are S.E.M. values.

may be accounted for different pharmacological bases of mediating the increases in I_{sc} and $[Ca^{2+}]_i$.

III.4.3. Cross desensitization experiments

As mentioned in chapter III.3, in the presence of ATP or UDP, the epithelia was stilll sensitive to the application of another agonists. In this experiment series, simultaneous measurement method was employed to elucidate the cellular mechanism(s) underlying the increase in I_{sc} induced by the second agonist in the presence of the first agoinst.

In the first series of experiment, the interaction between ATP and UTP was studied. Epithelia were first challenged with 100μM ATP, followed by 100μM UTP or *vice versa.* In the presence of ATP (N=6), UTP was able to evoke another change in R_f (ΔR_f) by 0.29±0.02 accompanied with the change in I_{sc} (ΔI_{sc}) by 8.9±1.3μA cm^{-2} (Figure III.4.(g)(A)). The UTP-induced R_f and I_{sc} were partially desensitized by 42.4±3.6% and 79.4±3.1% respectively.

In contrast, in the presence of UTP (N=5), ATP could only induce the ΔR_f by 0.03±0.01 and ΔI_{sc} by 1.6±0.7μA cm^{-2}. The ΔR_f and ΔI_{sc} induced by ATP were drastically desensitized by 90.9±1.5% and 88.1±5.3% respectively (Figure III.(4)(g)(B)).

Similarly, another series of experiments were done for UDP and UTP. In the presence of UDP (N=5), UTP could induce another ΔR_f by 0.24±0.05 and ΔI_{sc} by 14.4±3.5μA cm^{-2}. The ΔR_f and ΔI_{sc} induced by UTP were partially desensitized by 43.3±11.6% and 69.7±7.5% respectively (Figure III.(4)(h)(A)).

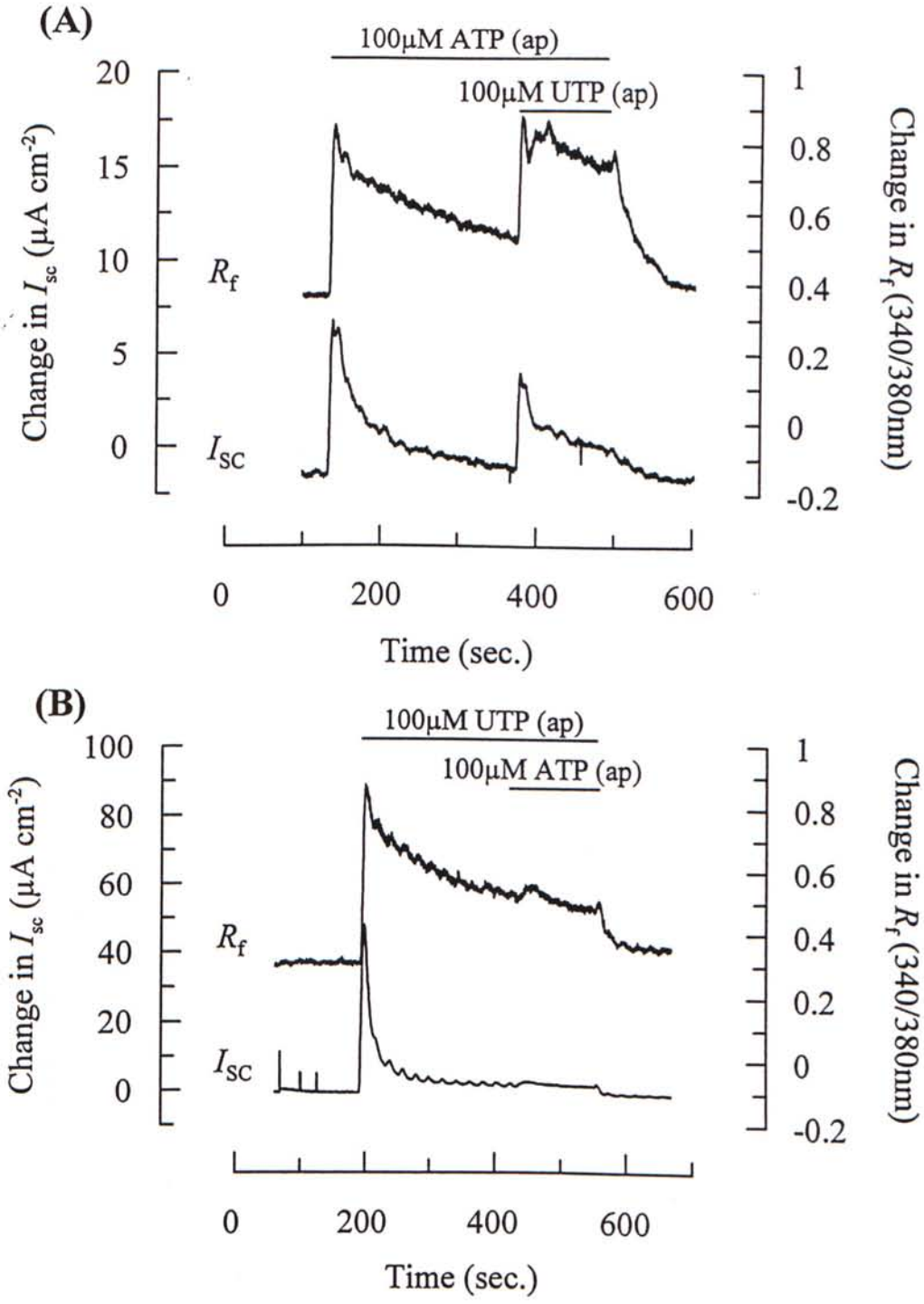

Figure III.4.(g)

Desensitizing effect on the **(A)** R_f and I_{sc} induced by UTP or **(B)** R_f and I_{sc} induced by ATP. Typical I_{sc} and R_f recordings showing the changes in I_{sc} that occur when cultured epithelia are stimulated by **(A)** ATP, followed by UTP or **(B)** *vice versa* to the apical (ap) solution. Essentially identical responses are obtained in 4-6 separate epithelia. Horizontal bars indicate the duration of application.

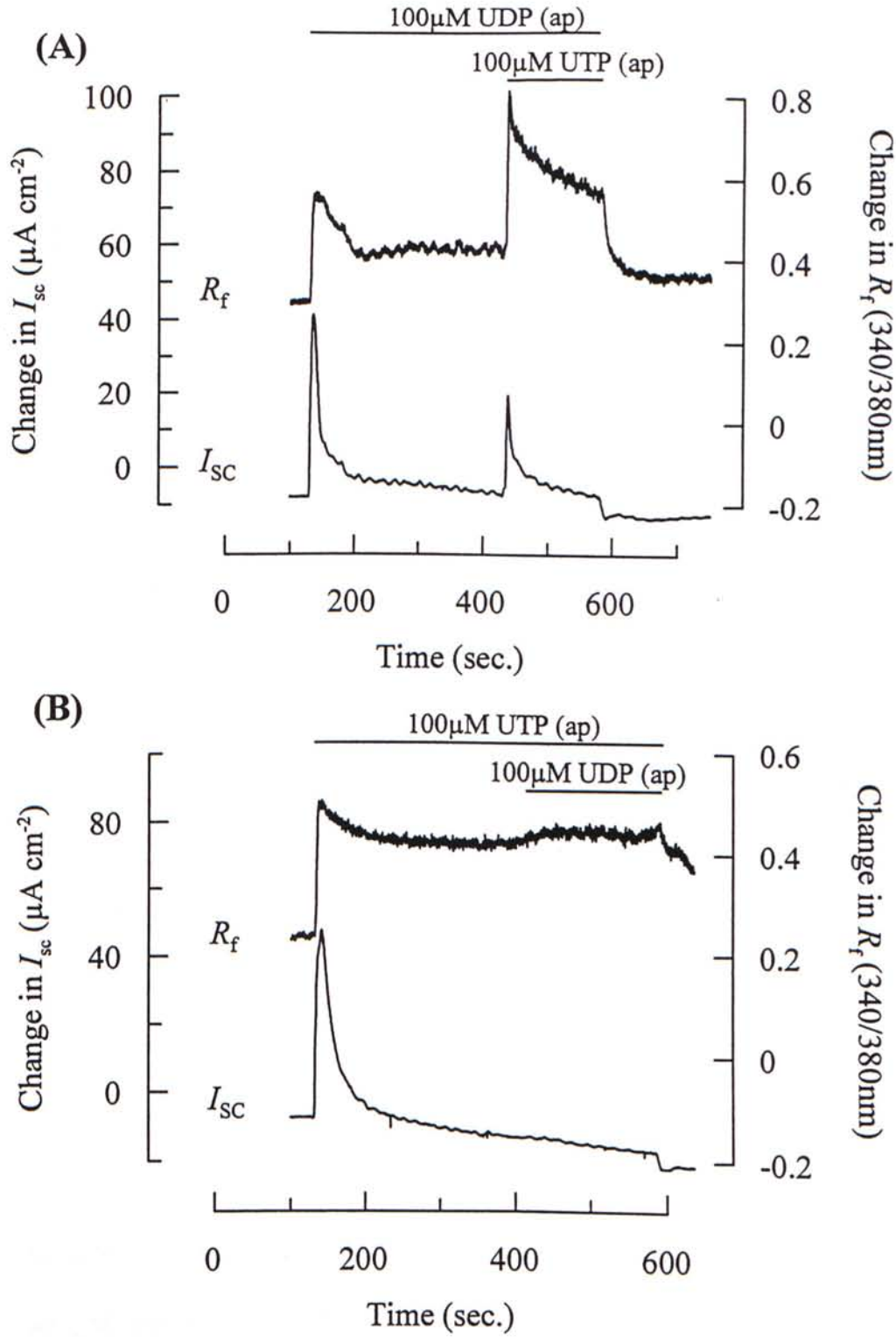

Figure III.4.(h)

Desensitizing effect on the **(A)** R_f and I_{sc} induced by UTP or **(B)** R_f and I_{sc} induced by UDP. Typical I_{sc} and R_f recordings showing the changes in I_{sc} that occur when cultured epithelia are stimulated by **(A)** UDP, followed by UTP or **(B)** *vice versa* to the apical (ap) solution. Essentially identical responses are obtained in 4-6 separate epithelia. Horizontal bars indicate the duration of application.

In the presence of UTP (N=5), UDP was only able to induce the ΔR_f by 0.03±0.01 and ΔI_{sc} by 0.3±0.3μA cm^{-2}. The ΔR_f and ΔI_{sc} induced by UDP were drastically desensitized by 85.3±5.1% and 98.7±1.3% respectively. (Figure III.(4)(h)(B)).

A final series of experiment was done for ATP and UDP. In the presence of ATP (N=5), UDP could induce another ΔR_f by 0.22±0.06 and ΔI_{sc} by 4.6±0.5μA cm^{-2}. The ΔR_f and ΔI_{sc} induced by UDP were partially desensitized by 21.9±19.5% and 62.8±4.2% respectively (Figure III.(4)(i)(A)).

Similarly, in the presence of UDP (N=4), ATP-induced R_f and I_{sc} were partially desensitized by 47.1±16.2% and 62.3±3.1% respectively. The ΔR_f and ΔI_{sc} induced by ATP after the prestimulation of UDP were 0.18±0.06 and 3.8±0.3μA cm^{-2} respectively (Figure III.(4)(i)(B)).

In summary, these findings clearly demonstrated that the I_{sc} induced by the second agonists were also mediated by a $[Ca^{2+}]_i$-dependent mechanism. However, the ion channels responsible for mediating of anion secretion were seemed to be quickly desensitized by the first agonist. After the initial increase to a definite peak, the I_{sc} would gradually returned to the basal level. The nucleotide-induced I_{sc} also seemed to be insensitive to the sustained elevation of $[Ca^{2+}]_i$. With ATP or UDP as the first agonist, addition of another nucleotide into the bathing solution was able to induce another increases in R_f accompanied with I_{sc}. Based on this phenomenon, we speculate that the second agonist could 'reactivate' the ion channels to elicit another increase in I_{sc} by evoking a further increase in $[Ca^{2+}]_i$. In other words, the ΔI_{sc} was sensitive to a change in $[Ca^{2+}]_i$, but not the sustainable elevation of $[Ca^{2+}]_i$.

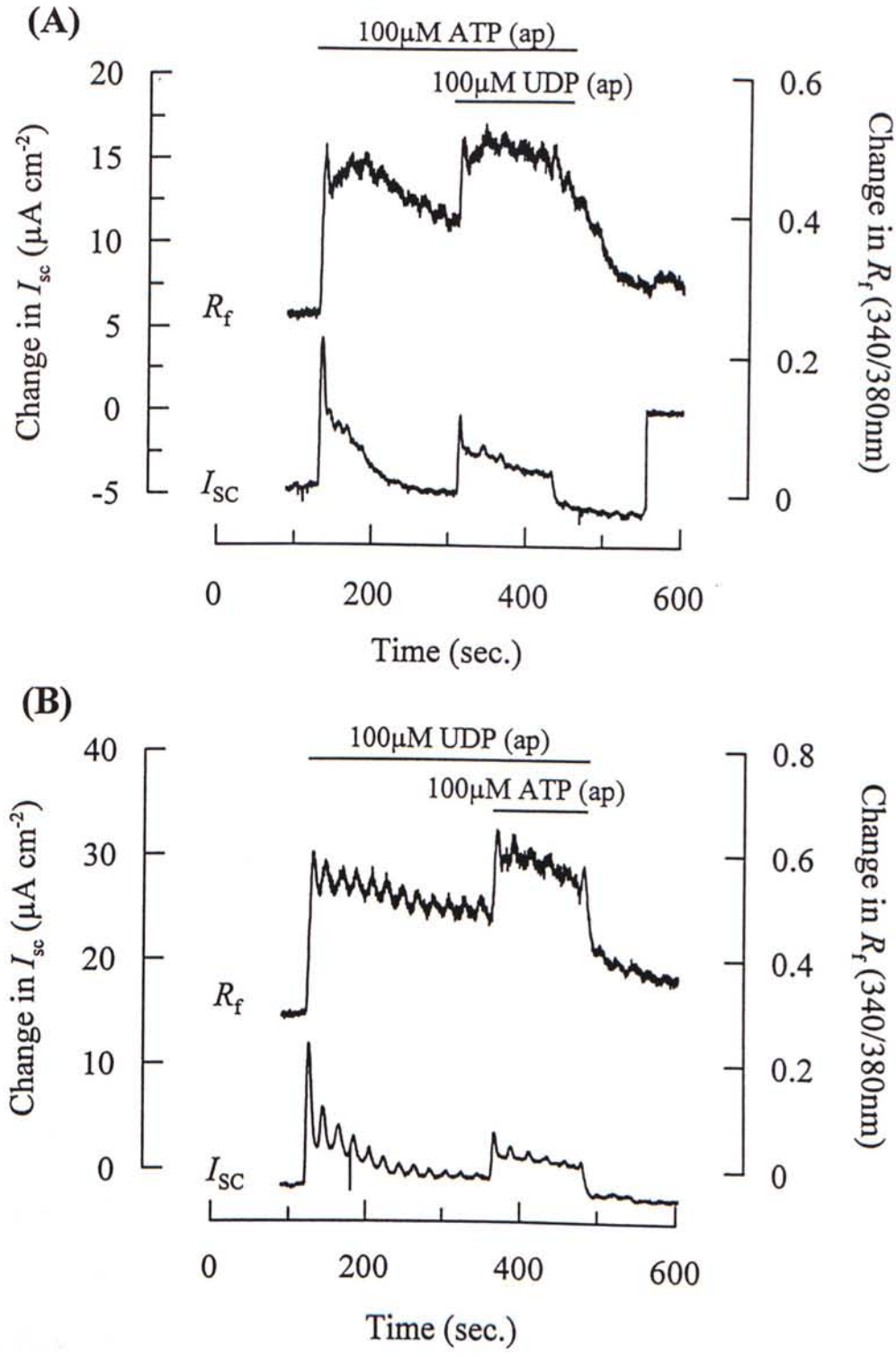

Figure III.4.(i)

Desensitizing effect on the **(A)** R_f and I_{sc} induced by UDP or **(B)** R_f and I_{sc} induced by ATP. Typical I_{sc} and R_f recordings showing the changes in I_{sc} that occur when cultured epithelia are stimulated by **(A)** ATP, followed by UDP or **(B)** *vice versa* to the apical (ap) solution. Essentially identical responses are obtained in 4-6 separate epithelia. Horizontal bars indicate the duration of application.

III.5. Evidence of a $[Ca^{2+}]_i$-independent I_{sc}-component induced by nucleotides

III.5.1. The time course of the ΔR_f and ΔI_{sc}

With the advent of the measurement technique, the kinetics of the ΔI_{sc} and ΔR_f induced by nucleotides could be investigated. These data suggests that the ATP-induced R_f (N=6) was preceded by the I_{sc}. The duration required for the ATP-induced I_{sc} to reach the peak after application (*i.e.* $\mathbf{T_{Isc}(control)}$) was 18.1±0.9 sec. As shown in figure III.5.(a)(A), the ATP-induced I_{sc} was faster than that of R_f to reach the peak. The time required for the ATP-induced R_f to reach the peak was 20.3±0.9 sec., which was 2.3±0.4 sec. after the peak of I_{sc} (*i.e.* $\mathbf{T_{lag}(control)}$).

Apart from ATP, similar patterns were also observed for UTP (N=8), UDP (N=4) and 5-Br-UTP (N=4). A summary of these data were shown in figure III.5.(a) and Table III.1.(a). The existence of a $\mathbf{T_{lag}(control)}$ would speculate the possibility of a $[Ca^{2+}]_i$-independent mechanism for mediating the increase in I_{sc}. However, under this circumstance, we could not exclude the possibility of a constant delay in capturing the R_f signals.

To rule out this possibility, cells were challenged with ionomycin, which elicits cellular responses exclusively *via* a $[Ca^{2+}]_i$-dependent mechanism. In contrast to nucleotides-evoked responses, the ionomycin-induced I_{sc} (N=4) was always preceded by the ΔR_f (Figure III.5.(b)). Based on this observation, the possibility of a delay in capturing the R_f signals could be excluded.

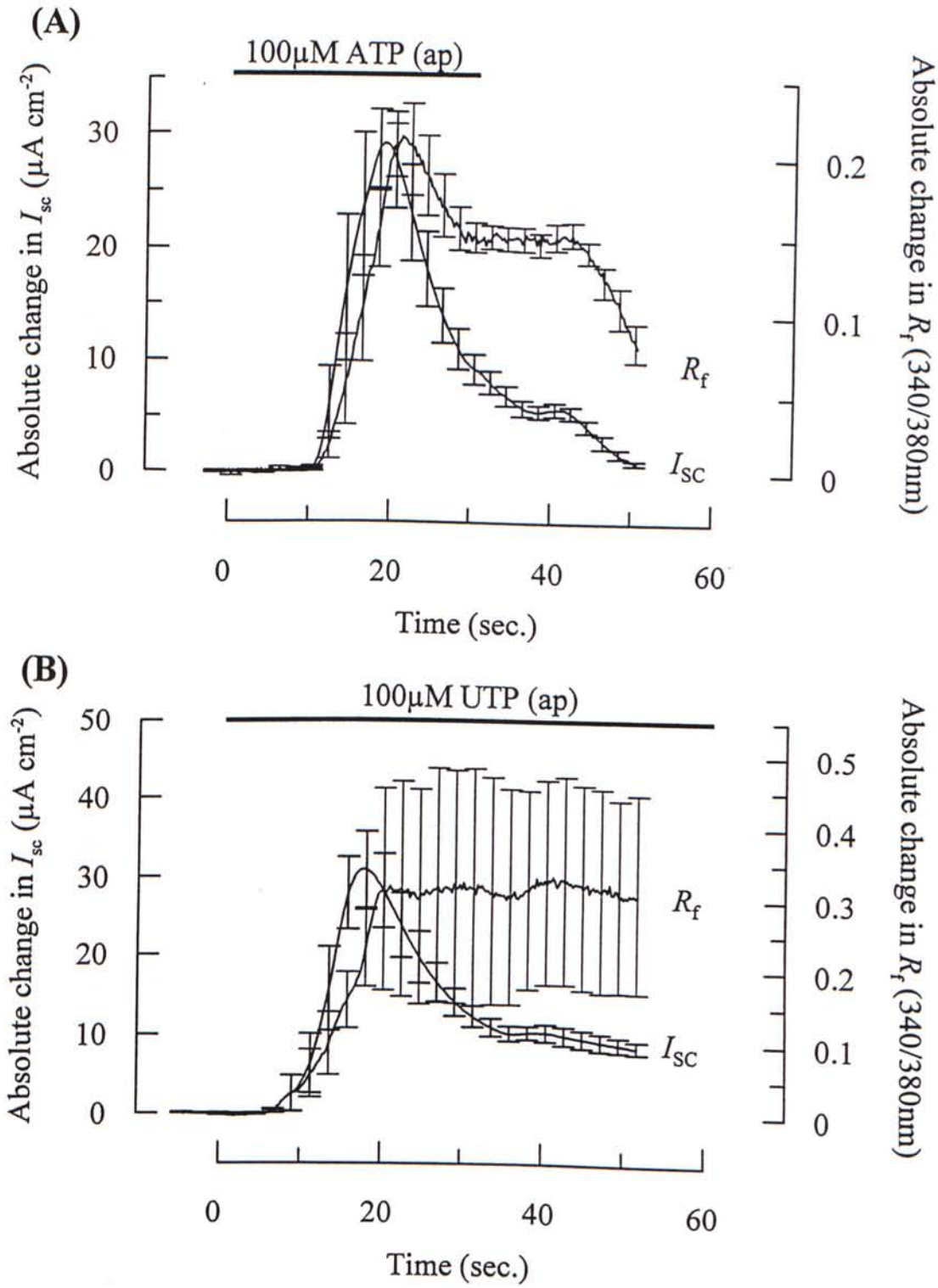

Figure III.5.(a)

Comparison of the time course for the nucleotide-induced R_f and I_{sc}. Epithelia were exposed to **(A)** ATP (N=6) or **(B)** UTP (N=8) at 100μM for a duration as indicated by the horizontal bars. The changes in R_f and I_{sc} were quantified as absolute changes in which the initial basal values were normalized as zero. Data are means for 6-8 separate epithelia. Bars and columns shown above are S.E.M. values.

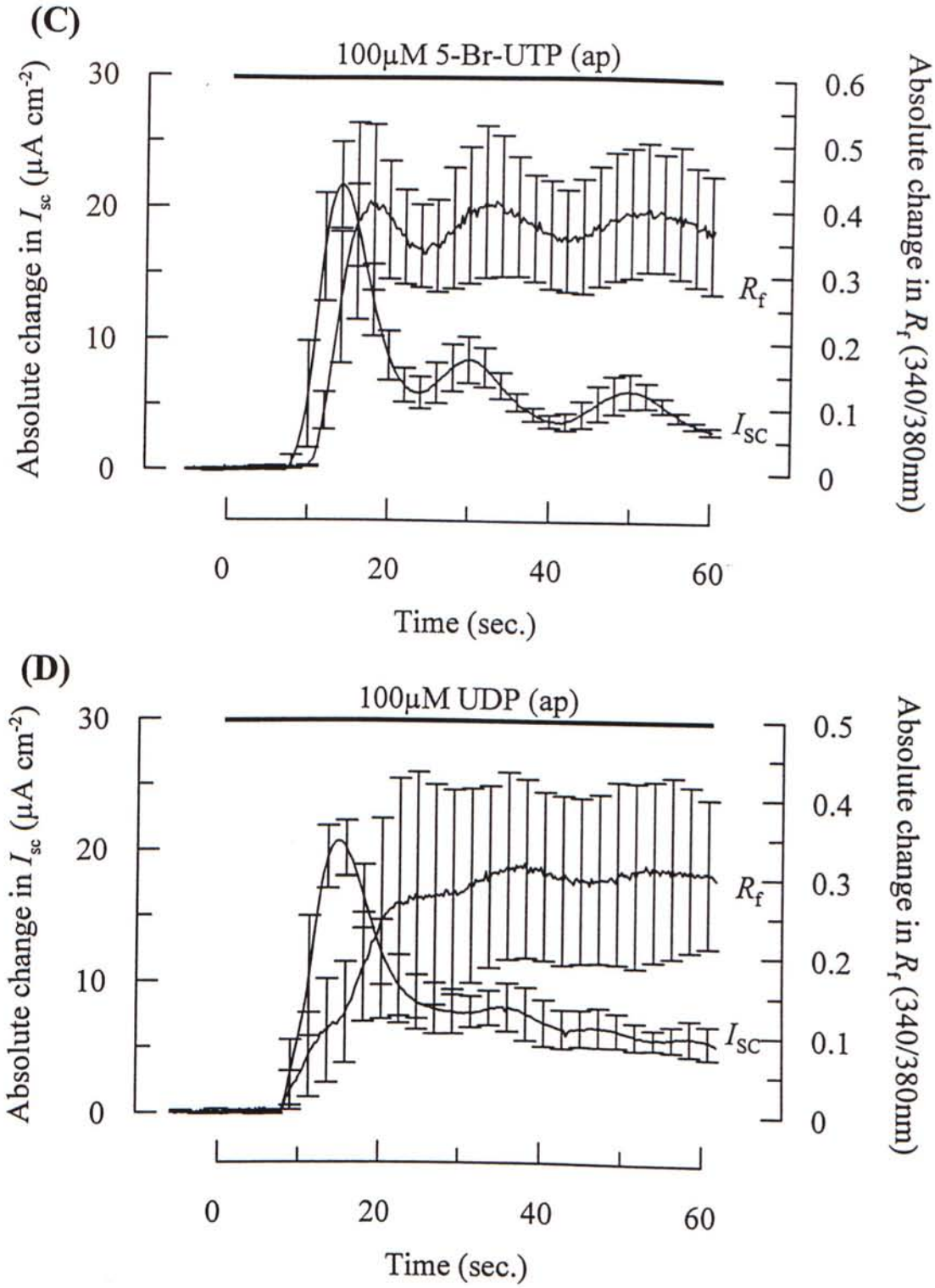

Figure III.5.(a)

Epithelia were exposed to **(C)** 5-Br-UTP (N=4) or **(D)** UDP (N=4) at 100μM for a duration as indicated by the horizontal bars. The changes in R_f and I_{sc} were quantified as absolute changes in which the initial basal values were normalized as zero. Data are means for 4 separate epithelia. Bars and columns shown above are S.E.M. values.

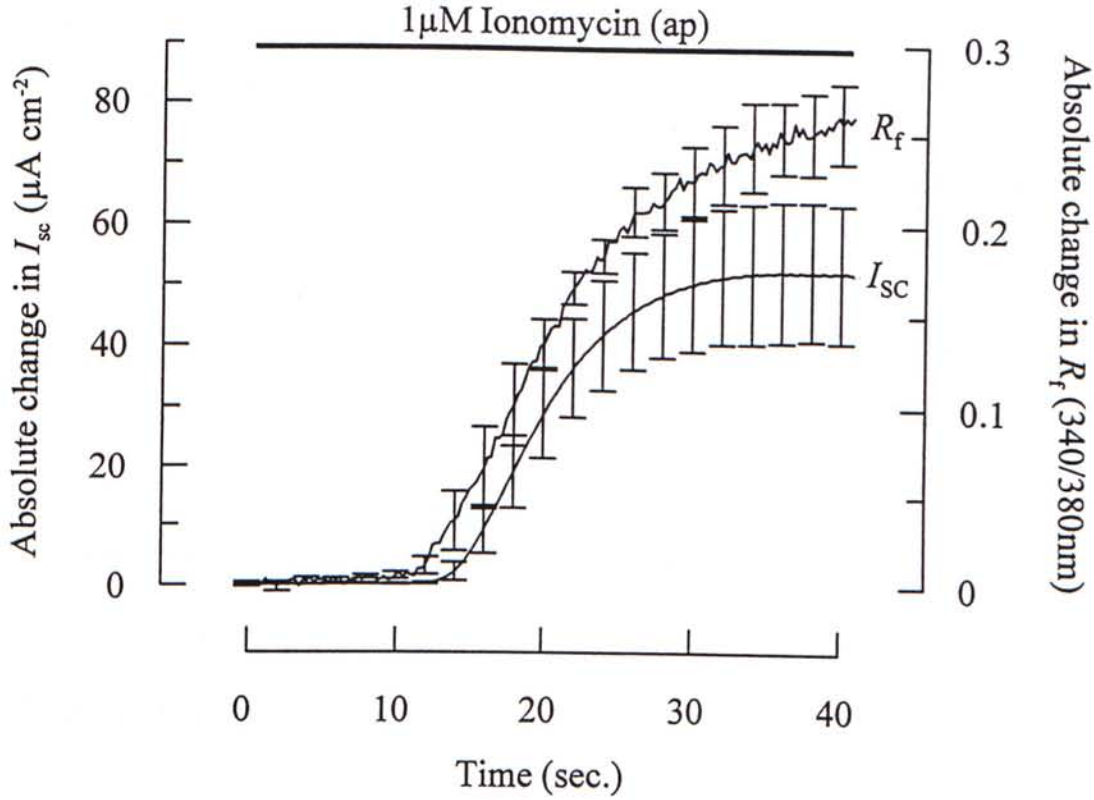

Figure III.5.(b)

Epithelia were exposed to 1μM Ionomycin (N=4) for a duration as indicated by the horizontal bar. The change in R_f and I_{sc} were quantified as absolute changes in which the initial basal values were normalized as zero. Data are means for 4 separate epithelia. Bars and columns shown above are S.E.M. values. Note the ionomycin induced R_f was always faster than that of I_{sc}.

Effect of BAPTA/AM

BAPTA/AM is a pharmacological tool which could presumably abolish any cellular responses mediated *via* a $[Ca^{2+}]_i$-dependent pathway by artificially increasing the cytosolic Ca^{2+} buffering capacity (Tsien, 1980). Therefore, in the following experiments, epithelia were pretreated with 50μM BAPTA/AM in order to further substantiate the possibility of a $[Ca^{2+}]_i$-independent pathway.

With the pretreatment of BAPTA, ATP (N=11) was only able to induce a small ΔI_{sc} by 3.8±1.4μA cm^{-2}. The time required for the ATP-induced I_{sc} (N=6) to reach the peak after application (*i.e.* $\mathbf{T_{Isc}(BAPTA)}$) was 88.3±5.6sec. (Figure III.5.(c)(A)). Under BAPTA pretreatment, ATP could still evoked a small but discernible ΔR_f by 0.15±0.03, although the peak of I_{sc} was even well-dissociated from the peak of R_f. The time required for the ATP-induced R_f to reach the peak was 156.3±14.7 sec., which was 67.9±16.5 sec. after the peak of I_{sc} (*i.e.* $\mathbf{T_{lag}(BAPTA)}$). Similar patterns were also observed in UTP (N=10), UDP (N=9) or 5-Br-UTP (N=11) induced the increases in I_{sc} and R_f. A summary of these data were shown in figure III.5.(c) and Table III.1.(b).

These data revealed that these nucleotides were still capable of inducing the increases in R_f after BATPA pretreatment. It is therefore important to note that a $[Ca^{2+}]_i$-dependent pathway could not be excluded even under BAPTA pretreatment.

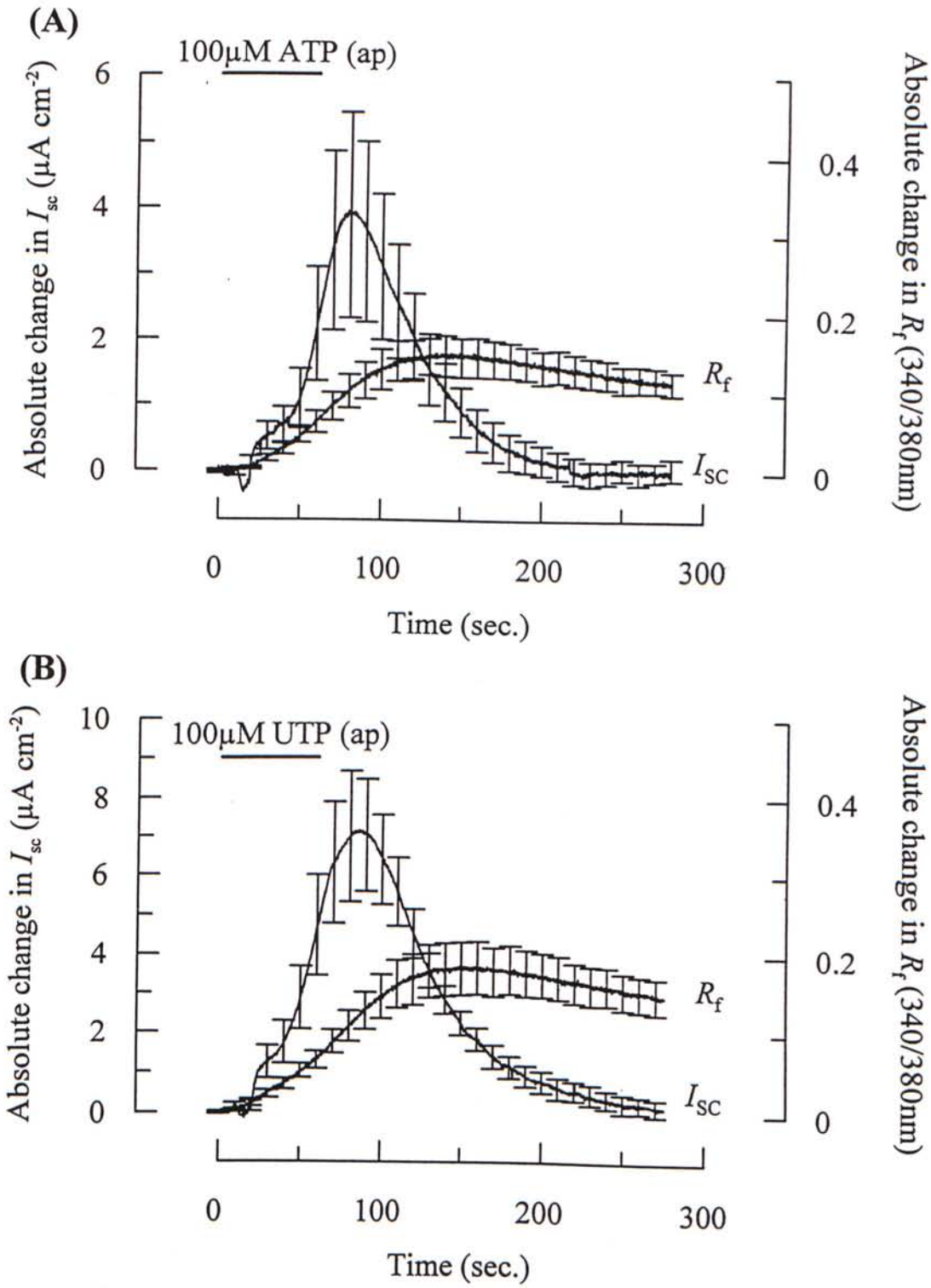

Figure III.5.(c)

Comparison of the time course for the nucleotide-induced R_f and I_{sc} after BAPTA/AM pretreatment. Epithelia were exposed to **(A)** ATP (N=11) or **(B)** UTP (N=10) at 100μM for 1 minute as indicated by the horizontal bars. The changes in R_f and I_{sc} were quantified as absolute changes in which the initial basal values were normalized as zero. Data are means for 10-11 separate epithelia. Bars and columns shown above are S.E.M. values.

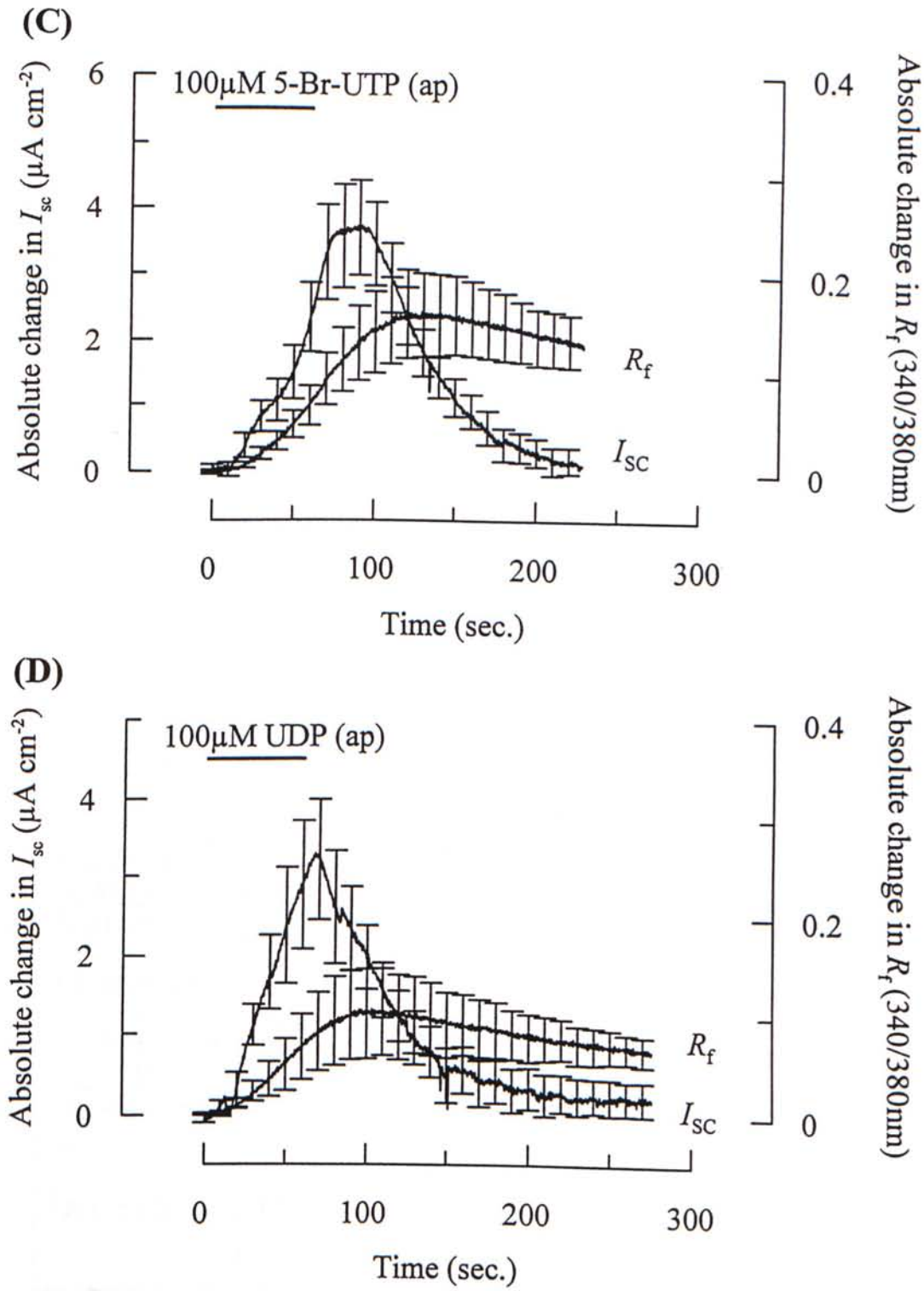

Figure III.5.(c)

Comparison of the time course for the nucleotide-induced R_f and I_{sc} after BAPTA/AM pretreatment. Epithelia were exposed to **(C)** 5-Br-UTP (N=11) or **(D)** UDP (N=10) at 100μM for 1 minute as indicated by the horizontal bars. The changes in R_f and I_{sc} were quantified as absolute changes in which the initial basal values were normalized as zero. Data are means for 9-11 separate epithelia. Bars and columns shown above are S.E.M. values.

Nucleotide	ATP (100μM)	UTP (100μM)	5-Br-UTP (100μM)	UDP (100μM)
T_{lsc}(control)/sec.	18.1±0.9 (N=6)	15.7±1.8 (N=4)	13.9±0.6 (N=4)	14.8±0.8 (N=4)
T_{lag}(control)/sec.	2.3±0.4	3.4±2.2	4.1±0.9	9.3±5.6
ΔI_{sc} at peak ($\mu A\ cm^{-2}$)	29.1±3.4	22.4±7.6	21.6±1.2	20.6±2.1
ΔR_f at peak	0.21±0.03	0.54±0.32	0.41±0.07	0.29±0.12

Table III.5.1.(a) Study of kinetics of the ΔR_f and ΔI_{sc} induced by nucleotides in control epithelia

Nucleotide	ATP (100μM)	UTP (100μM)	5-Br-UTP (100μM)	UDP (100μM)
T_{lsc}(BAPTA)/sec	88.3±5.6 (N=11)	89.6±0.4 (N=10)	86.4±3.9 (N=11)	102.7±26.4 (N=9)
Augmented delay in ΔI_{sc} in folds	3 times	5.7 times	6.2 times	5 times
T_{lag}(BAPTA)/sec	67.9±16.5	76.0±15.7	102.2±24.7	72.8±6.3
Augmented delay in T_{lag}(BAPTA) in folds	29.5 times	22.4 times	24.9 times	7.8 times
ΔI_{sc} at peak ($\mu A\ cm^{-2}$)	3.8±1.4	7.1±1.5	3.3±1.6	1.9±0.4
ΔR_f at peak	0.15±0.03	0.18±0.03	0.15±0.03	0.09±0.03

Table.III.5.1.(b) Study of kinetics of the ΔR_f and ΔI_{sc} induced by nucleotides in BAPTA-pretreated epithelia

III.5.2. Effect of ionomycin on the ΔI_{sc} and ΔR_f induced by nucleotides

To further explore the possibility of a $[Ca^{2+}]_i$-independent mechanism, a different approach was employed in which the epithelia were first stimulated with ionomycin. Application of ionomycin (0.3 μM) (N=18) induced the ΔR_f by 0.22±0.01 to a saturated $[Ca^{2+}]_i$ level accompanied with the ΔI_{sc} by 34.9±2.7μA cm^{-2}. This could abolish the any further increase in $[Ca^{2+}]_i$ induced by subsequent application of nucleotides.

Referring to figure III.5.(d)&(e), stimulating the epithelia with ATP (N=6), UDP (N=5) or UTP (N=4) at 100μM were still capable of evoking a further ΔI_{sc} without any discernible ΔR_f. A summary of these data was shown in figure III.5.(e)(B). No significant differences (P>0.05) were found between the ATP-induced I_{sc} (0.8±0.4μA cm^{-2}), the UDP-induced I_{sc} (1.2±0.5μA cm^{-2}) and the UTP-induced I_{sc} (1.4±0.5μA cm^{-2}).

III.5.3. Effect of thapsigargin on the ΔI_{sc} and ΔR_f induced by nucleotides

In this series of experiments, thapsigargin (*Tg*) was employed. *Tg* can inhibit the Ca^{2+}-ATPase of endoplasmic reticulum (Bradyden *et al.* 1989). Consequently, application of *Tg* (1μM) (N=48) induced the ΔR_f by 0.23±0.02 to a saturated $[Ca^{2+}]_i$ level accompanied with the ΔI_{sc} by 7.8±0.5μA cm^{-2}.

After the pretreatment of *Tg*, application of ATP (N=13) , UDP (N=6) or UTP (N=9) at 100μM were all able to initiate the further ΔI_{sc} without any significant ΔR_f (Figure III.5.(f)&(g)). Data analysis shown that the UTP-induced I_{sc} (3.3±0.9μA cm^{-2}) was significantly (P<0.05) greater than the ATP-induced I_{sc} (1.6±0.5μA cm^{-2}), but no

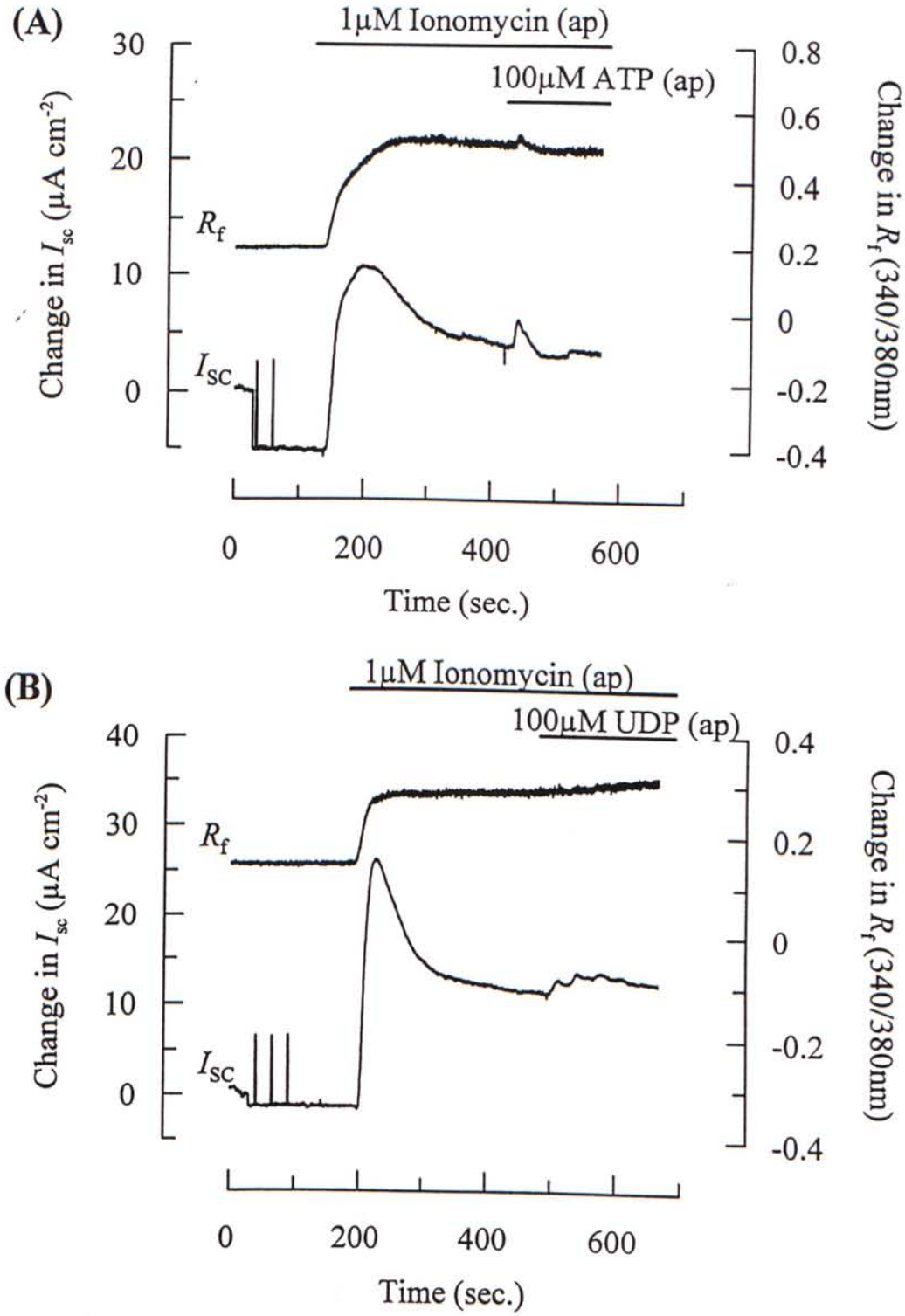

Figure III.5.(d)

Typical I_{sc} and R_f recordings obtained from simultaneous measurement. Epithelia were prestimulated with 1μM ionomycin followed by **(A)** ATP (N=6) or **(B)** UDP (N=6) at 100μM for a duration as indicated by the horizontal bars. Essentially similar results were obtained in 6 separate epithelia.

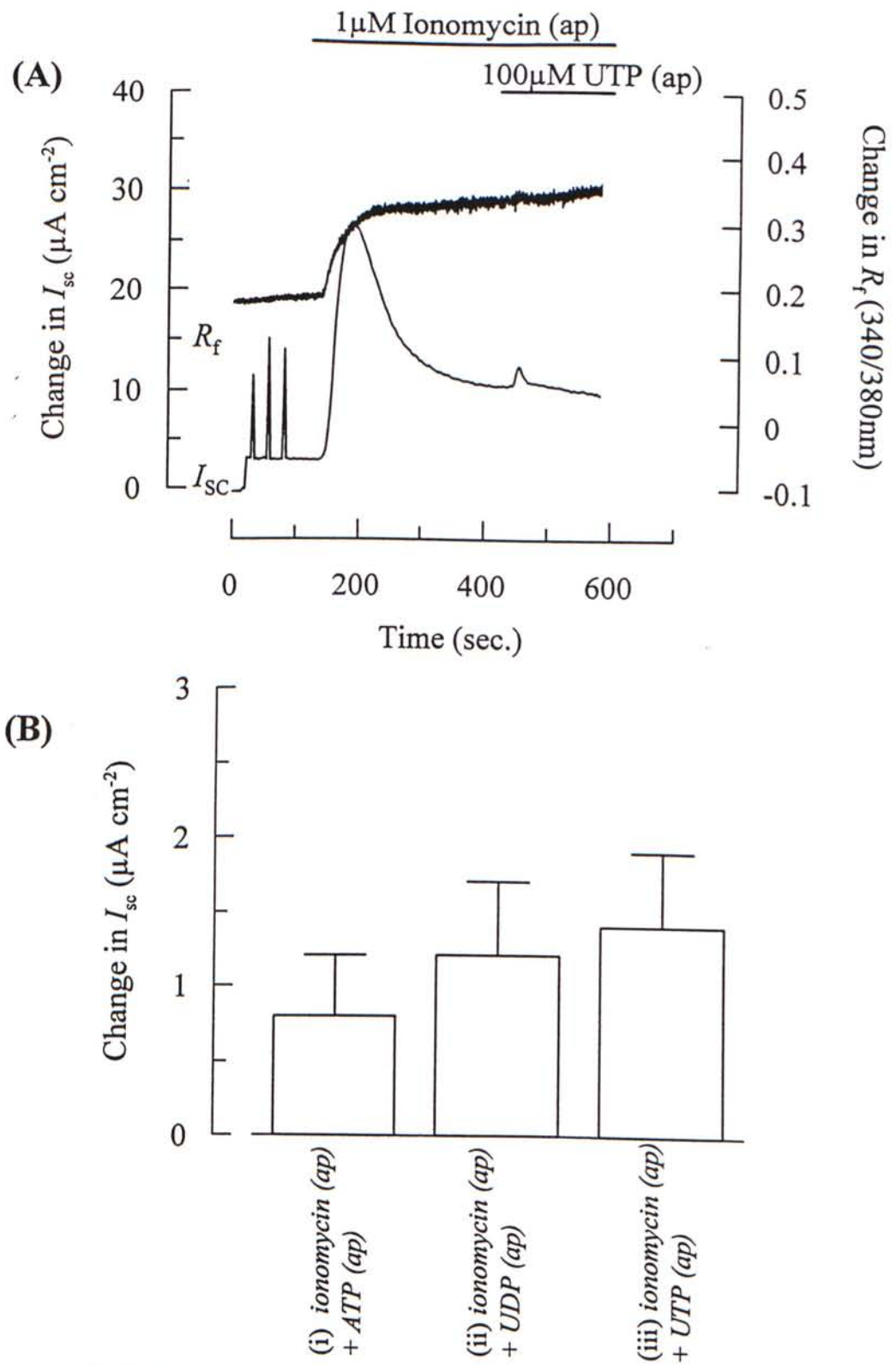

Figure III.5.(e)

(A) Typical I_{sc} and R_f recording obtained from simultaneous measurement. Epithelia were prestimulated with 1μM ionomycin followed by UTP. Essentially similar results were obtained in 4 separate epithelia. **(B)** Column chart summarizing the effect of pretreatment of 1μM ionomycin on **(i)** ATP 100μM (ap); **(ii)** UDP 100μM (ap) or **(iii)** UTP 100μM (ap) induced I_{sc}. Columns and bars are means ± S.E.M. for 4-6 separate epithelia.

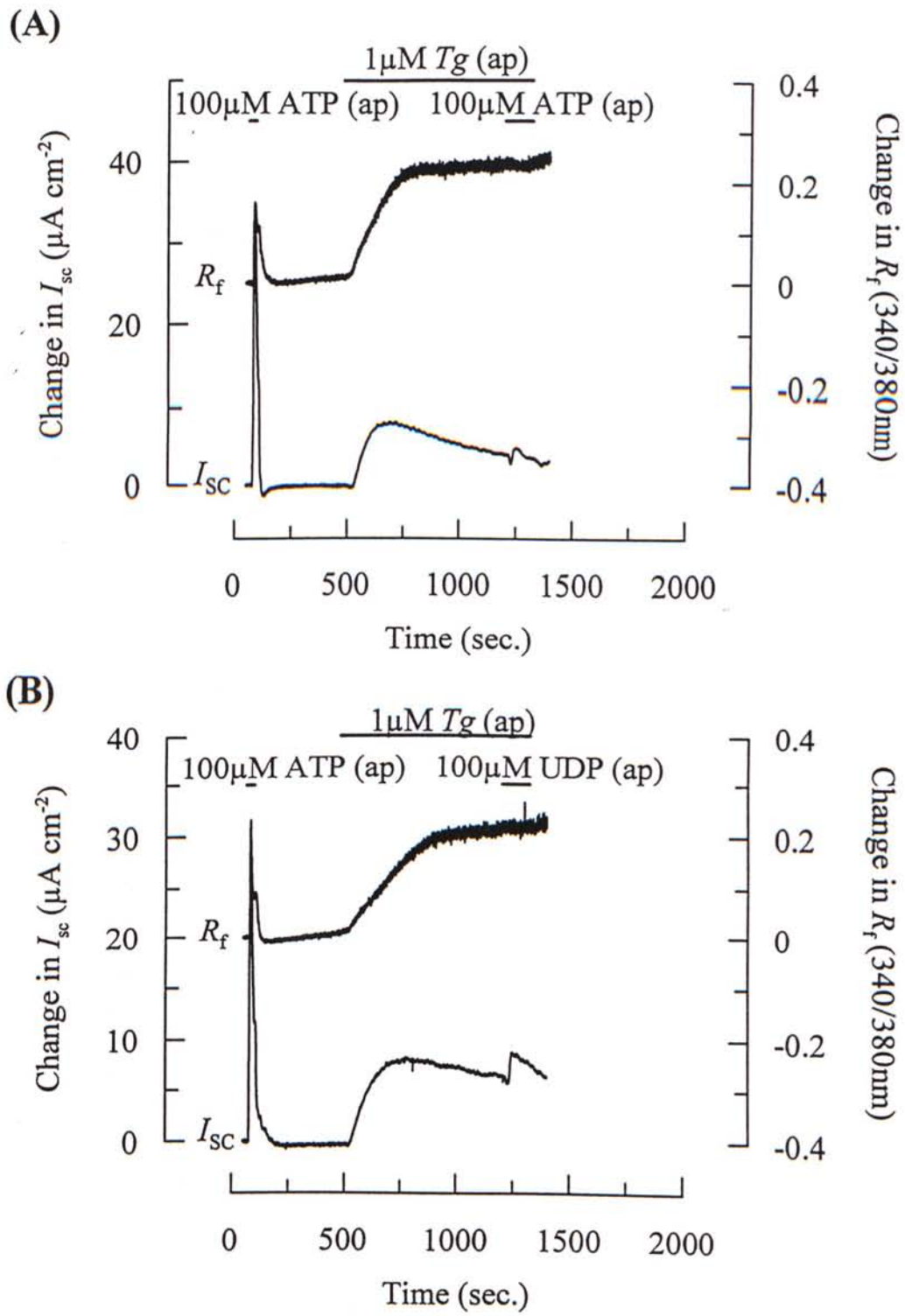

Figure III.5.(f)

Typical I_{sc} and R_f recordings obtained from simultaneous measurement. Epithelia were prestimulated with 1μM thapsigargin (*Tg*) followed by **(A)** ATP (N=13) or **(B)** UDP (N=6) at 100μM for a duration as indicated by the horizontal bars. Essentially similar results were obtained in 6-13 separate epithelia.

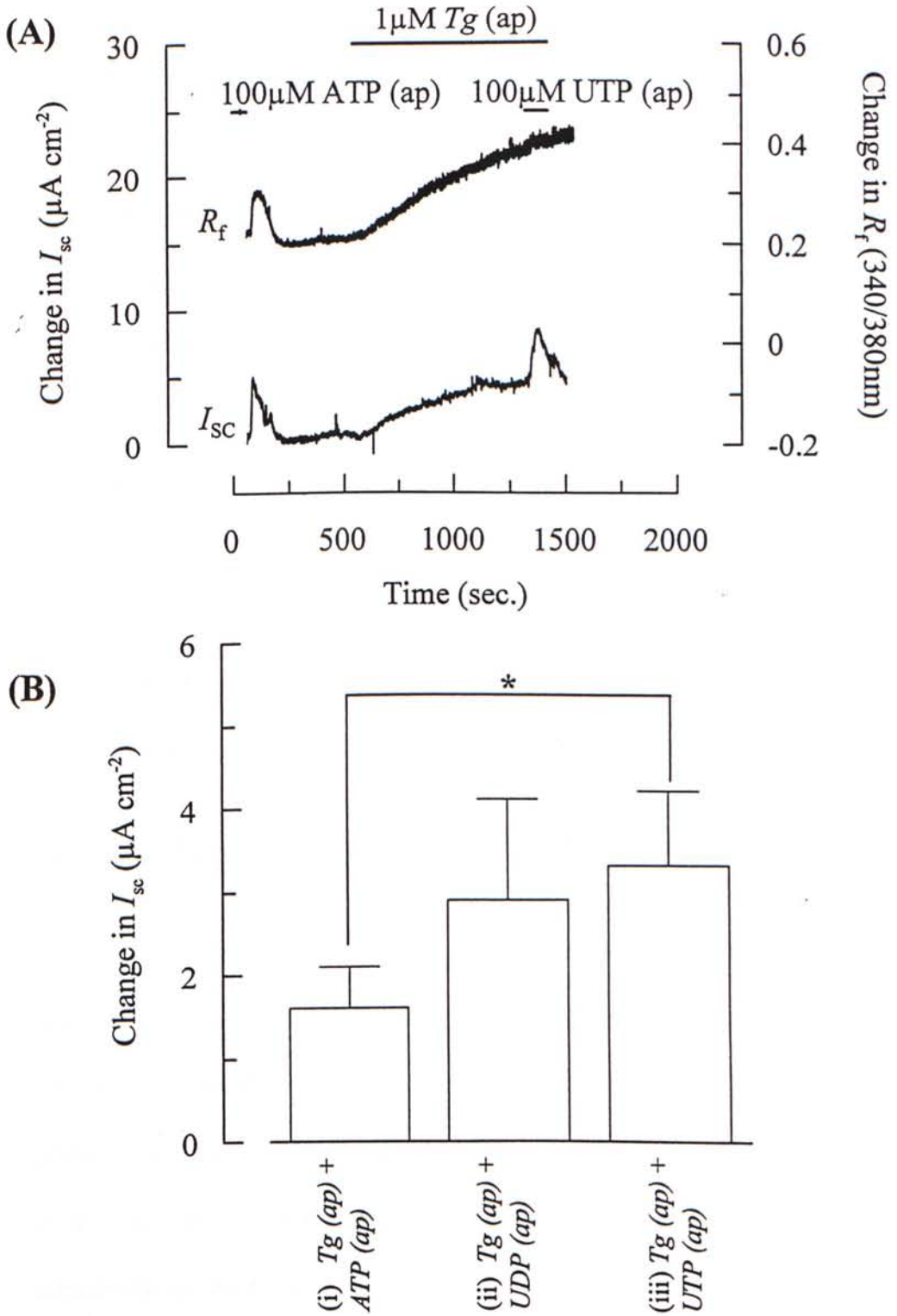

Figure III.5.(g)

(A) Typical I_{sc} and R_f recording obtained from simultaneous measurement. Epithelia were prestimulated with 1μM *Tg* followed by UTP. Essentially similar results were obtained in 9 separate epithelia. **(B)** Column chart summarizing the effect of pretreatment of 1μM *Tg* on **(i)** ATP 100μM (ap); **(ii)** UDP 100μM (ap) or **(iii)** UTP 100μM (ap) induced I_{sc}. Note the difference between the magnitude of ATP-induced I_{sc} and UTP-induced I_{sc} was significant (* $P<0.05$). Columns and bars are means ± S.E.M. for 6-13 separate epithelia.

significant differences were found between the ATP-induced I_{sc} and UDP-induced I_{sc} (2.9±1.2μA cm^{-2}), or that of UTP and UDP (Figure III.5.(g)(B)).

So far, these data presented above strongly suggested the extracellular nucleotides could activate the ΔI_{sc} *via* a $[Ca^{2+}]_i$-independent pathway. However, at the elevated R_f level induced by ionomycin or *Tg*, Fura-2 may be insensitive to any further increase in $[Ca^{2+}]_i$. To exclude this possibility, epithelia were stimulated with *Tg* followed by ionomycin.

Referring to figure III.5.(h), application of *Tg* (N=12) induced the ΔR_f by 0.20±0.02 to a sustained plateau accompanied with the ΔI_{sc} by 9.5±1.2μA cm^{-2}. Under such circumstances, addition of ionomycin was capable of eliciting the further ΔR_f by 0.04±0.02 accompanied with the ΔI_{sc} by 8.5±2.2μA cm^{-2}.

III.5.4. Effect of thapsigargin in nominal Ca^{2+}-free solution

On the other hand, we attempted to clarify whether the $[Ca^{2+}]_i$-independent I_{sc} required an elevated $[Ca^{2+}]_i$ for activation. Therefore, in this final series of experiments, Ca^{2+} was removed from the perfusing solution after the *Tg*-induced R_f reached its plateau. As shown in figure III.5.(i), the removal of external Ca^{2+} reduced the R_f by 0.10±0.02, whereas the I_{sc} was decreased sharply by 12.9±3.9μA cm^{-2} (N=5). Under such circumstances, addition of 100μM ATP to the apical bathing solution was able to trigger another ΔI_{sc} by 4.8±1.5μA cm^{-2}. It is interesting to note that the application of ATP could further reduce the R_f by 0.03±0.00 to a value (0.13±0.03) closed to the initial basal R_f (0.14±0.02).

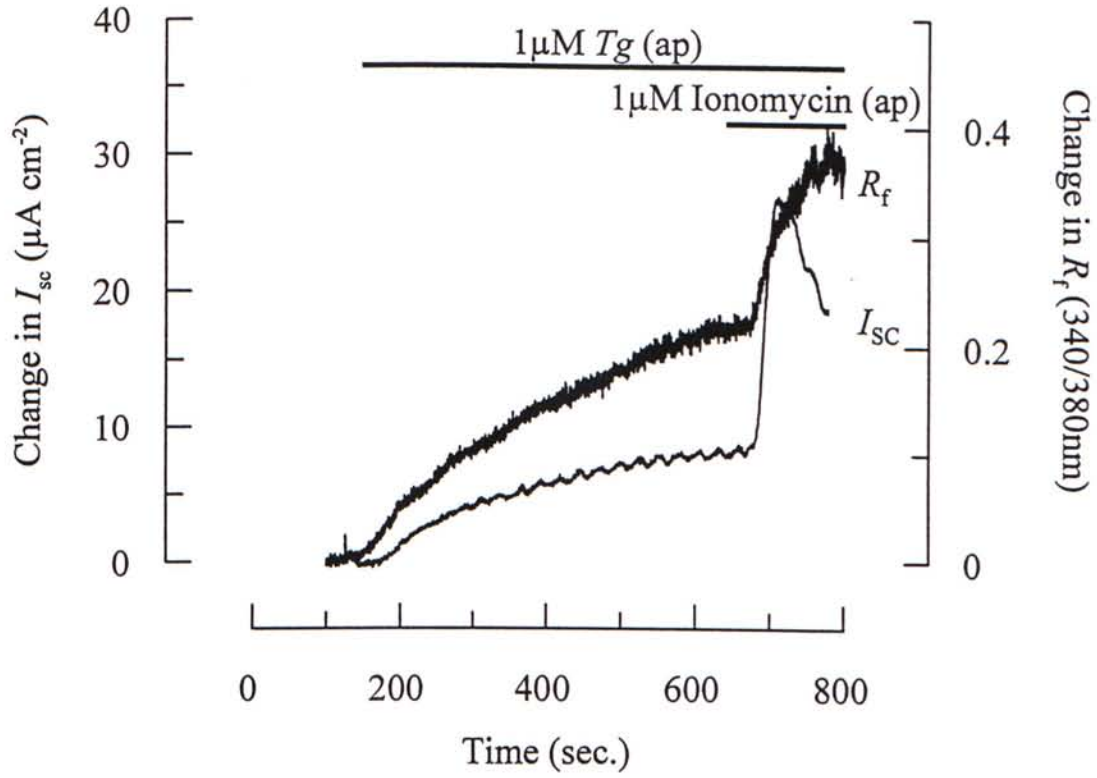

Figure III.5.(h)

Epithelia were prestimulated with 1μM *Tg* followed by 1μM ionomycin for a duration as indicated from the horizontal bars. Essentially similar results were obtained in 12 separate epithelia.

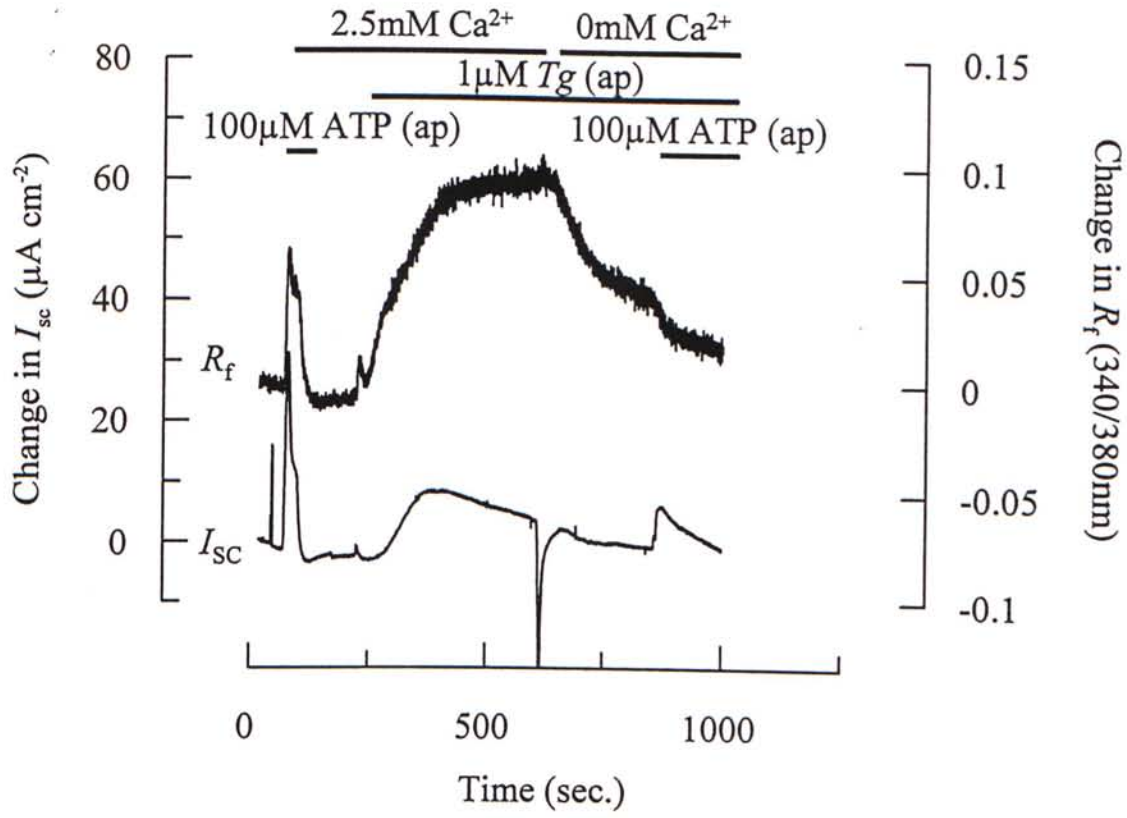

Figure III.5.(i)

Epithelia were prestimulated with 1μM *Tg* followed by removing Ca^{2+} from perfusing solution. After the removal of external Ca^{2+}, 100μM ATP was added for a duration as indicated by the horizontal bars. Essentially similar results were obtained in 5 separate epithelia.

Data analysis revealed that the magnitude of I_{sc} induced by ATP in Ca^{2+}-free solution (4.8±1.5μA cm^{-2}) was significantly larger than that in normal KH solution (1.6±0.5μA cm^{-2}). Such difference suggested that the elevated $[Ca^{2+}]_i$ induced by *Tg* might partially suppress the $[Ca^{2+}]_i$-independent I_{sc}.

Chapter IV. Discussion

IV.1. Role of extracellular nucleotides in epithelial tissues

Previous studies on cultured equine sweat gland epithelial cells had revealed that extracellular ATP could activate the mobilization of $[Ca^{2+}]_i$ accompanied with the electrogenic ion transport (Wilson *et al.* 1993; Ko *et al.* 1994). These findings suggested the involvement of a purinergic component in controlling the sudomotor system. More than one decade ago, extracellular ATP was once proposed as a co-transmitter with noradrenaline from sympathetic nerve endings (Burnstock, 1990). Our data from conventional I_{sc} measurement clearly demonstrated that the P_{2Y}-nucleotide receptors were predominantly located on the apical membrane (Wilson *et al.* 1996). The existence of P_{2Y}-nucleotide receptors on the apical membrane seemed to be a common feature in many other epithelial tissues; such as the epithelia of epididymis, airway, salivary gland and tracheal submucosal gland (Wong, 1988; Mason *et al.* 1991; Xu *et al.* 1996; Yamaya *et al.* 1996). The apically confined P_{2Y}-nucleotide receptors could not be activated by ATP released from periglandular nerves. Obviously, the apical predominance of the P_{2Y} receptors make their physiological role hard to infer, but it has been proposed that ATP, and possibly other nucleotides, may be released across the apical membranes of stimulated epithelia *via* ion channels (Reisin *et al.* 1994). The nucleotides released in this way could activate the apical receptors and so act as autocrine regulators of epithelial transport (Parr *et al.* 1994; Schwiebert *et al.* 1995; Wilson *et al.* 1996; Ko *et al.* 1997).

IV.2. Characterization of an ATP-insensitive P_{2Y}-nucleotide receptor

Evidences for the existence of a separate P_{2Y}-nucleotide receptor

To characterize the P_{2Y}-nucleotide receptor subtypes existing on the apical membrane, a series of cross desensitization experiments were carried out by employing the conventional I_{sc} technique. In this series of experiments, we found that in the presence of 100μM ATP in the apical bathing solution, application of either UTP, 5-Br-UTP or UDP were able to elicit the increases in I_{sc} with minimal desensitizing effects. These results suggest that the pyrimidine nucleotides could induce the increases in I_{sc} *via* an ATP-insensitive, separate receptor population. In fact, the existence of a separate pyrimidine receptor was proposed more than twenty years ago (Urquilla,1978). Concurrent to the findings from human nasal epithelial cells (Lazarowski *et al.* 1997), our results from cultured equine sweat gland epithelial cells was one of the most preceding reports about the existence of such an ATP-insensitive, pyrimidine-selective receptor on the epithelial tissues (Ko *et al.* 1997).

On the other hand, the potent desensitizing effects of UTP on the I_{sc} induced by ATP or UDP may be accounted for the stimulatory effects of UTP on both the ATP-sensitive (P_{2Y2}) and the ATP-insensitive (pyrimidine selective) receptors. In contrast, the prestimulation of either ATP or UDP could only exert a partial desensitizing effect on the UTP-induced I_{sc}. Actually, the coexistence of two different subtypes of P_{2Y} receptors were also well-established in many other cell types (Boehm *et al.* 1995; Yang *et al.*1996; Huber-Lang *et al.* 1997; Metioul *et al.* 1996; Kugelgen *et al.* 1997) as well as epithelial tissues such as MDCK cells (Zegarra-Moran *et al.* 1995; Firestein *et al.* 1996) and human nasal epithelial cells (Lazarowski *et al.* 1997).

Characterization of the ATP-insensitive P_{2Y}-nucleotide receptor

To further characterize the pharmacological properties of the ATP-insensitive receptor, epithelial monolayers were prestimulated with ATP so as to abolish any responses activated by P_{2Y2} receptor. Under ATP-prestimulated conditions, UDP, UTP, 5-Br-UTP or ADP were tested. In the presence of ATP, these nucleotides were able to initiate the increases in I_{sc} in a dose dependent manner. These data strongly indicated the presence of another subtype of P_{2Y} receptor on the apical membrane, which was insensitive to ATP. According to their effectiveness to induce the increases in I_{sc}, UDP was the most effective one, the following were UTP and 5-Br-UTP, whereas ADP was the least effective. Based on these data, we speculated that the pyrimidine-selective and ATP-insensitive receptor existing on the apical membrane belonged to P_{2Y6} subtype. Referring to a recent pharmacological study which based on the [^{3}H] inositol phosphates accumulation induced by different nucleotides at P_{2Y6} receptor, UDP was a potent agonist, whereas UTP, 5-Br-UTP and ADP were much less potent and ATP was essentially inactive (Nicholas *et al.* 1996).

Concurrently, pyrimidine selective P_{2Y}-receptors were also found in the apical membrane of cultured human airway epithelia (Lazarowski *et al.* 1997) and coloncytes (Inoue *et al.* 1997). The existence of the pyrimidine selective receptors on different epithelial tissues may further substantiate that these receptors could play a distinct role in the regulation of ionic secretion.

Possible interaction between ATP and UDP

In the present study, we found that ATP could partially desensitize the UDP-induced I_{sc} and *vice versa*. However, a pharmacological study of different P_{2Y}

subtypes performed by Nicholas (1996) had reported that purified UDP was essentially inactive at P_{2Y2} receptor, whereas ATP was also unable to induce any cellular responses at P_{2Y6} receptor. One possible explanation for the interaction between ATP and UDP was due to the depletion of common Ca^{2+} internal stores. Another possibility was the interactions between these two nucleotides at the receptor level. To circumvent this dilemma, the cross desensitizing protocol was carried out for ATP and bradykinin. ATP and bradykinin are acting on separate receptor families, and hence these unrelated agonists should not have any interaction at receptor level. According to our data, the desensitizing effect of ATP to bradykinin-induced I_{sc} suggested the partial desensitizing patterns among ATP and UDP could be due to the depletion of common Ca^{2+} internal stores, although the possibility of interaction between ATP and UDP at receptor level could not be excluded. Moreover, our data were also found to be consistent with another studies about the desensitizing effects on bradykinin-induced increases in $[Ca^{2+}]_i$ by ATP or UTP in a neuronal cell line (Czubayko *et al.* 1996).

IV.3. Expression of the novel ATP-insensitive receptor on a functionally polarized epithelia

Different cellular responses of non-polarized epithelial cells to functionally polarized epithelia

As mentioned in previous chapter, purified ADP and UDP were unable to elicit any responses in non-polarized epithelial cells in $[Ca^{2+}]_i$ measurement. However, these nucleoside diphosphates were able to elicit responses in functionally polarized epithelia in conventional I_{sc} measurement (Ko *et al.* 1997). These

controversial results suggested that the increase in I_{sc} induced by these diphosphates may be mediated through a $[Ca^{2+}]_i$-independent pathway. It could be also due to the non-polarized cells grown on glass coverslips in $[Ca^{2+}]_i$ measurement did not express the novel pyrimidine selective P_{2Y}-receptor.

However, our data from conventional I_{sc} measurement had demonstrated that the UDP-induced I_{sc} was sensitive to the BAPTA pretreatment. In other words, the UDP-induced I_{sc} was also depended on the $[Ca^{2+}]_i$ level at a certain extent, although the involvement of a $[Ca^{2+}]_i$-independent mechanism could not be excluded.

UDP and ADP induced the ΔR_f and ΔI_{sc} on functionally polarized epithelia

With the distinct advantage of simultaneous measurement, we could directly illustrate that the UDP or ADP induced I_{sc} required an elevation of $[Ca^{2+}]_i$ for activation. Apparently, these diphosphates were only able to induce the increases in $[Ca^{2+}]_i$ on functionally polarized epithelia, but were essentially inactive on non-polarized epithelial cells in $[Ca^{2+}]_i$ measurement. These results strongly suggested that the polarization of epithelia is a crucial step for the expression of the novel pyrimidine-selective P_{2Y} receptor on the epithelial monolayer. It is therefore possible that the polarized epithelial cells may express such a pyrimidine-selective receptor if maintained under the appropriate conditions (Inoue *et al.* 1997; Lazarowski *et al.* 1997). For the cells grown on permeable supports used in I_{sc} measurement, their polarization was confirmed by a previous study in which the cross-section of the epithelial monolayer was examined with electron microscopy (EM). The EM pictures clearly displayed the apical/basolateral polarity as well as the possessing of junctional complexes and short and numerous microvilli at the apical side (Ko *et al.* 1996*a*). Therefore, the equine sweat gland epithelial cells grown on permeable supports will

adopt a polarized phenotype. The unawareness of such a criterion for expressing the pyrimidine-selective receptor may greatly underestimate the occurrence of this novel receptor in many other epithelia (Dubyak and El-Moatassim,1993). In contrast to this novel receptor, the well-documented P_{2Y2}-receptor seemed to be present in both the polarized epithelial monolayer and non-polarized epithelial cells (Ko *et al.* 1994; Wilson *et al.* 1995; Wilson *et al.* 1998). Similar to our findings, a recent study on a human leukemic cell line had reported that the expression of different subtypes of P_{2Y} receptors was regulated by a programmed change at different developmental stages (Clifford *et al.* 1997).

IV.4. Involvement of a $[Ca^{2+}]_i$-independent I_{sc} induced by nucleotides

The time course of the nucleotides-induced increases in R_f and I_{sc}

In the present study, our data obtained from simultaneous measurement had revealed that the increase in R_f induced by nucleotides was always preceded by the increase in I_{sc}. The delay in the time course of the R_f to reach the peak after that of I_{sc} could suggest the possibility of a $[Ca^{2+}]_i$-independent I_{sc}. However, it may be still debatable that such a small delay could be due to a constant time lag in capturing the R_f signals during experiments. To circumvent this problem, epithelial monolayers were challenged with ionomycin, which could activate an increase in I_{sc} exclusively *via* a $[Ca^{2+}]_i$-dependent pathway. Obviously, our data had clearly shown that the ionomycin-induced R_f was always faster than that of I_{sc}. Therefore, we can rule out the possibility of a technical problem in capaturing the R_f signals.

The increases in R_f and I_{sc} after BAPTA pretreatment

In order to explore the possibility of a $[Ca^{2+}]_i$-independent I_{sc} component, epithelial monolayers were preincubated with BAPTA. BAPTA/AM is an intracellular Ca^{2+} chelator which could presumably abolish any cellular response mediated *via* the $[Ca^{2+}]_i$-dependent pathway by increasing the $[Ca^{2+}]_i$ buffering capacity (Boeynaems *et al.* 1993). Out of our expectation, the present findings had clearly demonstrated that BAPTA pretreatment was unable to completely abolish the increase in R_f induced by nucleotides. Therefore, under BAPTA pretreatment, the involvement of an elevation of $[Ca^{2+}]_i$ for inducing the I_{sc} could not be excluded. Nevertheless, it may be more important to note that under normal conditions without measuring $[Ca^{2+}]_i$, the assumption that BAPTA-treatment could completely abolish any $[Ca^{2+}]_i$-dependent event may be incorrect.

Nucleotide-induced I_{sc} after the prestimulation of ionomycin or thapsigargin

Due to the ineffectiveness of BAPTA, another experimental approach was employed in order to further substantiate the $[Ca^{2+}]_i$-independent I_{sc}. Two pharmacological tools: ionomycin and thapsigargin (*Tg*) were used so as to increase the R_f to a sustained elevated level. At an elevated $[Ca^{2+}]_i$, addition of nucleotides were unable to elicit any further increase in R_f but yet capable of evoking a discernible increase in I_{sc}. Unequivocally, these data strongly suggested that the nucleotides were able to stimulate a Cl^- conductance that did not rely on a change in $[Ca^{2+}]_i$. However, someone may argue that the fluorescence dye (Fura-2) we used in these experiments may be saturated. Nevertheless, our data also showed that ionomycin was still able to induce further increases in R_f and I_{sc} even under *Tg*-

prestimulated condition. Thus, we can exclude the possibility of the insensitivity of Fura-2 to any changes in $[Ca^{2+}]_i$ under such experimental condition. However, these results could not rule out the possibility that an elevated $[Ca^{2+}]_i$ level was required for the activation of this $[Ca^{2+}]_i$-independent I_{sc}. Therefore, the final series of experiments were done in which the *Tg*-prestimulated epithelia were exposed to Ca^{2+}-free bathing solution in order to return the elevated $[Ca^{2+}]_i$ to the basal level. Under such circumstances, ATP was able to elicit an increase in I_{sc}, and we can confirm the $[Ca^{2+}]_i$-independent I_{sc} induced by ATP did not require an elevated $[Ca^{2+}]_i$ level for activation. However, it was still remained unknown that why ATP could further reduce the R_f to the basal level in Ca^{2+}-free bathing solution.

The existence of such a $[Ca^{2+}]_i$-independent Cl^- conductance mediated by P_{2Y}-nucleotide receptor was also reported in airway epithelia (Stutts *et al.* 1994), tracheal epithelia (Hwang *et al.* 1996), intestinal epithelia (Inoue *et al.* 1997) and coloncytes (HT-29) (Guo *et al.* 1995; Guo *et al.* 1997). Nevertheless, to the best of my knowledge, our data was the first to provide a direct evidence of such a $[Ca^{2+}]_i$-independent I_{sc} measured from a simultaneous method. In contrast, the studies presented above were reported from separate patch clamp studies and $[Ca^{2+}]_i$ measurement from non-polarized cells (Guo *et al.* 1995; Guo *et al.* 1997) or separate $[Ca^{2+}]_i$ measurement from the non-polarized epithelial cells and conventional I_{sc} measurement (Stutts *et al.* 1994; Hwang *et al.* 1996; Inoue *et al.* 1997).

However, it was still remained unknown for the cellular component responsible for the $[Ca^{2+}]_i$-independent Cl^- conductance. In the airway epithelia, the $[Ca^{2+}]_i$-independent I_{sc} was proposed to be elicited by direct coupling of the P_{2Y}-nucleotide receptor with a ion channel or a G-protein subunit for mediating the Cl^-

secretion (Stutts *et al.* 1994). Nonetheless, another study had demonstrated that a Ptx-sensitive G-protein can directly regulate a Outwardly Rectified Chloride Channel (ORCCs) (Ismailov *et al.* 1996). To investigate the $[Ca^{2+}]_i$-independent Cl^- conductance, further experiments should be carried out to identify the chloride channels which are responsible for such a $[Ca^{2+}]_i$-independent mechanism.

In summary, the results presented above have contributed to the better understanding of the purinergic/pyrimidinergic regulation of epithelial secretion. Apart from the well-documented P_{2Y2}-receptor, which have been already clearly demonstrated in the previous study (Ko *et al.* 1994), our data from cross desensitization experiments had strongly suggested the existence of a novel pyrimidine-selective receptor on the apical membrane. Moreover, we had revealed that the formation of a polarized monolayer was crucial for the expression of this novel receptor on the apical membrane. The unawareness of such a criterion for expressing the novel P_{2Y}-receptor in the past years may underestimate its physiological role and importance in transepithelial ion transport. With the advancement of the measurement method, we could monitor the changes in I_{sc} and R_f concurrently. By employing this technique, we can demonstrate that the nucleotides-induced I_{sc} may involve a $[Ca^{2+}]_i$-independent component.

Chapter V. References

Bennett, W.D., Olivier, K.N., Zeman, K.L., Hohneker, K.W., Boucher, R.C. and Knowles, M.R. (1996). Effect of Uridine 5'-Triphosphate Plus Amiloride on Mucociliary Clearance in Adult Cystic Fibrosis. *Am. J. Respir. Crit. Care Med.* **153**, 1796-1801.

Bijman, J. and Quinton, P.M. (1984). Predominantly β-adrenegic control of equine sweating. *A. J. Physiol.* **246**, R349-R353.

Bijman, J. and Quinton, P.M. (1984). Influence of calcium and cyclic nucleotides on β-adrenegic sweat secretion in equine sweat gland . *A. J. Physiol.* **247**, C10-C13.

Bradyden, D.J., Hanley, M.R., Thastrup, O. and Cuthbert, A.W. (1989). Thapsigargin, a new calcium-dependent epithelial anion secretagogue. *Brit. J. Pharm.* **98**, 809-816.

Burnstock, G. (1980). Purinergic nerves and receptors. *Prog. Biochem, Pharmacol.* **16**, 141-154.

Burnstock, G. (1990). Noradrenaline and ATP as cotransmitters in sympathetic nerves. *Neurochem. Int.* **17**, 251-274.

Boehm, S., Huck, S. and Illes, P. (1995). UTP and ATP trigger transmitter release from rat sympathetic neurones via separate receptors. *Brit. J. Pharm.* **116**, 2341-2343.

Boeynaems, J.M. Heilporn, S. Broeders, F. and Braekman, J.C. (1993). Enhancement of the endothelial production of prostacyclin by substituted derivatives of BAPTA-AM. *European Journal of Pharm.* **233(1)**, 13-20.

Boeynaems, J.M., Communi, D., Pirotton, S., Motte, S. and Parmentier, M.. (1996). Involvement of distinct receptors in the actions of extracellular uridine nucleotides: *P_2 purinoceptors: localisation, function and transduction mechanisms..* (Ciba Foundation Symposium 198) John Wiley & Sons. pp266-277.

Chang, K., Hanaoka, K., Kumada, M. and Takuwa, Y. (1995). Molecular cloning and functional analysis of a novel P_2 nucleotide receptor. *J. biol. Chem.* **270**, 26152-26158.

Clifford, E.E., Martin, K.A., Dalal, P., Thomas, R. and Dubyak G.R. (1997). Stage-specific of P_{2Y} receptors, ecto-apyrase and ecto-5'-nucleotidase in myeloid leukocytes. *A. J. Physiol.* **273**, C973-C987.

Cockcroft, S. and Stutchfield, J. (1989). ATP stimulates secretion in human neutrophils and HL60 cells *via* a pertussis toxin-sensitive guanine nucleotide-binding protein coupled to phospholipase C. *FEBS Lett.* **245**, 25-29.

Communi, D., Pirotton, S., Parmentier, M. and Boeynaems, J.M. (1995). Cloning and functional expression of a human uridine nucleotide receptor. *J. biol. Chem.* **270**, 30849-30852.

Communi, D., Pirotton, S., Parmentier, M. and Boeynaems, J.M. (1996). Cloning, functional expression and tissue distribution of the human P_{2Y6} receptor. *Biochem. Biophys. Res. Commun.* **222**, 303-308.

Communi, D. and Boeynaems, J.M. (1997). Receptors responsive to extracellular pyrimidine nucleotides. *Trends in Pharmacol. Sci.* **18**, 83-86.

Czbayko, U. and Reiser, G. (1996). Desensitisation of P_{2U} receptor in neuronal cell line. *Biochem. J.* **320**, 215-219.

Dubyak, G.R. and El-Moatassim, C. (1993). Signal transduction via P_2-purinergic receptors for extracellular ATP and other nucleotides. *A. J. Physiol.* **265**, C577-C606.

Dubyak, G.R., Cowen, D.S. and Meuller, L.M. (1988). Activation of inositol phospholipid breakdown in HL60 cells by P_2-purinergic receptor for extracellular ATP. Evidence for a mediation by both pertussis toxin-sensitive and pertussis toxin-insensitive mechanisms. *J. biol. Chem.* **263**, 18108-18117.

Erb, L, Garrad, R., Wang, Y., Quinn, T., Turner, J.T. and Weisman G.A. (1995). Site-directed mutagensis of P_{2U}-purinoceptors: Positively charged amino acids in transmembrane helices 6 & 7 affect agonist potency and efficacy. *J. bioil. Chem.* **270**, 4185-4188.

Filtz, T.M., Harden, T.K. and Nicholas, R.A. (1997). Structure, Pharmacological Selectivity, and Second Messenger Signaling Properties of G-protein coupled P_2-purinergic receptors: *Puriinergic Approaches in Experimental Therapeutics.* (Kenneth, A.J. and Jarvis, M.F.) ©Wiley-Liss, Inc. pp39-53.

Firestein, B.L. Xing, M., Hughes, R.J., Corvera, C.U. and Insel, P.A. (1996). Heterogeneity of P_{2U}- and P_{2Y}-purinergic receptor regulation of phospholipases in MDCK cells. *A. J. Physiol.* **271**, F610-F618.

Gogelein, H., Dahlem, D., Englert, H.C. and Lang, H.J. (1990).Flufenamic acid, mefenamic acid and niflumic acid inhibit single nonselective cation channels in the rat exocrine pancreas. *FEBS Letters.* **268**, 79-82.

Guo, X., Merlin, D., Harvey, R.D. Laboisse, C. and Hopfer, U. (1995). Stimulation of Cl^- secretion by extracellular ATP does not depend on increased cytosolic Ca^{2+} in HT-29.cl16E. *A. J. Physiol.* **269**, C1457-C1463.

Guo, X., Merlin, D., Harvey, R.D. Laboisse, C. and Hopfer, U. (1997). Pharmacological Evidence that Calcium is Not Required for P_2-Receptor-Stimulated Cl^- Secretion in HT-29.cl16E. *J. Membrane Biol.* **155**, 239-246.

Harden, T.K., Boyer, J.L. and Nicholas, R.A. (1995). P_2-purinergic receptors: Subtype-Associated Signaling Responses and Structure. *Annu. Rev. Pharmacol. Toxicol.* **35,** 541-579.

Harden, T.K., Lazarowski E.R. and Boucher, R.C. (1997). Release, metabolism and interconversion of adenine and uridine nucleotides: implications for G-protein coupled P_2 receptor agonist selectivity. *Trends in Pharmacol. Sci.* **18,** 43-46.

Huber-Lang, M., Fishcer, K.G. Gloy, J., Schollmeyer, P., Kramer-Guth, A., Greger, R. and Pavenstadt, H. (1997). UTP and ATP induce different membrane voltage responses in rat mesangial cells. *A. J. Physiol.* **272**, F704-F711.

Hwang, T.H., Schwiebert, E.M., and Guggino, W.B. (1996). Apical and basolateral ATP stimulates tracheal epithelial chloride secretion via multiple purinergic receptors. *A. J. Physiol.* **270**, C1611-C1623.

Inoue, C.N., Woo, J.S., Schwiebert, E.M., Morita, T., Hanaoka, K., Guggino, S.E. and Guggino, W.B. (1997). Role of purinergic receptors in chloride secretion in Caco-2 cells. *A. J. Physiol.* **272**, C1862-C1870.

Ismailov, I.I., Jovov, B., Fuller, C.M., Derdiev, B.K., Keeton, D.A. and Benos, D.J. (1996). G-protein Regulation of Outwardly Rectified Epithelial Chloride Channels Incorporated into Planar Bilayer Membranes. *J. Biol. Chem.* **271**, 4776-4780.

Johnson, K.G. (1975). Sweat gland function in isolated perfused skin. *J. Physiol.* **250**, 633-649.

Kao, J.P.Y. (1994).Practical aspects of measuring $[Ca^{2+}]_i$ with fluorescent indicator: *Methods in cell biology.* **Vol. 40.** Academic Press, Inc. pp155-181.

Kao, J.P.Y. (1994).Practical aspects of measuring $[Ca^{2+}]_i$ with fluorescent indicator: *Methods in cell biology.* **Vol. 40.** Academic Press, Inc. pp155-181.

Kingston, J.K., Geor, R.J. and McCutcheon, L.J. (1997).Rate and composition of sweat fluid losses are unaltered by hypohydration during prolonged exercise in horses. *J. Appl. Physiol.* **83(4)**, 1133-1143.

Kleyman, T.R. and Cragoe, E.J. Jr. (1988). Amiloride and its analogs as tools in the study of ion transport. *J. of Membr. Biol.* **105(1)**, 1-21.

Ko, W.H., O'Dowd, J.J.M., Pediani, J.D., Elder, H.Y., Bovell, D.L., Jenkinson, D.M. and Wilson, S.M. (1994). Extracellular ATP can activate autonomic signal transduction pathways in cultured equine sweat gland epithelial cells. *J. exp. Biol.* **190**, 239-252.

Ko, W.H., Chan H.C., Chew, S.B.C. and Wong, P.Y.D. (1996*a*). Ionic mechanisms of Ca^{2+}-dependent electrolyte transport across equine sweat gland epithelium. *J. Physiol.* **493**, 885-894.

Ko, W.H., Chan H.C. and Wong, P.Y.D. (1996*b*). Anion secretion induced by capacitative Ca^{2+} entry through apical and basolateral membranes of cultured equine sweat gland epithelium. *J. Physiol.* **497**, 19-29.

Ko, W.H., Wilson, S.M. and Wong, P.Y.D. (1997). Purine and pyrimidine nucleotide receptors in the apical membranes of equine cultured epithelia. *Brit. J. Pharm.* **121**, 150-156.

Kugelgen, I.V., Norenberg, W., Illes, P., Schobert, A. and Starke, K. (1997). Differences in the mode of stimulation of cultured rat sympathetic neurons between ATP and UDP. *Neuroscience.* **78**, 935-941.

Larsen, E.H., Novak, I., and Pedersen, P.S. (1989). Cation transport by sweat ducts in primary culture. Ionic mechanisms of cholinergically evoked current osicillations. *J. Physiol.* **424**, 109-131.

Lazarowski, E.R., Paradiso, A.M., Watt, W.C., Harden, T.K. and Boucher, R.C. (1997). UDP activates a mucosal-restricted receptor on human nasal epithelial cells that is distinct from the P_{2Y2}-receptor. *Proc. Natl. Acad. Sci.USA.* **94**, 2599-2603.

Mason, S.J., Paradiso, A.M. and Boucher, R.C. (1991). Regulation of ion transport and intracellular calcium by extracellular ATP in normal human and cystic fibrosis airway epithelium. *Brit. J. Pharm.***103**, 1649-1656.

McConaghy, F.F., Hodgson, D.R., Evans, D.L. and Rose, R.J. (1995). Equine sweat composition: effects of adrenaline infusion, exercise and training. *Equine Vet. J. Suppl.* **Nov(20)**, 158-164.

Metioui, M., Amsallem, H., Alzola, E., Chaib, N., Elamani, A., Moran, A., Marino, A. and Dehaye, J.P. (1996). Low affinityy purinergic receptor modulates the response of rat submandibular glands to Carbachol and substance P. *J. Cellular Physiol.* **168**, 462-475.

Montgomery, I., Jenkinson, D.M. and Elder, H.Y. (1982). The effects of thermal stimulation on the ultrastructure of the fundus and duct of the equine sweat gland. *J. Anat.* **135**, 13-28.

Nguyen, T., Erb, L., Weisman, G.A., Marchese, A., Heng, H.H.Q., Garrad, R.C., George, S.R., Turner, J.T. and O'Dowd, B.F. (1995). Cloning, expression, and chromosomal localization of the human uridine nucleotide receptor gene. *J. biol. Chem.* **270**, 30845-30848.

Nicholas, R.A., Watt, W.C., Lazarowski, E.R., Li, Q. and Harden T.K. (1996). Uridine Nucleotide Selectivity of Three Phospholipase C-Activating P_2 Receptors:

Identification of a UDP-Selective, a UTP-Selective, and an ATP-and UTP-Specific Receptor. *Mol. Pharmacol.* **50**, 224-229.

Parr, C.E., Sullivan, D.M., Paradiso, A.M., Lazorowski, E.R., Birch, L.H., Olsen, J.C., Erb, L., Weisman, G.A., Boucher, R.C. and Turner, J.T. (1994). Cloning and expression of a human P_{2U} nucleotide receptor, a target for cystic fibrosis pharmacotherapy. *Proc. Natl. Acad. Sci. U.S.A.* **91**, 3275-3279.

Paradiso, A.M., Mason, S.J., Lazarowski, E.R. and Boucher, R.C. (1995). Membrane-restricted regulation of Ca^{2+} release and influx in polarized epithelia. *Nature*. **377**, 643-646.

Reisin, I.L., Pratt, A.G., Abraham, E.H., Amarat, J.F., Gregory, R.J., Austello, D.A. and Cantiello, H.F. (1994). The cystic fibrosis conductance regulator is a dual ATP and chloride channel. *J. Biol. Chem.* **269**, 20584-20591.

Schachter, J.L., Li, Q., Boyer, J.L., Nicholas, R.A. and Harden, T.K. (1996). Second mesenger cascade specificity and pharmacological selectivity of the human P_{2Y1} receptor. *Brit. J. Pharmacol.* **118**, 167-173.

Schwiebert, E.M., Egan, M.E., Hwang, T.H., Fulmer, S.B., Allen, S.S., Cutting, G.R. and Guggino, W.B. (1995). CFTR regulates outwardly rectifying chloride channels through an autocrine mechanism involving ATP. *Cell.* **81**, 1063-1073.

Snow, D.H. (1977). Identification of the receptor involved in adrenaline mediated sweating in horse. *Res. vet. Sci.* **23**, 246-247.

Stutts, M.J., Fitz, J.G., Paradiso, A.M., and Boucher, R.C. (1994). Multiple modes of regulation of airway epithelial chloride secretion by extrracellular ATP. *A. J. Physiol.* **267**, C1442-C1451.

Tsien, R.Y. (1980). New calcium indicators and buffers with high selectivity against magnesium and protons: design, synthesis, and properties of prototype structures. *Biochemistry*. **19(11)**, 2396-404.

Urquilla, P.R. (1978).Prolonged contraction of isolated human and canine cerebral arteries induced by uridine 5'-triphosphate. *Stroke*.**9**, 133-136.

Ussing, H.H. and Zerah, K. (1951).Active transport of sodium as the source of electric current in the short-circuited isolated frog skin. *Acta Physiol. Scand.***23**, 112-127.

Wilson, S.M., Elder, H.Y., Jenkinson, D.M. and McWilliams, S.A. (1988). The effects of thermally induced activity in *vivo* upon the levels of sodium, chlorine and potassium in the epithelia of the equine sweat gland. *J. exp. Biol.* **136**, 489-494.

Wilson, S.M., Pediani, J.D., Ko, W.H., Bovell, D.L., Kitson, S., Montgomery, I., Brown, U.M.O., Smith, G.L., Elder, H.Y. and Jenkinson, D.M. (1993).

Investigation of stimulus-secretion coupling in equine sweat gland epithelia using cell culture techniques. *J. exp. Biol.* **183**, 279-299.

Wilson, S.M., Ko, W.H., Pediani, J.D., Rakhit, S., Nichol, J.A. and Bovell, D.L. (1995). Calcium-dependent regulation of membrane ion permeability in a cell line derived from the equine sweat gland epithelium. *Comp. Biochem. Physiol.* **111A(2)**, 215-221.

Wilson, S.M., Rakhit, S., Murdoch, R., Pediani, J.D., Elder, H.Y., Baines, D.L., Ko, W.H. and Wong P.Y.D. (1996). Activation of Apical P_{2U} Purine receptors permits inhibition of Adrenaline-evoked cyclic AMP accumulation in cultured equine sweat gland epithelial cells. *J. exp. Biol.* **199**, 2153-2160.

Wilson, S.M., Law, V.W.Y., Pediani, J.D., Allen, E.J., Wilson, G., Khan, Z. and Ko, W.H. (1998). Nucleotide-evoked calcium signals and anion secretion in equine cultured epithelia that express apical P_{2Y2} receptors and pyrimdine nucleotide receptors *Brit. J. Pharm.* **124**, 832-838.

Wong, P.Y.D. (1988). Control of anion and fluid secretion by apical P_2-purinoceptors in the rat epididymis. *Brit. J. Pharm.* **95**, 1315-1321.

Xu, X., Diaz, J., Zhao, H. and Muallem, S. (1996). Characterization, localization and axial distribution of Ca^{2+} signalling receptors in rat submandibular salivary gland ducts. *J. Physiol.* **491**, 647-662.

Yamaya, M., Sekizawa, K., Kakuta, Y., Ohrui, T., Sawai, T. and Sasaki, H. (1996). P_{2U}-purinoceptor regulation of chloride secretion in cultured human tracheal submucosal glands. *A. J. Physiol.* **270**, L979-L984.

Yang, S., Buxton, I.L.O., Probert, C.B., Talbot, J.N. and Bradley, M.E. (1996). Evidence for a discrete UTP receptor in cardiac endothelial cells. *Brit. J. Pharm.* **117**, 1572-1578.

Zegarra-Moran, O. Romeo, G., Galietta, L.J.V. (1995). Regulation of transepithelial ion transport by two different purinoceptors in the apical membrane of canine kidney (MDCK) cells. *Brit. J. Pharm.* **114**, 1052-1056.

Publications

Papers:

Wilson, S.M., **Law, V.W.Y.**, Pediani, J.D., Allen, E.A., Wilson, G., Khan, Z.E. and Ko, W.H. (1998). Nucleotide-evoked calcium signals and anion secretion in equine cultured epithelia that express apical P2Y2 receptors and pyrimidine nucleotide receptors. *British Journal of Pharmacology*, **124**, 832-838.

Ko, W.H., **Law, V.W.Y.** and Wilson, S.M.
Different effects of two Ca^{2+}-mobilising agonists, thapsigargin and ATP, upon transepithelial anion secretion in cultured equine epithelia. (in preparation)

Abstracts:

Wilson, S.M., Ko, W.H., Khan, Z., Pediani, J.D., **Law, V.W.Y.** and P.Y.D. Wong. (1997). Nucleotide-evoked anion secretion and calcium signals in equine cultured epithelia. *Journal of Physiology*, **505.P**, 64P.

Ko, W.H., **Law, V.W.Y.** and Wilson, S.M. (1998).Simultaneous measurement of short circuit current (I_{sc}) and $[Ca^{2+}]_i$ in equine cultured epithelia. *Journal of Physiology*, **506.P**, 126P.

Law, V.W.Y., Wilson, S.M. and Ko, W.H. (1998). Simultaneous measurement of calcium signal and anion secretion in cultured equine sweat gland epithelia. *The FASEB Journal*. **12(4)**, A123,